Civil Aviation Authority

Safety Regulation Group

CAA PAPER 2012/01

The Application of Advanced Anomaly Detection to Tail Rotor HUMS Data

Based on a report prepared for the CAA by GE Aviation Systems Limited

www.caa.co.uk

Civil Aviation Authority

Safety Regulation Group

CAA PAPER 2012/01

The Application of Advanced Anomaly Detection to Tail Rotor HUMS Data

Based on a report prepared for the CAA by GE Aviation Systems Limited

---

December 2012

© Civil Aviation Authority 2012

All rights reserved. Copies of this publication may be reproduced for personal use, or for use within a company or organisation, but may not otherwise be reproduced for publication.

To use or reference CAA publications for any other purpose, for example within training material for students, please contact the CAA at the address below for formal agreement.

ISBN 978 0 11792 794 0

Published December 2012

Enquiries regarding the content of this publication should be addressed to:
Flight Operations 2, Safety Regulation Group, Civil Aviation Authority, Aviation House, Gatwick Airport South, West Sussex, RH6 0YR.

This document is available in electronic format at www.caa.co.uk/publications

Table of Contents

Report

List of Tables

List of Figures

Foreword

The research reported in this paper was funded by the Safety Regulation Group of the UK Civil Aviation Authority (CAA) and Oil & Gas UK, and was performed by GE Aviation (GE). The work follows on from the review of the state of the art regarding the extension of HUMS to rotor health monitoring published in CAA Paper 2008/05.

The objective of the study reported here was to demonstrate the application of the advanced anomaly detection (AAD) methods successfully developed and applied to HUMS transmission data by GE (see CAA Paper 2011/01) to the rotor system data already routinely collected on in-service helicopters. In view of the findings published in CAA Paper 2008/05, the scope of this work was restricted to tail rotor systems.

The CAA accepts the findings of this study, and notes the following points:

1. Using AAD it is possible to detect tail rotor defects in Vibration Health Monitoring (VHM) data, but warnings are unlikely to be much in advance of the end of the flight preceding the 'failure' flight. On-board, post-flight indications would therefore be required for such a scheme to be effective.

2. Both axial and radial accelerometer data is required for effective detection of tail rotor defects.

3. Tail rotor VHM data was found to be particularly susceptible to instrumentation problems. A low noise, high reliability VHM system is required for effective tail rotor health monitoring.

4. Better results might be obtained by:

    a. analyzing VHM data captured during unsteady flight conditions;
    b. measuring vibration data on board the tail rotor rather than in the fuselage.

    These concepts could usefully be investigated.

CAA believes applying VHM directly to rotors is a worthwhile area of research, and encourages the development of these systems. The CAA is committed to supporting such programmes where possible and is participating in the AgustaWestland Rotorcraft Technology Validation Programme (RTVP) which contains a significant section on rotor HUMS. Although it will likely not be possible to release the results of this programme into the public domain, given the costs and facilities required for the work that needs to be performed, CAA believes that this represents the best way forward at this time.

Safety Regulation Group
December 2012

Glossary

AAD	Advanced Anomaly Detection
AFH	Air Frame Hours
AHUMS™	(Advanced) HUMS, developed by GE Aviation initially for Bell helicopter types
CAA	The United Kingdom Civil Aviation Authority
CF	Canadian Forces
CI	Condition Indicator
CVFDR	Cockpit Voice Flight Data Recorder
EuroHUMS™	HUM system developed by GE Aviation for Eurocopter
FS	Fitness Score
GE	General Electric
HUMS	Health and Usage Monitoring System
IF	Influence Factor
IHUMS	Integrated HUMS
MooN	M out of N
MPOG	Minimum Pitch On Ground
MR	Main Rotor
PA	Probability of Anomaly
RTB	Rotor Tracking and Balancing
SG	Savitzky-Golay
TGB	Tail rotor Gear Box
TR	Tail Rotor
VHM	Vibration Health Monitoring

Executive Summary

Under an extension to Contract No. 841, GE Aviation conducted a helicopter rotor HUMS study to review the status of rotor health monitoring research, and also accidents caused by rotor system failures (Reference [2]). This study identified two Main Rotor (MR) failure cases and three Tail Rotor (TR) cases for which HUMS data were available. In neither of the MR cases (a MR blade failure and a cracked blade yoke) was there any evidence in the currently acquired HUMS data of fault-induced changes that could have provided warning of the failure. However, in all three TR cases an investigation performed after the incident or accident revealed some fault-related information in the HUMS vibration data. It was therefore concluded that there may be potential to improve airworthiness through the application of new analysis techniques such as Advanced Anomaly Detection (AAD) to HUMS TR vibration data.

Under a further extension to Contract No. 841, GE Aviation has applied its AAD technology to HUMS vibration data from three TR-related accidents and incidents, and also a database of historical Bristow 332L IHUMS data, to evaluate the potential airworthiness and maintenance benefits that could be obtained. The analysis consisted of three primary elements; anomaly modelling of single and multiple TR harmonics, merging data from different acquisitions stored in different database tables (e.g. to allow TR axial and radial data to be modelled together), and automated trend analysis.

A blade failure occurred on the two bladed TR of a Bell 412 helicopter. Several anomaly models built with different combinations of vibration harmonics responded to the fault. While a univariate model responded to the specific characteristics of this individual fault, fusing multiple TR harmonics in an anomaly model also gave a clear fault indication. A trend detection algorithm also showed that the period immediately prior to the accident could be identified as part of a trend. The results indicated that a TR AAD alert could have been triggered on the flight prior to a refuelling stop that occurred before the final flight.

A failure occurred on one of the arms of the pitch change spider on the 5 bladed TR of a Super Puma. Multiple anomaly models were built using axial and radial TR data and all models clearly responded to the failure. In this case, the frequencies could be predicted from knowledge of the failure mode. The trend detection algorithm identified a clear trend on the aircraft immediately prior to the accident. The results show that a TR alert could have been triggered after the first flight of the day of the accident, with the failure occurring on the second flight.

The third incident involved a Super Puma with a cracked flapping hinge retainer on one of the 5 TR blades. The available accident data was limited although an anomaly model built using recreated tail rotor gearbox data was able to identify the accident aircraft as anomalous. In this case the existing IHUMS had triggered an alert, but a subsequent maintenance inspection failed to identify the developing flapping hinge retainer crack.

The Bristow Super Puma TR ‘maintenance study’ (analysing maintenance-related TR faults) used IHUMS data that was limited to radial measurements only, but included both amplitude and phase. According to the maintenance data, there were repeated occurrences of similar faults, however the TR vibration data showed trends in different TR harmonics, and it was not possible to identify any consistent pattern between the harmonics in the TR vibration data and particular fault types. However instrumentation faults could affect all harmonics. Nevertheless, results showed that the outputs from anomaly models combining amplitude and phase information were primarily dependent on magnitude rather than phase. Therefore it was concluded that using the phase data did not provide any improvement in the ability to detect TR faults. The analysis indicated that multiple TR harmonics can be combined in a single model to provide a general fault detection capability, while a separate 1T model remains useful to identify balance issues.

Some limited further analysis was performed on the Bell 412 HUMS TR data. Anomaly models were built on processed vibration harmonics from the radial and axial accelerometers. It was concluded from this short anomaly modelling exercise that TR faults appear to be generally more visible in the axial dataset rather than the radial. Cross correlating axial and radial data sets can help to distinguish between instrumentation errors and potential faults.

The report makes a number of recommendations. It is recommended that, when implementing an AAD capability for the helicopter rotor drive system, AAD models are also included for the TR.

Consideration should be given to the application of appropriate data pre- and post processing techniques to enhance the AAD results. Pre-processing may include the use of techniques to identify data trends and the careful use of smoothing techniques if data is noisy. Post-processing can include anomaly model output trend identification and severity assessment.

TR Vibration Health Monitoring (VHM) may provide a late indication of a potential TR hub or blade failure. Therefore, where possible, HUMS data should be downloaded and reviewed between flights. For system upgrades and future systems, consideration should be given to the feasibility of providing on-ground post flight indications of MR and TR vibration monitoring alerts on a Multi-Functional Display in the cockpit.

It is recommended that, for TR VHM, the measurement set is standardised where possible. Data should be acquired from both radial and axial accelerometers and should, as a minimum, include measurements at Minimum Pitch on Ground (MPOG) and in normal cruise of all significant harmonics.

VHM can provide TR health information, however instrumentation problems can cause a significant number of false alarms. Providing high reliability instrumentation and the elimination of signal noise should be key requirements for the design and installation of accelerometers and wiring harnesses for TR VHM.

Consideration should be given to further research into health monitoring techniques that would be applicable to both the MR and TR. This could include areas such as the investigation of the potential use of vibration data acquired during unsteady flight conditions, and the investigation of the emergent rotating-frame sensing technologies including data transfer from the rotor system to the non-rotating fuselage equipment.

Report

1 Introduction

Health and Usage Monitoring Systems (HUMS), incorporating comprehensive rotor drive system Vibration Health Monitoring (VHM), have contributed significantly to improving the safety of rotorcraft operations. However, experience has also shown that, while HUMS has a good success rate in detecting defects, not all defect related trends or changes in HUMS data are adequately detected using current threshold setting methods. Earlier research conducted as part of the CAA's main rotor gearbox seeded defect test programme demonstrated the potential for improving fault detection performance by applying unsupervised machine learning techniques, such as clustering, to seeded fault test data. Therefore in 2004 the CAA commissioned a further programme of work titled "Intelligent Management of Helicopter Vibration Health Monitoring Data: Application of Advanced Analysis Techniques In-Service" (CAA Contract No. 841). Under this contract GE Aviation developed and trialled an Advanced Anomaly Detection (AAD) system for analysing HUMS rotor drive system VHM Condition Indicators (CIs). The work was carried out in partnership with Bristow Helicopters, analysing IHUMS data from Bristow's European AS332L fleet. The results are presented in Reference [1].

Under an extension to Contract No. 841, GE Aviation conducted a helicopter rotor HUMS study to review the status of rotor health monitoring research, and also accidents caused by rotor system failures (Reference [2]). This was motivated by the perception that, whilst rotor drive system VHM is a mature technology and an integral part of a helicopter HUMS, the same cannot be said for rotor system health monitoring, despite the fact that the numbers of helicopter accidents caused by rotor failures and drive system failures are comparable. Although rotor vibration is monitored by HUM systems and used for rotor tracking and balancing purposes (RTB), there are currently few recognised techniques for the detection and diagnosis of rotor fault induced vibration. Previous research work conducted in the area was on a largely theoretical, analytical basis, and was considered to have shown some potential, but there was no further development towards a working demonstration or a practical rotor monitoring system.

The accident analysis performed for the rotor HUMS study identified two Main Rotor (MR) failure cases and three Tail Rotor (TR) cases for which HUMS data was available. In neither of the MR cases (an S76 main rotor blade failure and a cracked 332L blade yoke) was there any evidence in the currently acquired HUMS data of fault-induced changes that could have provided warning of the failure. Therefore, whilst previous theoretical analysis indicates some potential for providing airworthiness benefits from improved monitoring techniques based on rotor vibration and blade track measurements, it is likely that some MR failures will remain undetectable.

In all three TR cases an investigation performed after the incident or accident revealed some fault-related information in the HUMS vibration data. In one case, an increase in 1/rev vibration had triggered a HUMS alert, but this was misdiagnosed, resulting in incorrect maintenance being performed. In the other two cases there were increases in vibration harmonics for which thresholds are not currently set. It was therefore concluded that the greatest potential to improve airworthiness is through the application of AAD to HUMS TR vibration data.

Under a further extension to Contract No. 841, GE Aviation was funded to research the application of its AAD technology to in-service HUMS TR vibration data, and evaluate the potential airworthiness and maintenance benefits that could be obtained. The objectives of the work were to:

1 Build anomaly models on HUMS data from three TR-related accidents and incidents to assess the ability of the models to detect the different TR failure mechanisms causing these incidents and accidents, and the warning times that could be provided.

2 In addition, analyse a database of historical Bristow 332L IHUMS data and correlate anomaly model outputs with TR faults and maintenance actions recorded in Bristow's 332L maintenance database to assess the ability of the anomaly models to provide a better indication of faults resulting in TR maintenance actions.

The results of the TR research work are presented in this report. Section 2 describes the application of AAD to HUMS TR data and also describes the data acquired for the research. The results of the accident and incident data analysis are presented in Section 3, and the results of the analysis of faults resulting in maintenance are presented in Section 4. Finally, conclusions and recommendations from the research work are given in Section 5.

2 Application of AAD to HUMS TR data

This section introduces the HUMS AAD capability that was developed for CAA Contract No. 841, together with the TR data that has been analysed in this work.

2.1 HUMS Advanced Anomaly Detection

A brief overview is presented here of GE Aviation's HUMS AAD capability that has been applied to the acquired HUMS TR data. The key elements of the AAD process are illustrated in Figure 2-1. A full description of this process is presented in Reference [1].

2.1.1 Data pre-processing and modelling

Different pre-processing is applied to the input HUMS CI data to enable two types of model to be built for each monitored component (e.g. a gear, shaft or bearing): an 'absolute' and a 'trend' model. The absolute models identify combined CI values that are anomalous in absolute terms, whereas the trend models identify anomalous combined CI trends, irrespective of the absolute values of the indicators.

The pre-processing for the absolute models can vary according to the modelling requirements. In some cases no pre-processing may be applied. For the rotor drive system analysis described in Reference [1] a median filter was applied to remove up to two successive outliers in the time series data. For some of the TR data analysis described in later sections of this report a smoothing algorithm was applied to characterise the underlying behaviour of what could be 'noisy' data (i.e. where there may be significant point-to-point variability). For the rotor drive system trend models a 'moving median difference' algorithm was applied to extract trend information. Following each new acquisition, the median of the time history was re-calculated and subtracted from the newly acquired value to provide a normalised value. This technique reduced the impact of early post-installation trends, because the normalised value would gradually recover back to the median base line level.

Prior to model building, using either available maintenance information or the results of an analysis of step changes in the data, the training data set is divided up into separate 'Component Fits'. A Component Fit is a combination of a particular assembly (e.g. a gearbox) installed in a particular aircraft for a particular time period. If the assembly is removed for maintenance, then installed in a different aircraft, it is given a different Component Fit ID.

Using the pre-processed data for selected combinations of HUMS CIs, anomaly models were constructed for each monitored component. The anomaly models are based on Gaussian Mixture Models (GMMs, which are a type of probabilistic cluster model), and provide detailed density mappings of the data. They are specifically designed for anomaly detection, and are not standard mixture models. The clusters in a model can rotate to represent correlations between CIs. This does not have a large impact on the anomalies detected for the type of data being analysed here, but it does allow more diagnostic information to be derived from the model, such as a de-correlation between CIs.

The models are then adapted so that they reject any abnormalities existing in the training data. A carefully designed automatic 'model adaptation' process detects regions in the model's cluster space that are not representative of normal behaviour,

then removes the associated clusters. The adaptation process is complex, but is controlled by a simple tuning parameter. The final model provides a poor fit to samples in the training data that are outliers. A significant amount of effort was expended developing the novel automated model adaptation process, as this is key to the successful building of models using in-service data containing various unknown anomalies.

The resulting models are sophisticated statistical representations of the data generated from in-service experience, fusing sets of CIs (i.e. vibration features) to reduce a complex data picture into a single parameter time history called a 'Fitness Score' (FS) trace. The FS measures the degree of abnormality in the input data and mirrors the shape of any significant data trends. It represents a 'goodness of fit' criterion, indicating how well data fits a model of normality. Therefore the FS has a decreasing trend as data becomes increasingly abnormal.

Another novel feature of the modelling process is that this does not require data to be categorised as training, test or validation (which is a common practice in data modelling to ensure that built models will generalise to data not used for training). All data can contribute to a model, and the standard procedure for building a model is to use all available historical data apart from cases that are known a-priori to be anomalous. This also has the advantage that online model updates can be performed as new data are acquired. The ability to update models is important, particularly for a new aircraft type where data is initially limited.

2.1.2 Generating anomaly alerts and diagnostic information

Alert thresholds can be, and sometimes are, set on the anomaly model FS outputs. The disadvantage of this approach is that these thresholds are model-specific, as FS values vary between models. Therefore the FS output can be converted into a 'Probability of Anomaly' (PA) value, which is a normalised probability measure that ranges between 0 and 1. For each model there is a PA distribution which is an extreme value distribution. An FS value is passed to the PA distribution and a PA value is returned. Most FS values will return a PA of 0 because most acquisitions will be normal. The PA distribution is built using a model-based prediction of outlying data. The PA values provide a measure that is normalised across models, which allows model outputs to be compared. An alerting threshold can be defined using the PA values, which greatly simplifies the threshold setting process.

A default PA threshold is normally applied that is common to all models and components (the FS equivalent of this PA threshold will be different for each model). The default threshold for an individual model, however, can be changed if it is considered that the alert rate is too high or low.

Diagnostic information about an anomaly model and its inputs (i.e. HUMS CIs) can be provided by another type of model prediction known as 'Influence Factors' (IFs). There are different types of IF, each type producing a different view on a model or input variable. An acquisition will generate a single IF predicted value for each CI used to train a model. IF time histories provide information regarding the influence of HUMS CIs on the fused Fitness Score. These traces are not the same as plots of CIs as they are assessing the contribution of individual CIs to a statistical measure of abnormality. Unlike CIs, IFs are normalised and can be directly compared. Although multiple types of IF are generated for GE Aviation's internal use, with each type being designed to provide different information about a model or an input feature, normally only one type of IF would be presented to the operator. This would

be the one that most closely matches the trends the operator would observe in the HUMS CI data.

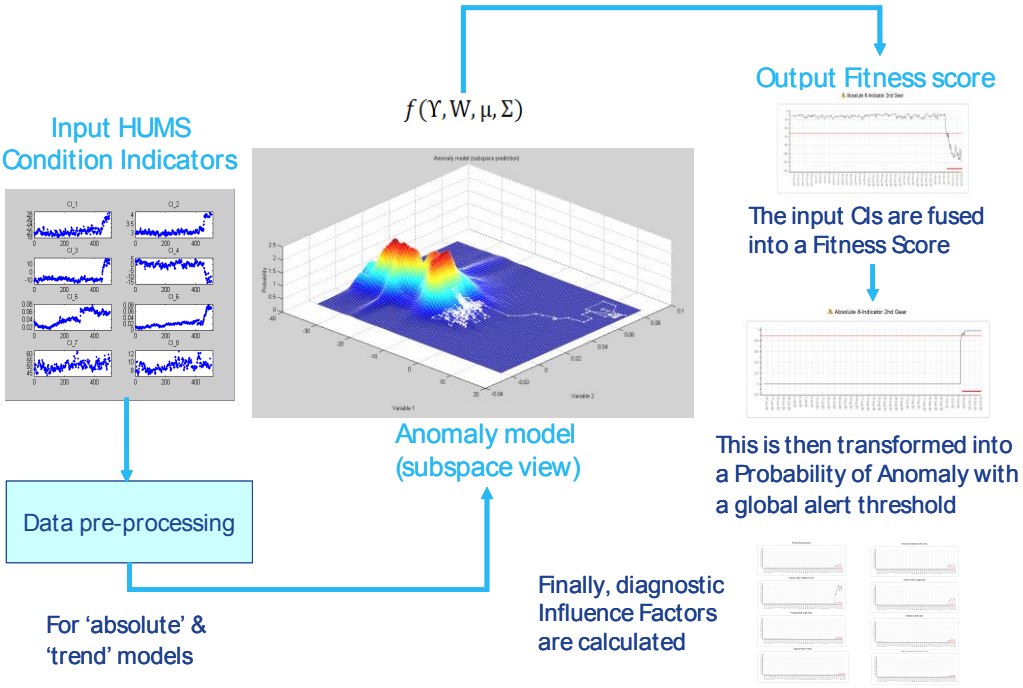

Figure 2-1: Advanced Anomaly Detection Process

2.2 HUMS TR data

Although there are variations between aircraft types and HUM systems, TR data normally consist of the measurement of vibration amplitudes at multiple harmonics of TR rotation in different aircraft regimes from two accelerometers mounted in radial and axial directions. Once per Rev (1/rev) amplitude and phase measurements are also acquired for TR balancing (these acquisitions may be pilot initiated).

For this work TR data has been acquired from the following three different HUM systems.

- Super Puma Mk1 data from the Meggitt Avionics IHUMS
- Super Puma Mk1 data from the EuroHUMS™ produced by GE Aviation for Eurocopter
- Bell 412 (CF Griffon) data from the GE Aviation AHUMS™

A summary of the available TR measurements from these HUM systems is given in Table 2-1. Whilst the measurements performed by the EuroHUMS™ and AHUMS™ are the same, there are some notable differences between these and the measurements performed by the IHUMS. For example the IHUM system acquires both amplitude and phase data, but only from a single accelerometer mounted in the radial direction.

In addition to the TR measurements, Tail rotor GearBox (TGB) output shaft 1/rev (SO1) and 2/rev (SO2) vibration measurements from a TGB mounted accelerometer are also available. As demonstrated in the HUMS AAD in-service trials described in Reference [1], these measurements can also provide information on TR faults.

Table 2-1: HUMS Tail Rotor Data

System	Aircraft	Regime	Measurements
IHUMS	Super Puma Mk1	MPOG 125 Knots Cruise TGB Output – Cruise only	TR harmonics 1, 2, 3, 4, 5, 10T Radial accelerometer only All measurements have phase Data also available at 115Kts, Climb, Descent, Hover and Turn. TGB output SO1, SO2
EuroHUMS™	Super Puma Mk1	MPOG Normal Cruise TGB Output – Cruise only	TR harmonics 1, 2, 3, 4, 5, 6, 7, 8, 9T Radial and Axial accelerometers No phase data TGB output SO1, SO2
AHUMS™	CF Bell 412 (Griffon)	MPOG Normal Cruise TGB Output – Cruise only	TR harmonics 1, 2, 3, 4, 5, 6, 7, 8, 9T Radial and Axial accelerometers No phase data TGB output SO1, SO2

2.3 Data acquired for the research

2.3.1 Accident/incident data

Details of the three TR accidents and incidents analysed in this project are given in Section 3.1. HUMS data were available from two of these – the accident to Canadian Forces (CF) Bell 412 (Griffon) CH146420 on 18th July 2002, and the ditching of Super Puma 9M-STT on 18th June 2005. No HUMS data were readily available from the incident on Super Puma G-PUMH on 27th September 1995, however this could be reconstructed from HUMS data plots in the AAIB report (Reference [3]).

2.3.2 Database of TR data for model building and maintenance related fault investigation

Databases of TR and TGB output data were created for building anomaly models for the analysis of the accident and incident data described in Section 2.3.1. In addition,

the database of Bristow Super Puma IHUMS data were also used to investigate TR faults causing maintenance actions. The CF Bell 412 (Griffon) AHUMS™ database contained data from 51 aircraft in the period of June 2006 to December 2007. The Super Puma EuroHUMS™ database contained data from 25 aircraft, covering a range of dates. The Bristow Super Puma IHUMS database contained data from 20 aircraft, starting between August 2005 and September 2006, and including data up to the end of December 2008.

2.3.3 Database of TR maintenance data

For the analysis of Bristow Super Puma TR faults causing maintenance actions, access was provided to Bristow's Super Puma maintenance database to identify actions carried out on the aircraft. These were studied to identify any correlations between maintenance actions and rotor faults identified by the anomaly models.

There were 471 records of TR maintenance actions for the aircraft in the IHUMS database. The principle actions could be broadly categorised as pitch link actions, flap hinge actions, spindle and sleeve actions, and rotor balance actions. Other actions included torn boot replacements and inspections, etc. Servicing actions such as re-greasing of the TR are not recorded in the database (Bristow records these separately under routine maintenance). A distribution of the approximate frequency of the different maintenance actions is shown in Figure 2-2. The figure shows that the most common type of action is related to the maintenance of the pitch links. It should be noted that some individual maintenance records included more than one type of maintenance action; the 471 records detailed 494 separate maintenance actions.

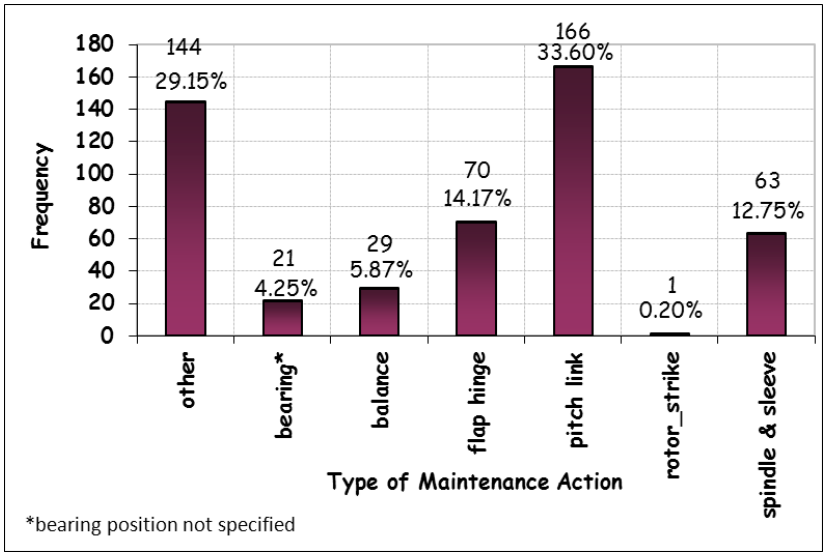

Figure 2-2: Frequency of Maintenance Action Types

The TR maintenance data were also used to identify TR replacements so that the Bristow IHUMS TR data set could be divided up into different Component Fits (i.e. combinations of a particular TR installed in a particular aircraft for a particular period of time).

3 Accident/Incident Data Analysis

3.1 Summary of accident/incident details

3.1.1 Canadian Forces Bell 412 (Griffon), CH146420

The information presented here is obtained from Reference [4]. On the 18th July 2002 Canadian Forces CH146420 was in cruise flight returning from a SAR mission, when the TR failed due to a fatigue crack initiating from a small damage site on the skin of the rotor blade about 18.5 inches from the tip of one blade .

Figure 3-1: TR Blade Failure

The initiation site for the fatigue failure was a nick on the blade which was most likely caused by contact with a stone or similar object. The nick had a depth of 0.008 inches (the maintenance manual common to all Bell 412 operators states a maximum tolerance of 0.003 inches) and was 0.06 inches long. Over the following flying hours the nick developed into a crack which, once through the skin thickness, began growing simultaneously towards the leading and trailing edges of the aluminium skin. As the crack grew the load shedding caused an increase in load (and stress) in the stainless steel leading edge which propagated the crack into the leading edge spar. The crack then grew to such a size that the remaining structure could not carry the normal operating loads and it failed. The outward 18.5 inch of the TR blade separated and flew up striking the main rotor blade. The resulting TR unbalance caused an overload failure of the TGB shaft (TR input shaft), which resulted in the TR assembly separating from the aircraft.

In order to determine the fatigue crack growth rate, a fractography analysis of the crack striation pattern and numbers was conducted using a scanning electron microscope and a transmission electron microscope, together with a crack debris analysis and a review of the Bell 412 baseline design spectrum and certification process. This indicated that a fatigue crack would take approximately 56 airframe hours (AFH) to develop into a crack resulting in blade failure. Bell Helicopter then used the actual CVFDR data from the accident aircraft in comparison to the Bell 412 baseline design spectrum to establish the actual failure timeframe. This indicated the following crack propagation times.

60 AFH (failure -16.86 hrs) – Time to crack through material thickness
71 AFH (failure -5.86 hrs) – Crack reaches 0.1” length

74.5 AFH (failure -2.36 hrs) - Crack reaches 0.25" length
75.3 AFH (failure -1.56 hrs) – Crack reaches Critical Length of 4.14"
76.86 AFH – Complete Blade Failure

3.1.2 Super Puma, 9M-STT

On 18th June 2005 Super Puma 9M-STT was ditched in the sea following increasing vibration (Reference [5]). Inspection of the TR revealed a broken arm on the pitch change spider (Figure 3-2).

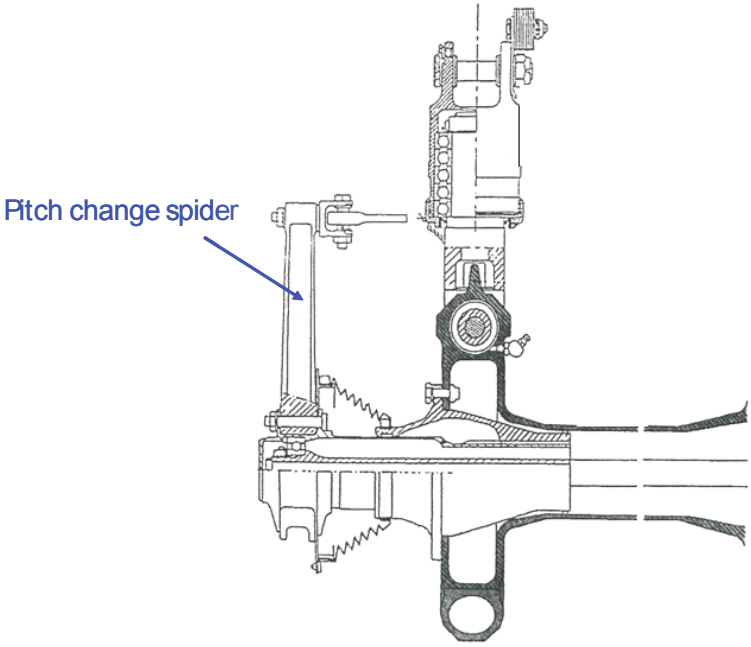

Figure 3-2: TR Pitch Change Spider

Flight information is shown in the following table. The accident occurred on the second flight of the day, and the aircraft had made two flights on the previous day.

Flight Number	Date	Start Time (GMT)	End Time (GMT)	Duration
1	17/6/05	04:57	07:15	2:18
2	17/6/05	07:38	08:33	0:55
3	18/6/05	00:28	02:52	2:24
Last	18/6/05	03:34	04:09 approx	0:35

3.1.3 Super Puma, G-PUMH

The information presented here is obtained from Reference [3]. On 27th September 1995 Super Puma G-PUMH left Aberdeen at 7:02am. At 7:29am, while cruising at 3,000ft and 120kts, there was a sudden onset of severe airframe vibration. A MAYDAY was issued at 7:52am and the aircraft was diverted and landed safely at

8:21am. Subsequent examination revealed that a TR blade flapping hinge retainer had fractured on one side (Figure 3-3).

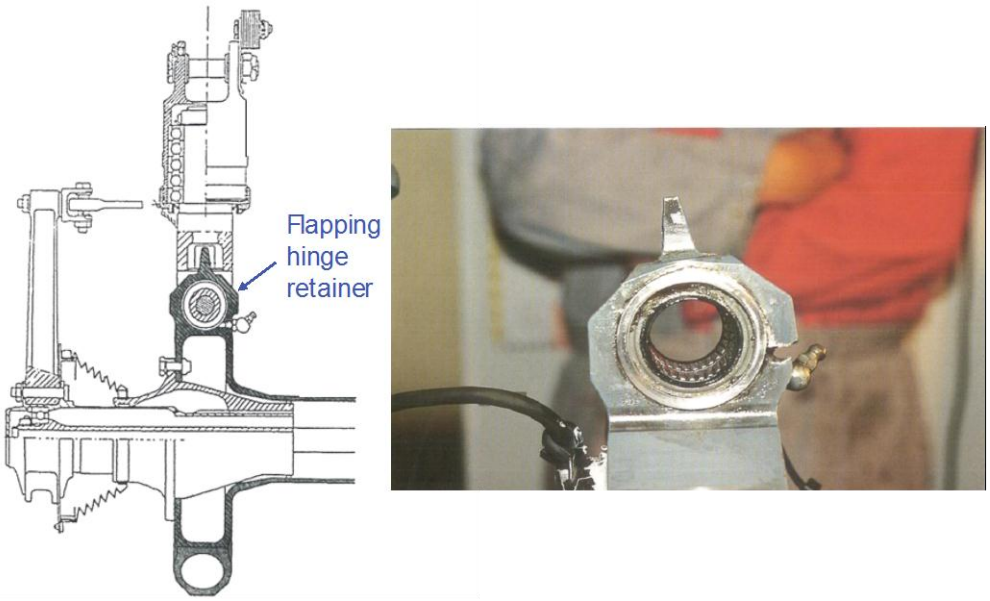

Figure 3-3: TR Flapping Hinge Retainer

The commander considered the vibration period to be nearer 4R (4x main rotor speed) than 1R. The main rotor tracking appeared normal and engine torque and other engine parameters were normal. The general airframe vibration was severe, but there was no obvious lateral component, no significant vibration was felt through the collective lever and that felt through the yaw pedals seemed in sympathy with the airframe. The most significant control vibration was felt through the cyclic control; this was greater fore and aft than laterally. Despite the vibration the 1st officer had full control movement and normal response.

Maintenance Record:

Task	Airframe hours	Date
Rebalance of tail rotor	14050	13/9/95
50hr check	14053	14/9/95
50hr check	14105	22/9/95
3000hr 'on condition' check of tail rotor head requirement issued	14105	22/9/95
IHUMS trend investigation suspected shaft imbalance associated with tail rotor gearbox output shaft 1R – Additional work sheet raised for removal of tail rotor blades, pitch change spider, fairings.	14105	22/9/95
3000hr 'on condition' check of tail rotor head completed	14105	26/9/95
Rebalance of tail rotor	14105	26/9/95

During the 50 flying hours before the incident, some vibration in the vertical plane of the TR was recorded by the IHUM system; it did not exceed the alert threshold until 22/9/95. Only 25 minutes was logged between 22nd and 26th Sept. The IHUMS indications were attributed by the engineer involved to slight 'free play' in the TR gearbox shaft bearings. The vibration was temporarily resolved by rebalancing. Final separation of the fracture face and the onset of severe vibration occurred about 27 minutes into the incident flight.

After the incident the TGB was examined and it was observed that the flapping hinge retainer at the blue blade position had fractured on one side in the plane of the greasing point, and had opened up under centrifugal loads by approximately 6-7mm. The surfaces of the fracture showed some corrosion and markings typical of fatigue progression. Evidence of rotation of the bushes in the bore indicated that the flapping moments had not been eliminated by the flap bearing; the only way for this to happen was if the flap bearing became stiff. The unresolved flapping moments would have induced stresses in the flapping hinge retainer, which the shaft was unable to withstand.

The crack had clear evidence of growth by fatigue over most of its length from an origin close to one end, on the inside face of the bore. There was corrosion pitting that was about 7-10 microns in depth in the region of the origin, 7mm from one end. The total crack length was 67mm, having propagated in a slow stable manner in both directions from the origin. The remaining material had failed in a ductile rupture mode.

When the crack extended to the external surface and reached 50mm in length it would have started to open up significantly under centrifugal loads, causing the observed increased vibration on IHUMS. With the aircraft shut down and centrifugal loads removed the crack closed up again. Crack length was estimated at 54mm at the time the IHUMS data began to show a divergent trend. The IHUMS triggered an alert 5 flight hours before the incident. At the last rebalancing the effect of the undetected crack was eliminated by increasing the weights on the opposite blades. During the incident flight the crack progressed to a length where the remaining material fractured, causing severe vibration.

3.2 Accident/incident AAD results

3.2.1 Canadian Forces Bell 412 (Griffon), CH146420

The database created for the CF412 aircraft contained TR data for 56 aircraft. This included about 3,500 acquisitions of TR gearbox parameters SO1 and SO2, and 3,700 acquisitions of TR 1 to 9T axial and radial vibration amplitudes (i.e. vibration at the first 9 harmonics of TR rotational frequency), in the Normal Cruise phase. The database also contained about 11,000 acquisitions of TR harmonics gathered in the phase Minimum Pitch on Ground (MPOG).

Analysis of the data was conducted with particular attention focused on the accident aircraft (ID 46420). Figure 3-4 through Figure 3-12 show the 1T to 9T radial harmonics for Aircraft 46420. Figure 3-13 through Figure 3-21 show the corresponding harmonics for the axial data. Figure 3-22 shows the acquisitions for gearbox parameter SO1. Data for SO2 was not available for this aircraft. The figures relate to data captured during the Cruise phase. The figures are plotted together with +/-3SD bands derived for from the entire fleet.

The clearest failure related trends were in the 1T and 5T axial and radial vibration together with the gearbox SO1 measurements. Trends were observed in both the Cruise phase and the MPOG phase. Figure 3-22 shows a trend in the SO1 values starting on 19th June just prior to the accident. Figure 3-4 shows a step change in the 1T radial data on 23rd October 2000. Since the next acquisition is not until 24th January 2001 it may be that maintenance actions were performed during this time. The amplitude values then remain fairly constant but at an elevated level until the 5th June; the values are at the high end of the envelope of acquisitions for this parameter (although the 3SD lines have been distorted by the presence of spikes in other aircraft acquisitions). Another step change is then also observed on the 19th June and therefore may indicate further maintenance actions. However, from about the 6th July the amplitude of the harmonic is seen to start trending up. An initial peak is reached on the 7th July before falling back but then the trend continues over the next six acquisitions until the 18th July. Similar behaviour is observed in the 1T axial data, although the step change on the 23rd October is not clear (Figure 3-13). Nevertheless, the amplitude values are higher in the period February to June than the preceding period. The step change on the 19th June is clear and whilst a peak is again observed on the 7th July the value is not significant. The continuing trend up to the 18th July is more significant in the axial data than the radial data. This would be expected as the radial measurements can be affected by both TR unbalance and component faults, whereas axial measurements are in the axis of the thrust generated loadings and could exercise faults.

The most significant trends are observed in the 5th harmonic. Figure 3-8 shows the 5T radial measurements where a trend is seen to begin around the 29th May and generally increases until the end of the acquisition period. A significant jump in values is seen on the 18th July where values reach three standard deviations above the mean. Again, similar behaviour is observed in the axial measurements but with the trend appearing significantly stronger (Figure 3-17). It would be expected that increased vibration would be observed in the 1T data as a result of deflection of the blade. However, the 5T trend could not be predicted and is believed to be due to excitation of a blade bending mode, as the frequencies of the blade modes would decrease as the crack developed.

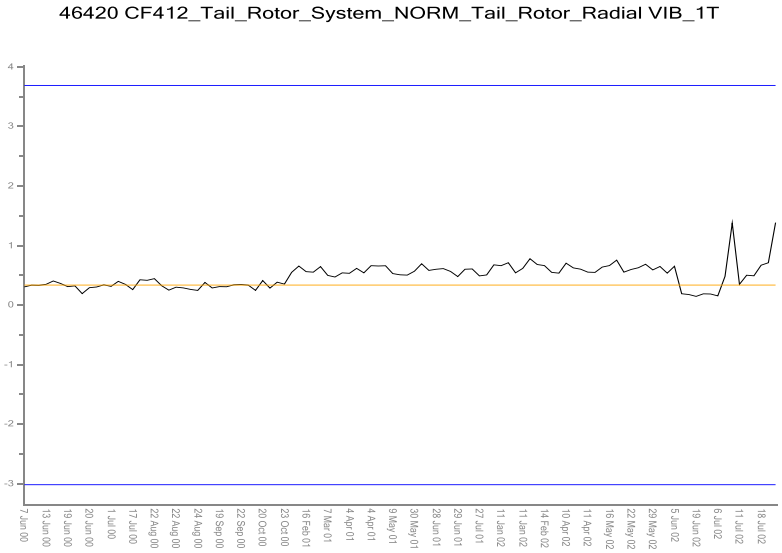

Figure 3-4: CF412 Radial Vib 1T for Aircraft 46420

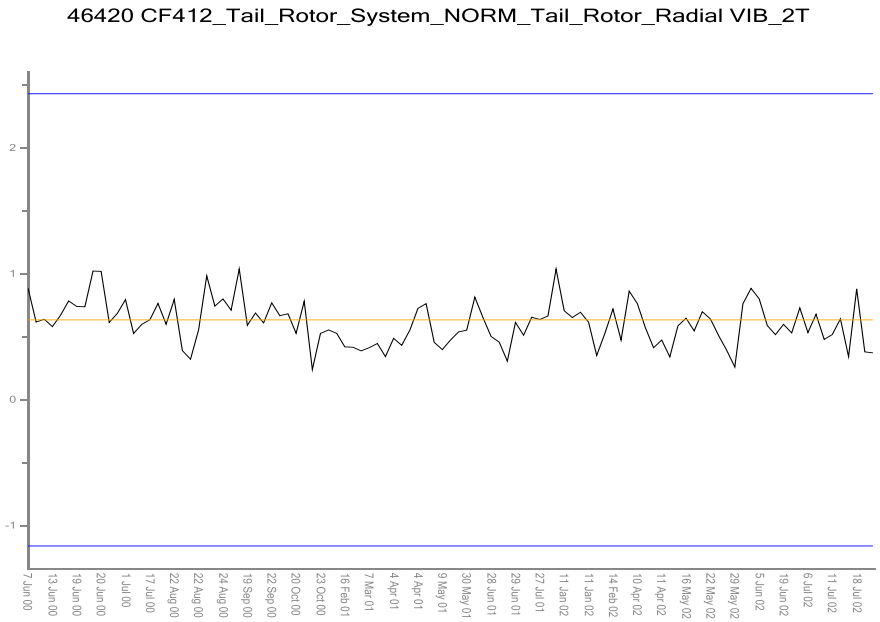

Figure 3-5: CF412 Radial Vib 2T for Aircraft 46420

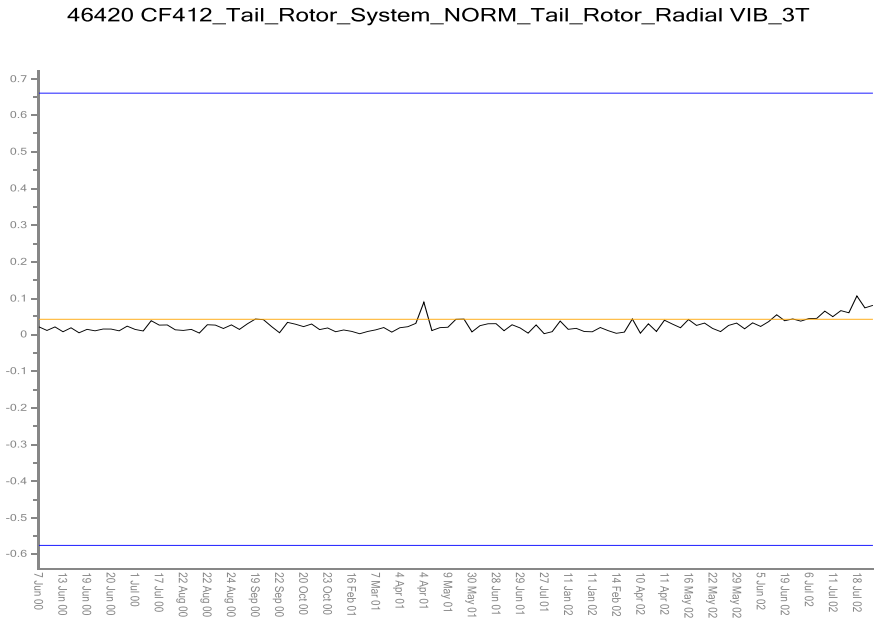

Figure 3-6: CF412 Radial Vib 3T for Aircraft 46420

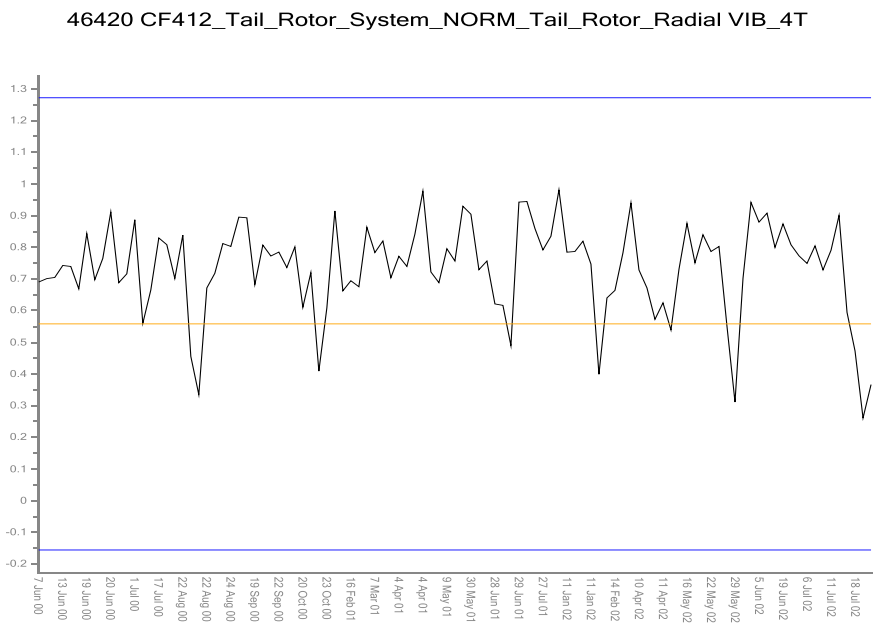

Figure 3-7: CF412 Radial Vib 4T for Aircraft 46420

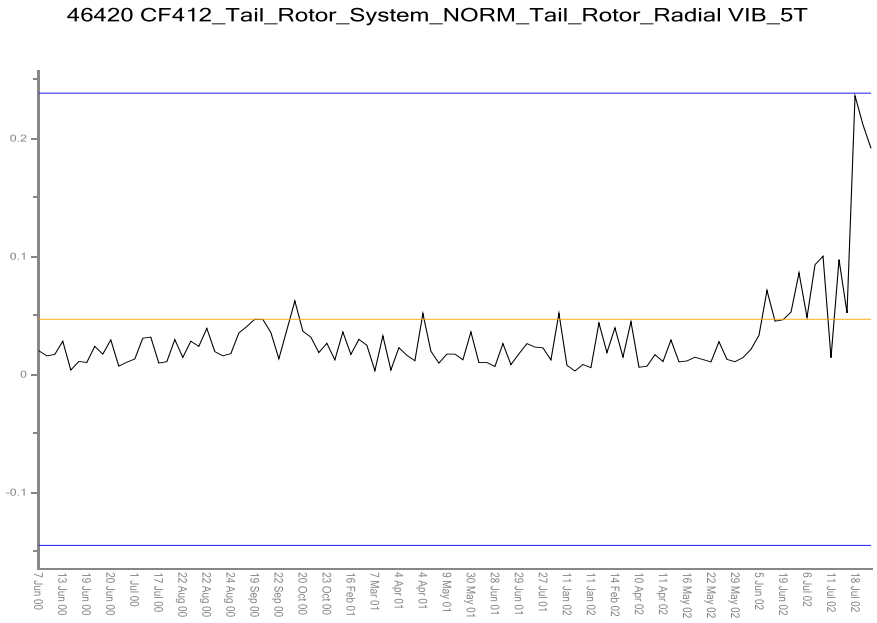

Figure 3-8: CF412 Radial Vib 5T for Aircraft 46420

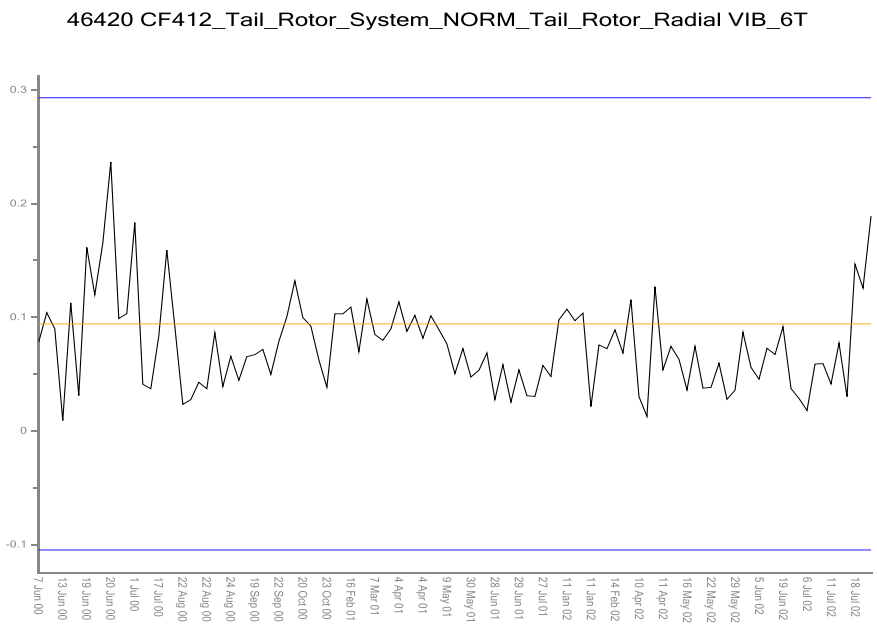

Figure 3-9: CF412 Radial Vib 6T for Aircraft 46420

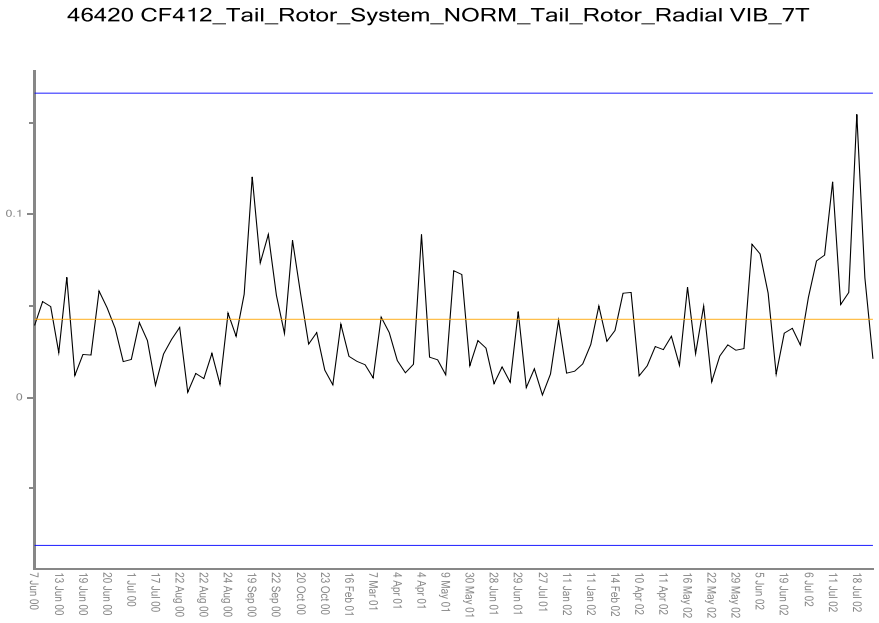

Figure 3-10: CF412 Radial Vib 7T for Aircraft 46420

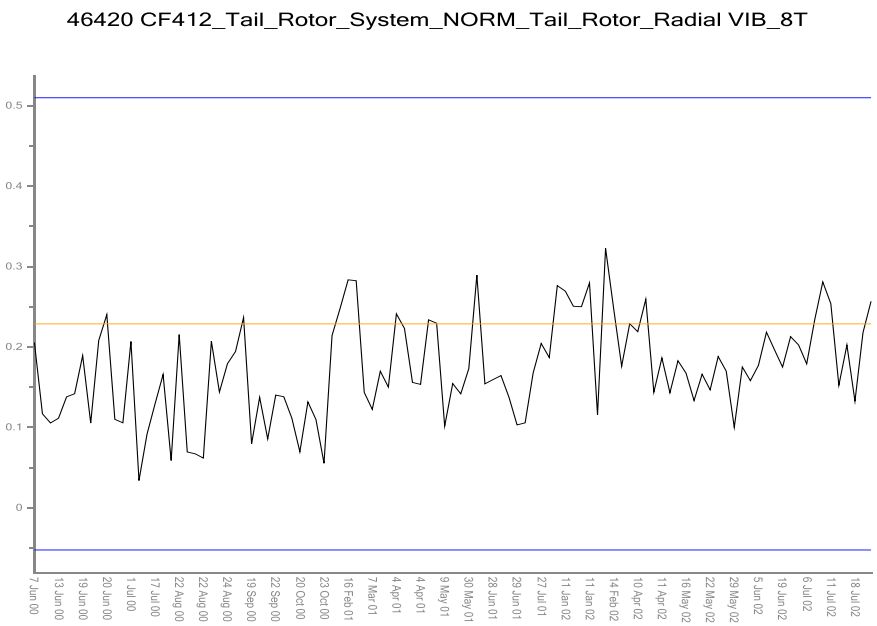

Figure 3-11: CF412 Radial Vib 8T for Aircraft 46420

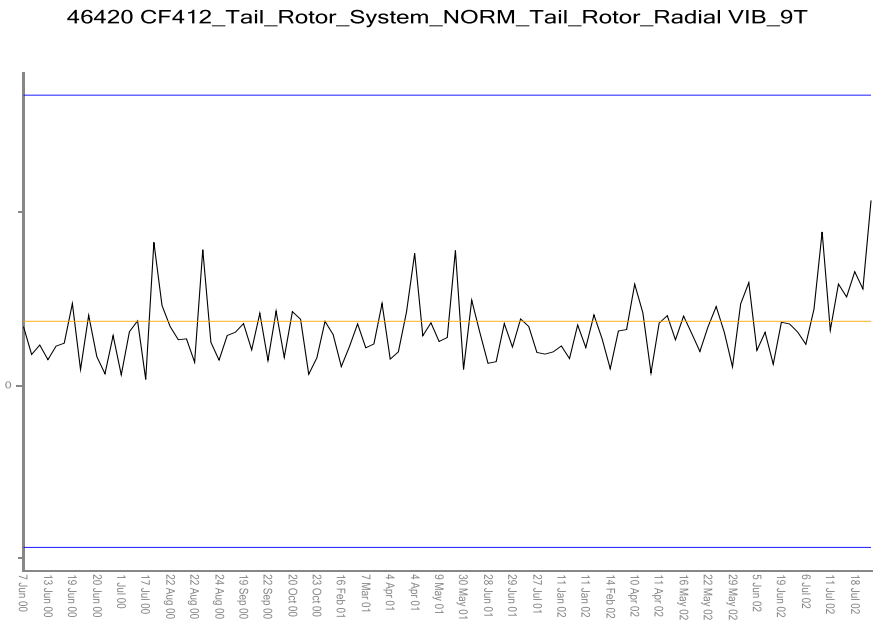

Figure 3-12: CF412 Radial Vib 9T for Aircraft 46420

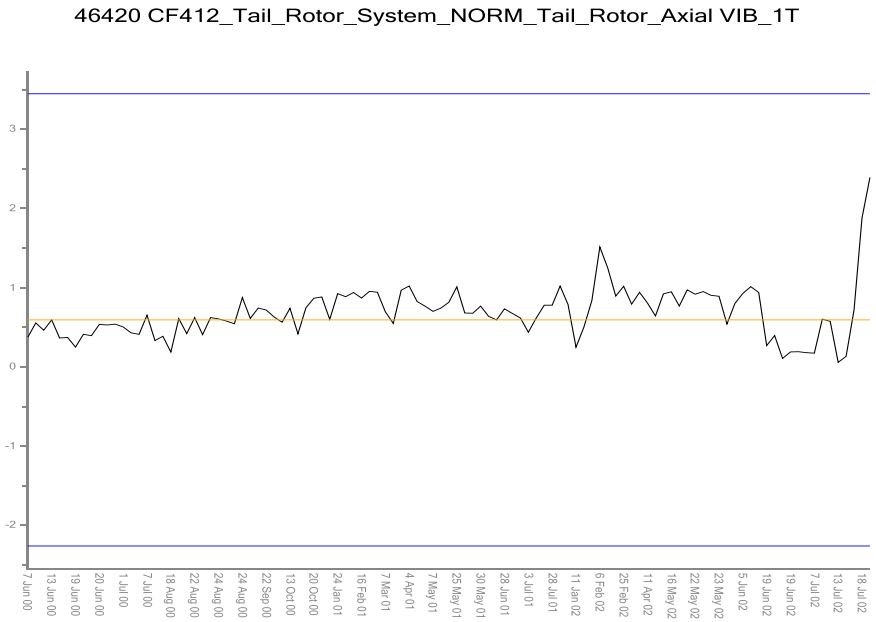

Figure 3-13: CF412 Axial Vib 1T for Aircraft 46420

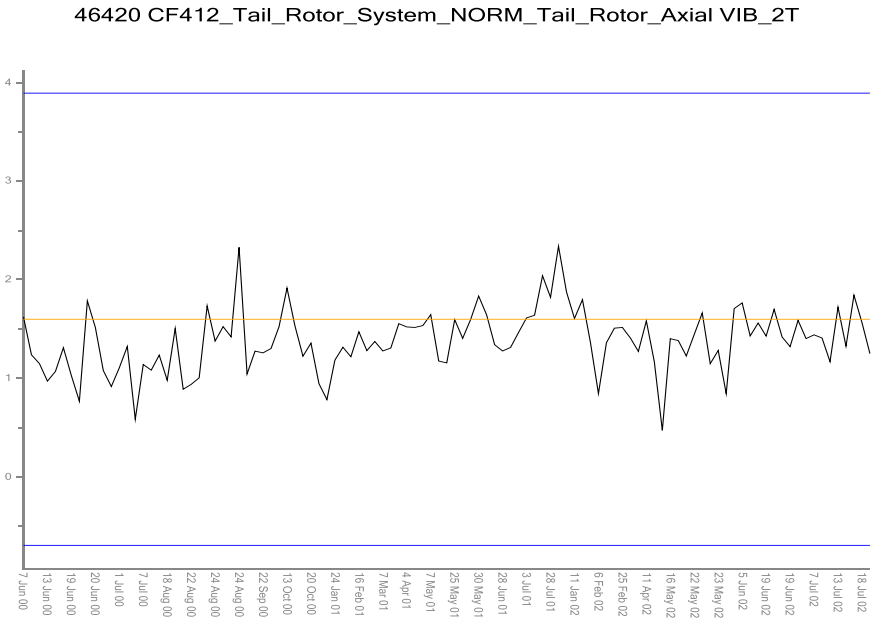

Figure 3-14: CF412 Axial Vib 2T for Aircraft 46420

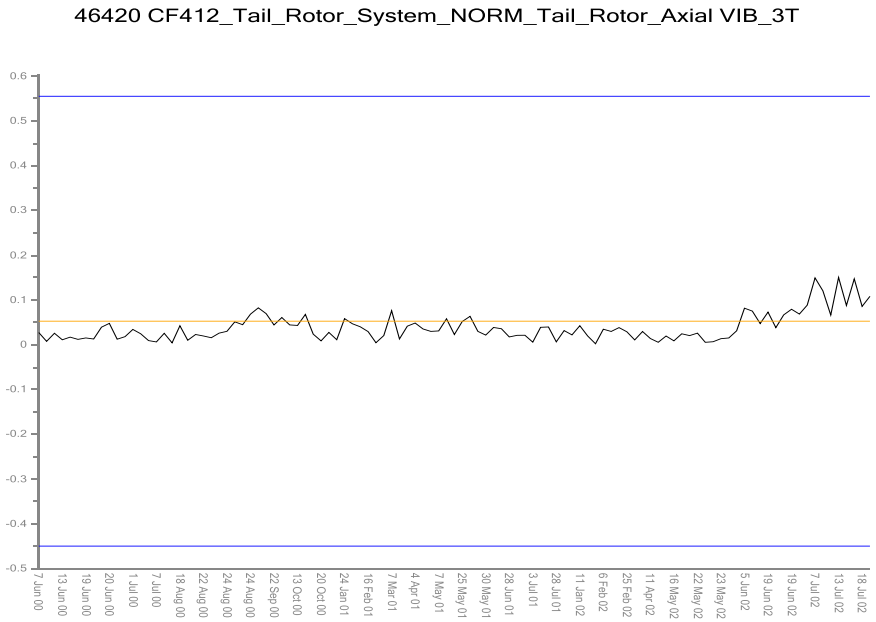

Figure 3-15: CF412 Axial Vib 3T for Aircraft 46420

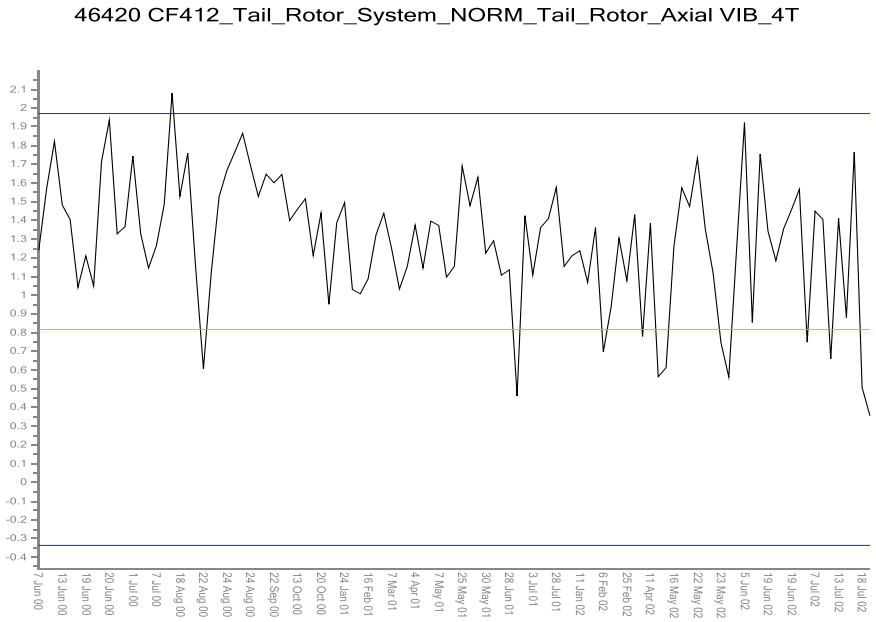

Figure 3-16: CF412 Axial Vib 4T for Aircraft 46420

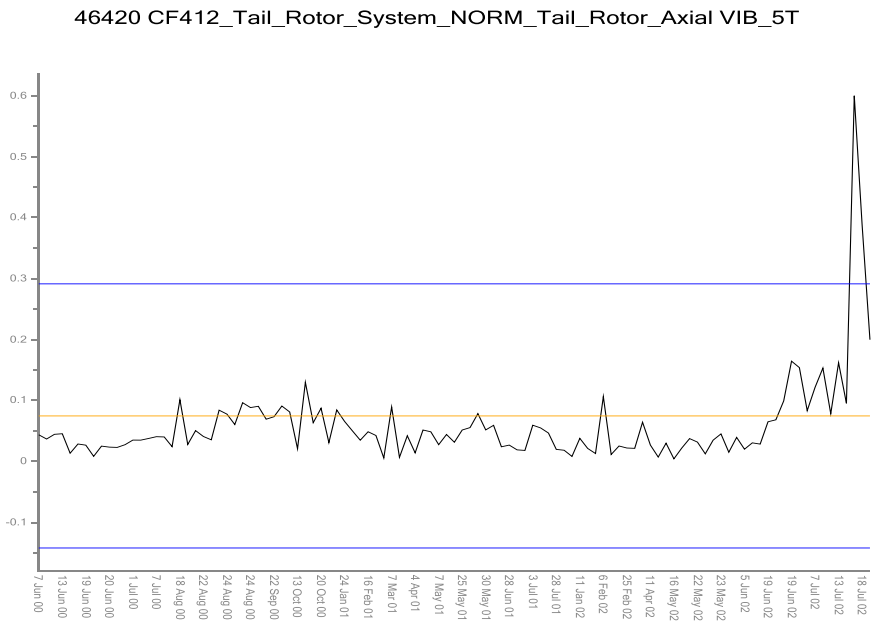

Figure 3-17: CF412 Axial Vib 5T for Aircraft 46420

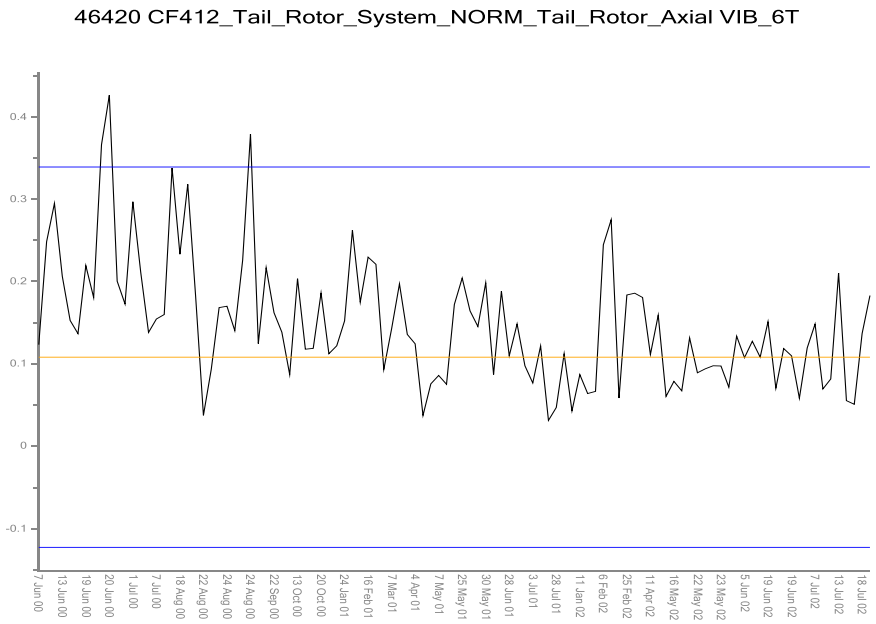

Figure 3-18: CF412 Axial Vib 6T for Aircraft 46420

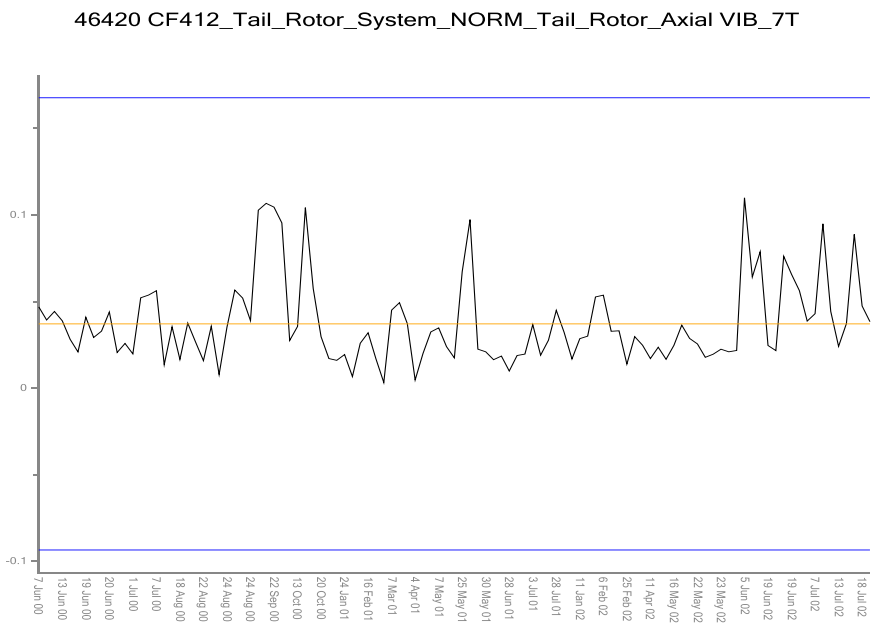

Figure 3-19: CF412 Axial Vib 7T for Aircraft 46420

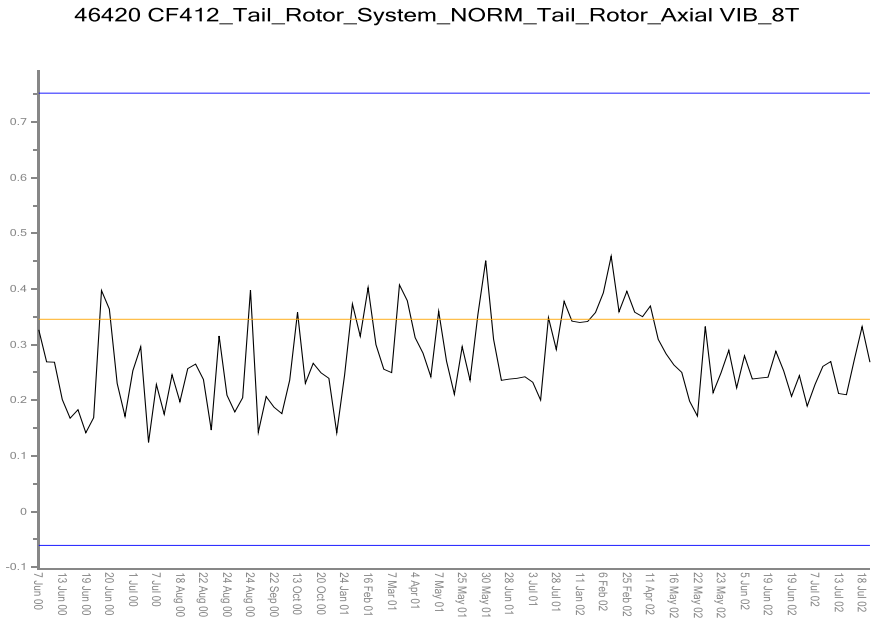

Figure 3-20: CF412 Axial Vib 8T for Aircraft 46420

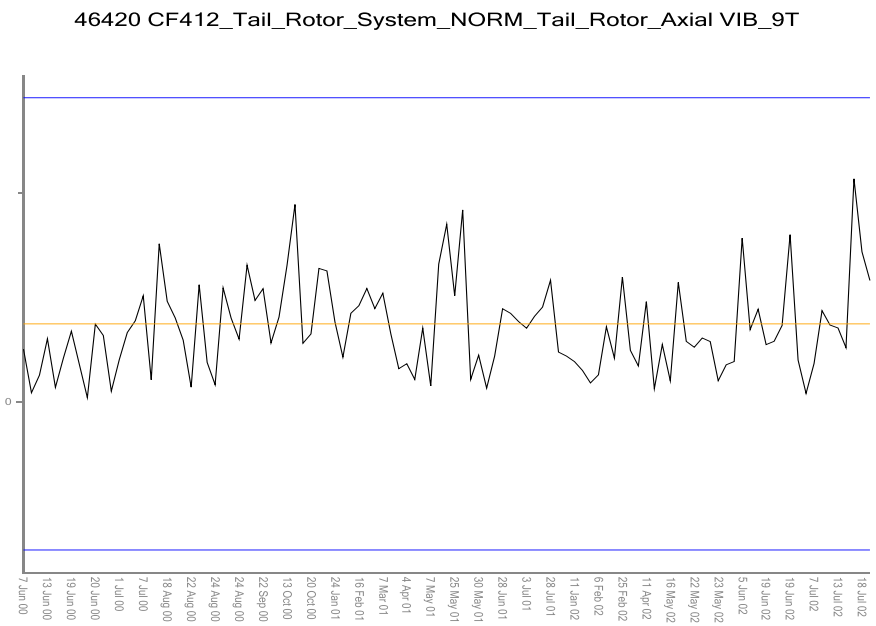

Figure 3-21: CF412 Axial Vib 9T for Aircraft 46420

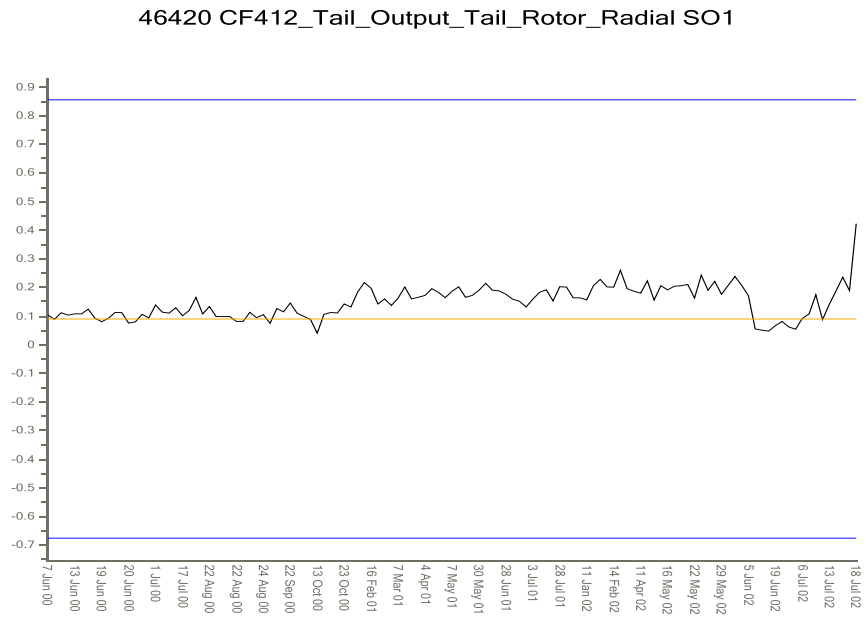

Figure 3-22: CF412 Gearbox SO1 for Aircraft 46420

Five separate single parameter absolute AAD models were built for 1T Radial, 5T Radial, 1T Axial, 5T Axial and SO1 parameters. Two additional models were built using two parameters each: a 1T and 5T Radial model and a 1T and 5T Axial model. The models were built using data from the Cruise phase only; models using MPOG data were not constructed. Similar model behaviour would be expected using the MPOG data because similar trends had been observed, however, the data generally

contained more noise than the Cruise data and it would be anticipated that detecting the anomalies would be more difficult.

The results of the AAD models indicated that they all responded to the anomaly, however, the most anomalous results were generally caused by instrumentation faults in other aircraft. The faults were generally characterised by short duration spikes in the data, which gave the most significant levels of abnormality, i.e. lowest minimum Fitness Scores. For each model, the Fitness Scores were normalised by the mean and standard deviation of the Fitness Score values calculated over all the acquisitions for all the aircraft. The minimum value for each aircraft was extracted and the values ranked in descending order of magnitude. The top 20 ranked orders of significance for the seven anomaly models are given for a selection of the highest ranked aircraft in Table 3-1.

The table identifies the aircraft through their ID numbers, the ID for the accident aircraft is 46420 (all other aircraft have been de-identified). The values for the accident aircraft have been highlighted in the table. The aircraft does appear significant with respect to other aircraft. However as indicated previously, the absolute levels of significance are biased by instrumentation faults in other aircraft so that it can appear statistically small. For example for the 1T Axial model the minimum Fitness Score appeared to be only 0.287 standard deviations below the mean. This is due to the value of the normalisation parameters used. In other words, the standard deviation used to normalise the Fitness Scores appeared much larger than expected due to instrumentation faults and was not representative of the actual data distribution. The results were regenerated after the Fitness Score standard deviation was recalculated to provide a more representative value for the statistic. In this case, a trimmed mean and trimmed standard deviation were calculated for the 1T Axial model. Trimmed statistics are more robust in the presence of outliers. The statistics were calculated by ordering the Fitness Scores for all acquisitions of all the aircraft in ascending order and excluding the top and bottom 2.5% of the data, i.e. the statistics were calculated from 95% of the total number of values. The trimmed statistics were used to normalise the minimum Fitness Scores for all aircraft. This will not affect the rankings calculated previously, so the accident aircraft still appears significant with respect to the other aircraft but it does provide a more realistic assessment of the statistical significance of the minimum Fitness Score: in this case the Fitness Score significance was raised to 11 standard deviations below the mean.

The ranking of Aircraft 46420 appears similar for most of the models. Nevertheless, the aircraft is highest ranked in the 5T Axial model with a rank of 3. The two aircraft having more extreme values than Aircraft 46420 were probably suffering from instrumentation faults. This result is as expected from the previous discussion and indicates the significance of the 5T axial data. It is noted that this was not commented on in the accident report. The 1T Radial model ranks the aircraft lowest in significance with a rank of 13. The average rank over all the models was 9.

Table 3-1: Ranked Orders of Significance for Minimum Fitness Score: Univariate Models

Rank	ID	Axial 1T	ID	Axial 5T	ID	Radial 1T	ID	Radial 5T	ID	SO1	ID	Radial 1&5T	ID	Axial 1&5T
1	AC-1	-32.256	AC-1	-52.292	AC-1	-15.336	AC-1	-46.588	AC-1	-25.538	AC-1	-14.0156	AC-1	-27.8336
2	AC-2	-15.649	AC-5	-9.2866	AC-27	-15.336	AC-27	-6.9552	AC-27	-25.538	AC-5	-14.0156	AC-2	-12.4219
3	AC-3	-4.8964	46420	-4.5238	AC-28	-15.336	AC-29	-6.6576	AC-5	-8.0290	AC-29	-14.0156	AC-5	-6.5270
4	AC-4	-3.7527	AC-4	-3.8349	AC-20	-14.061	AC-31	-6.1634	AC-33	-2.8313	AC-27	-14.0156	AC-4	-3.7121
5	AC-5	-1.9994	AC-3	-3.3383	AC-29	-13.949	AC-20	-5.4401	AC-28	-2.3725	AC-30	-14.0156	AC-3	-3.5639
6	AC-6	-0.8310	AC-20	-1.8749	AC-30	-12.838	AC-5	-3.1846	AC-32	-2.2349	AC-28	-14.0156	AC-7	-1.4104
7	AC-7	-0.8036	AC-19	-1.7064	AC-5	-12.008	AC-30	-2.5585	AC-29	-0.6584	AC-20	-14.0156	46420	-0.6760
8	AC-8	-0.376	AC-21	-1.3660	AC-31	-8.0360	AC-28	-1.5299	46420	-0.4695	AC-31	-7.9948	AC-6	-0.5953
9	46420	-0.2869	AC-15	-1.0583	AC-32	-2.9768	AC-33	-0.9984	AC-3	-0.3466	AC-32	-3.1797	AC-19	-0.3490
10	AC-9	-0.1504	AC-17	-1.0449	AC-33	-0.6149	46420	-0.7038	AC-19	-0.2847	AC-33	-1.0331	AC-20	-0.2886
11	AC-10	-0.1373	AC-10	-1.0229	AC-34	-0.3206	AC-32	-0.4640	AC-22	-0.1773	AC-34	-0.4217	AC-8	-0.2846
12	AC-11	-0.1325	AC-22	-1.0059	AC-19	-0.2919	AC-21	-0.4633	AC-6	-0.1163	46420	-0.3163	AC-17	-0.2260
13	AC-12	-0.1177	AC-7	-0.9617	46420	-0.1714	AC-36	-0.4076	AC-31	-0.088	AC-19	-0.2589	AC-22	-0.2070
14	AC-13	-0.1033	AC-16	-0.9520	AC-3	-0.0905	AC-15	-0.3758	AC-14	-0.0846	AC-3	-0.0891	AC-16	-0.1719
15	AC-14	-0.0955	AC-23	-0.8736	AC-22	-0.0277	AC-19	-0.3383	AC-12	-0.0791	AC-22	-0.063	AC-21	-0.1549
16	AC-15	-0.0776	AC-24	-0.6064	AC-6	-0.0102	AC-16	-0.2649	AC-2	-0.0769	AC-6	-0.0273	AC-15	-0.1246
17	AC-16	-0.0760	AC-6	-0.5856	AC-2	0.0066	AC-17	-0.2573	AC-9	-0.0668	AC-21	0.0018	AC-18	-0.1142
18	AC-17	-0.0560	AC-25	-0.5815	AC-12	0.0177	AC-35	-0.2328	AC-13	-0.0510	AC-2	0.0076	AC-23	-0.1109
19	AC-18	-0.0558	AC-18	-0.5527	AC-14	0.0184	AC-6	-0.1885	AC-37	-0.0392	AC-36	0.0098	AC-12	-0.1105
20	AC-19	-0.0524	AC-26	-0.5153	AC-35	0.0266	AC-22	-0.1686	AC-35	-0.0353	AC-15	0.0100	AC-10	-0.1100

Radial and axial TR acquisitions were merged together using airframe hours. A window of 2 hours was placed on the merging criteria such that data from the radial and axial tables that were more than this period apart would not be joined. Data that did not consist of both a radial and an axial acquisition could not be used for subsequent anomaly model building and were excluded from the merged data set. This resulted in a loss of approximately 5% of the data (134 axial and 288 radial acquisitions), i.e. where individual acquisitions could not be related. However, no data was lost from the accident aircraft. Merging was also performed between the TR axial, TR radial and gearbox SO1 databases. This resulted in the loss of a higher proportion of the data: 937 Axial, 1091 Radial and 695 SO1 acquisitions could not be merged. This equates to approximately 30% of the available data and is due to the differing scheduling and priorities of the rotor and gearbox analyses. However, none was lost from the final portion of accident data.

Anomaly models were built using the merged data. The models included two 2 parameter models, one 4 parameter model and a 5 parameter model. The models were: a 1T axial and 1T radial model (Both 1T), a 5T axial and 5T radial model (Both 5T), 1T axial, 1T radial, 5T axial and 5T radial (Both 1&5T) and a model that also used the gearbox input SO1 together with the four TR harmonics of interest (Both 1&5T & SO1). The models were trained and tested. The Fitness Score results for each model were normalised by the mean and standard deviations of all the Fitness Score values for that model and the minimum Fitness Score value was extracted for each aircraft. The top 20 ranked orders of significance for the four multivariate models are given for a selection of the highest ranked aircraft in Table 3-2. The rankings were similar to the results for the univariate models: the average ranking over the four models was slightly lower at Rank 13. Again, the levels of significance were biased by the presence of instrumentation errors so that the absolute level of significance appeared statistically small. In other words, the standard deviation used to normalise the Fitness Scores appears much larger than expected due to instrumentation faults and was not representative of the actual data distribution. The normalising parameters (mean and standard deviation) were re-calculated using 5% trimmed statistics to provide more representative values for the distribution. The minimum Fitness Scores for all aircraft from the five parameter model were extracted and normalised by the trimmed statistics. As indicated previously, this does not modify the ranking of the aircraft with respect to one another but does give a better representative value for the statistical significance of the results. In this case significance for Aircraft 46420 was raised from 1.238 standard deviations below the mean (see Table 3-2) to 24 standard deviations below the mean. This result simply indicates that the level of anomaly detected is more significant than it initially appears and that the anomaly was identified.

Table 3-2: Ranked Orders of Significance for Minimum Fitness Score: Multivariate Models

Rank	ID	Both 1&5T	ID	Both 1T	ID	Both 5T	ID	Both 1 & 5T & SO1
1	AC-1	-16.075	AC-1	-22.429	AC-1	-36.995	AC-1	-15.580
2	AC-27	-13.480	AC-27	-12.770	AC-20	-6.820	AC-24	-15.580
3	AC-20	-9.386	AC-2	-9.846	AC-31	-6.811	AC-5	-15.580
4	AC-5	-8.672	AC-28	-7.052	AC-29	-5.755	AC-27	-15.580
5	AC-2	-7.998	AC-29	-5.677	AC-27	-5.332	AC-33	-6.952
6	AC-29	-6.853	AC-20	-5.644	AC-5	-3.911	AC-28	-3.883
7	AC-30	-6.552	AC-30	-5.205	AC-30	-2.415	AC-32	-2.657
8	AC-28	-6.299	AC-5	-4.805	AC-28	-1.466	AC-4	-2.104
9	AC-31	-6.003	AC-3	-3.482	AC-33	-0.916	AC-3	-1.544
10	AC-3	-2.980	AC-4	-2.323	AC-4	-0.871	AC-19	-1.492
11	AC-4	-1.675	AC-31	-2.064	AC-3	-0.675	46420	-1.238
12	46420	-1.107	AC-6	-0.548	46420	-0.669	AC-2	-0.844
13	AC-33	-0.741	AC-32	-0.539	AC-36	-0.267	AC-34	-0.740
14	AC-7	-0.663	AC-7	-0.454	AC-19	-0.257	AC-22	-0.255
15	AC-32	-0.524	AC-33	-0.362	AC-7	-0.253	AC-7	-0.167
16	AC-6	-0.481	46420	-0.274	AC-21	-0.235	AC-15	-0.147
17	AC-22	-0.274	AC-34	-0.250	AC-15	-0.231	AC-6	-0.145
18	AC-34	-0.157	AC-19	-0.247	AC-10	-0.227	AC-16	-0.137
19	AC-21	-0.150	AC-8	-0.209	AC-17	-0.202	AC-36	-0.137
20	AC-19	-0.116	AC-10	-0.088	AC-16	-0.184	AC-17	-0.133

A trend detection algorithm has been developed that can identify developing trends while reducing the influence of noise caused by instrumentation faults. If a trend is identified it's severity can be quantified at each acquisition using the difference between the value of the current acquisition and the value at 5 points before when the trend was first identified. This figure was used to ensure that the entire trend period is captured.

The trend algorithm was applied to the Fitness Scores for the four parameter model, Table 3-3. Nine aircraft out of the 51 in the merged database were identified as having trends; Aircraft 46420 was ranked sixth based on severity. The higher ranked aircraft were interrogated and the trends were attributed to instrumentation faults with the exception of Aircraft 46425. This showed anomalies in the 1T, 5T and 9T axial data and in the 1T and 5T radial data. The reason for the anomalies is unknown. The trend algorithm was also applied to the five parameter model and similar results were obtained.

In summary, various univariate and multivariate anomaly models have been built and a trend algorithm has been developed to extract potentially anomalous trends. All the models reacted to the anomaly in the accident aircraft although the most extreme Fitness Scores were generated on aircraft with suspected instrumentation faults.

Fusing multiple TR harmonics in an anomaly model in this case did not give a clearer indication than the univariate models but could provide more robust trend detection based on output Fitness Score values.

Table 3-3: Ranked Trend Detection Results for Model Both 1&5T (no other trends were detected)

ID	Start Index	End Index	Min Fitness Score	Severity
46425	144	149	-800.00	-172.32
AC-5	75	79	-431.62	-47.28
AC-28	12	14	-313.54	-32.94
AC-27	13	31	-670.87	-23.71
AC-31	14	16	5.64	-9.82
46420	100	103	-55.18	-6.90
AC-22	36	43	-13.73	-2.45
AC-8	15	15	-5.70	-2.09
AC-35	41	51	-1.29	-0.93

3.2.2 Super Puma, 9M-STT

The second accident case was for a EuroHUMS™ equipped Super Puma with a broken arm on the pitch change spider for the five bladed TR. The HUMS database available for the analysis contained data for 25 aircraft. The data again included TGB outputs SO1 and SO2 and 1T to 9T axial and radial vibration in cruise and at MPOG. There were approximately 13,000 TGB acquisitions, 24,000 axial vibration acquisitions and 45,000 radial acquisitions.

The signal averages from the TR axial vibration acquisitions in cruise showed a 5/rev waveform before the fault developed. However, as one arm of the pitch change spider failed, one of the 5 peaks in the waveform disappeared, Figure 3-23. In the frequency domain, this appeared as 1/rev modulation of the 5/rev blade pass frequency signal. The signal traces for the radial vibration of Aircraft 9M-STT are given in Figure 3-24 through Figure 3-32. The corresponding signal traces for the axial vibration are given in Figure 3-33 through Figure 3-41. The signal traces for the TGB SO1 and SO2 parameters are given in Figure 3-42 and Figure 3-43. The clearest failure related trends were in 1T, 4T, 6T, 9T axial and radial vibration. In this case, the frequencies could be predicted from a knowledge of the failure mode.

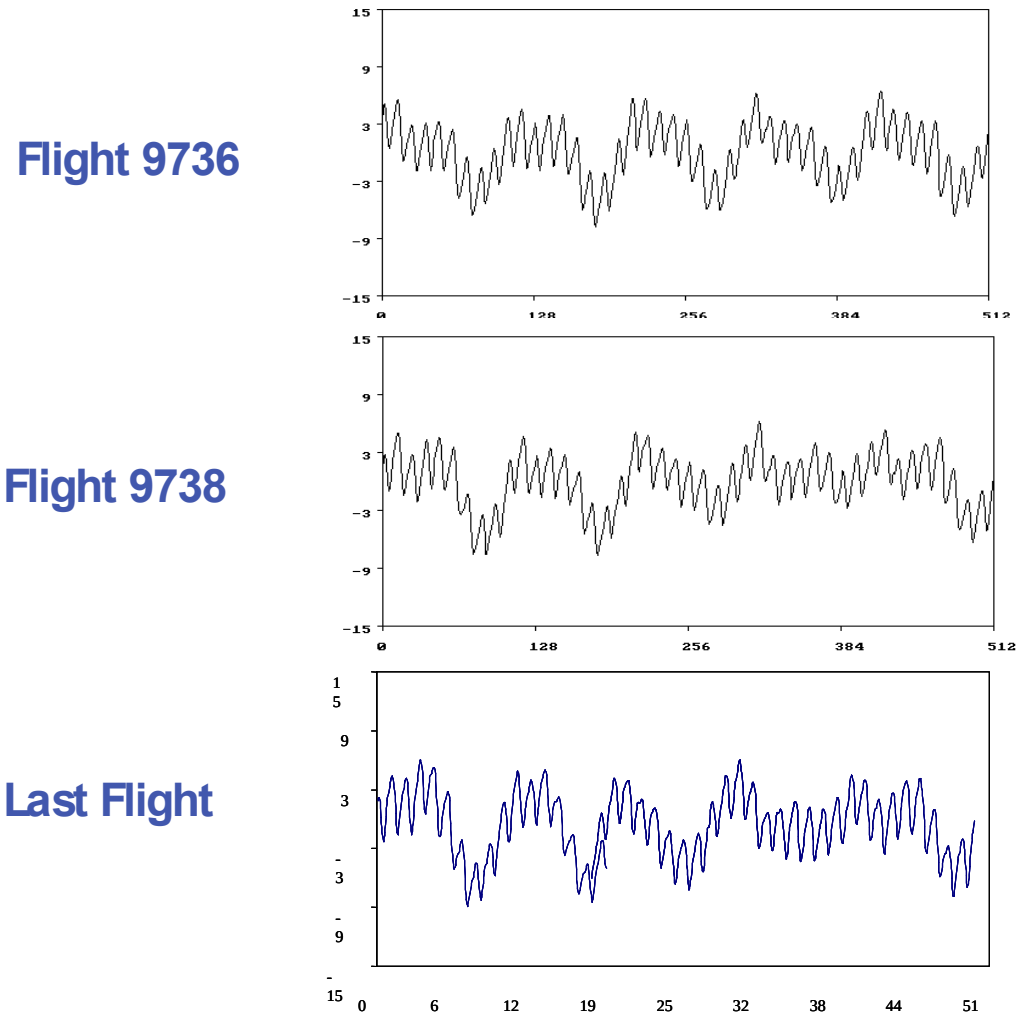

Figure 3-23: Aircraft 9M-STT: Tail Rotor NORM Axial Signal Averages

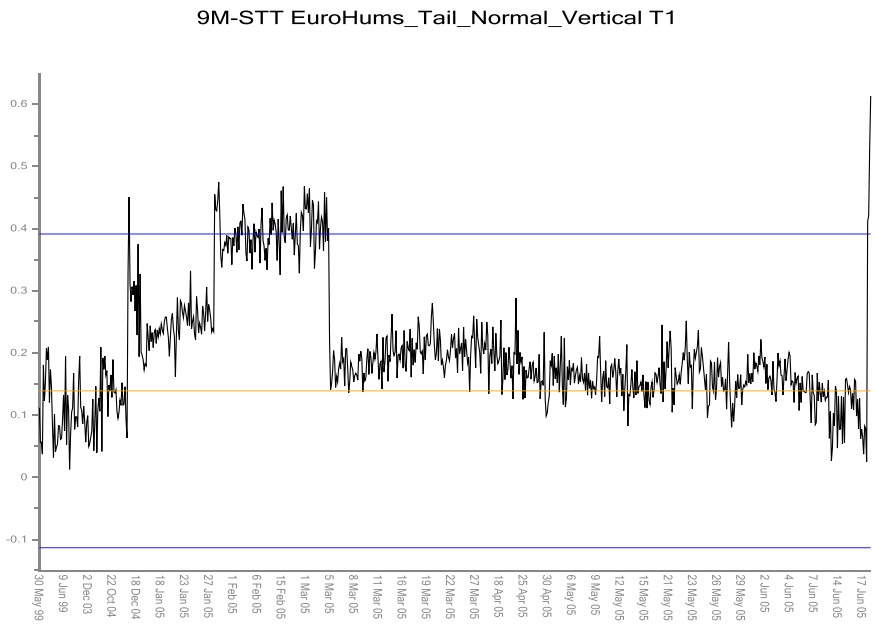

Figure 3-24: EuroHUMS™ Radial Vib 1T for Aircraft 9M-STT

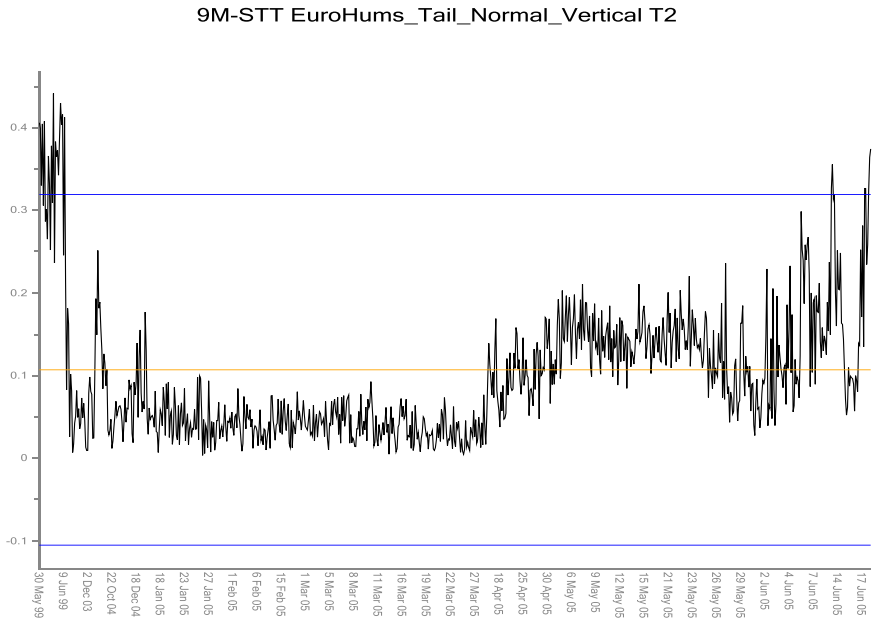

Figure 3-25: EuroHUMS™ Radial Vib 2T for Aircraft 9M-STT

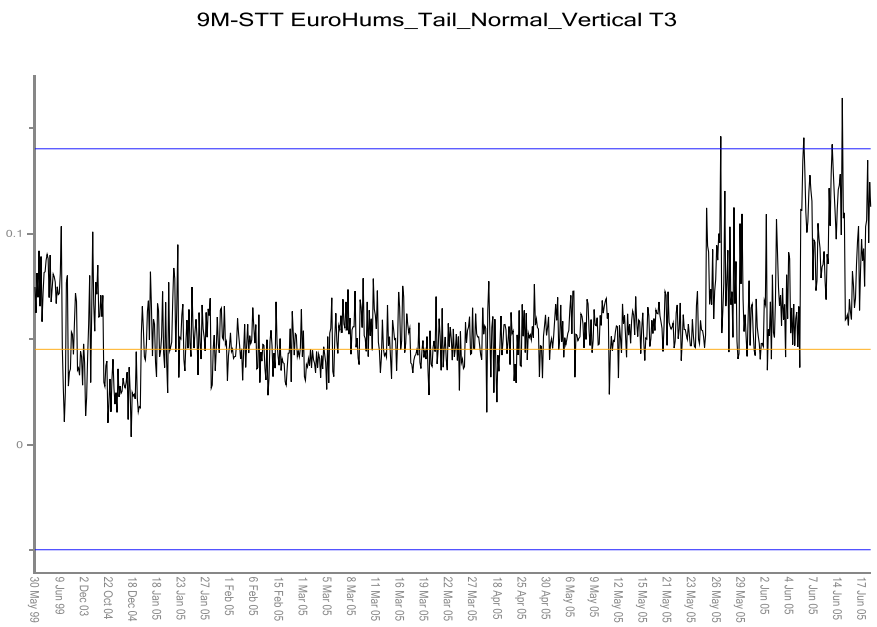

Figure 3-26: EuroHUMS™ Radial Vib 3T for Aircraft 9M-STT

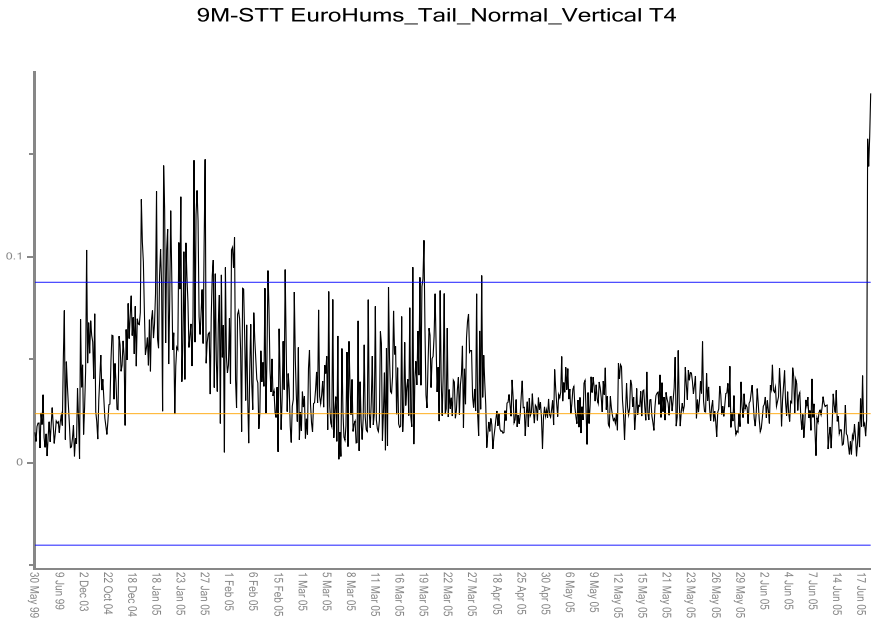

Figure 3-27: EuroHUMS™ Radial Vib 4T for Aircraft 9M-STT

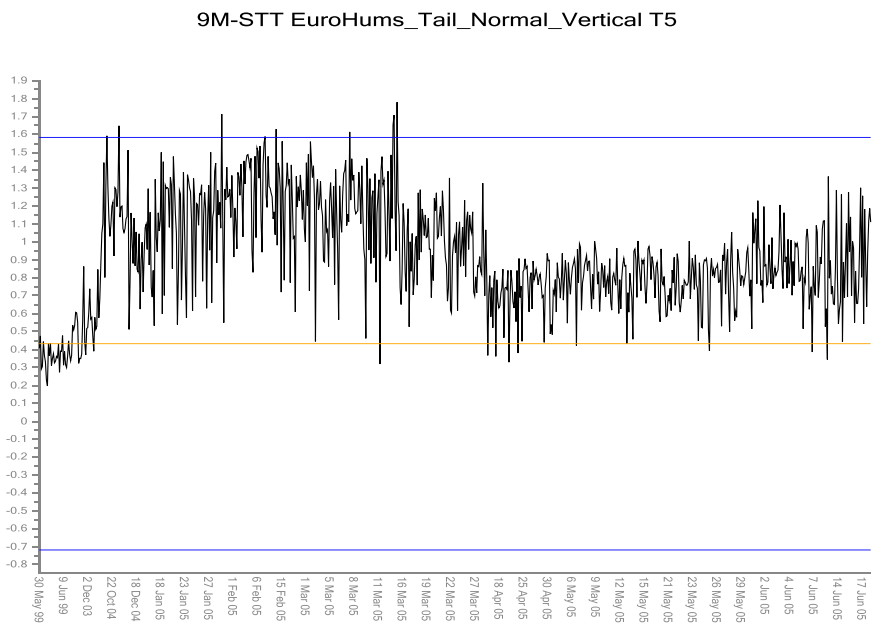

Figure 3-28: EuroHUMS™ Radial Vib 5T for Aircraft 9M-STT

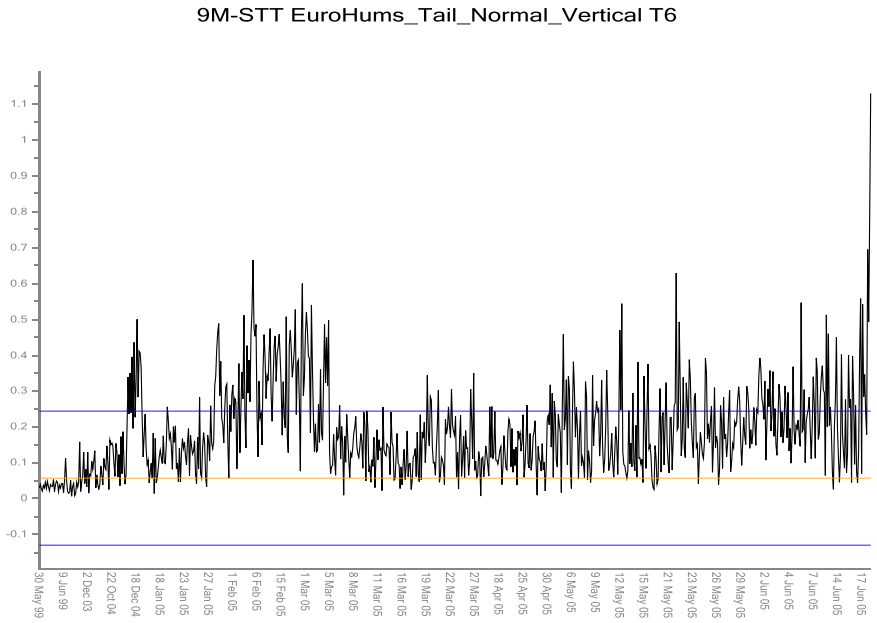

Figure 3-29: EuroHUMS™ Radial Vib 6T for Aircraft 9M-STT

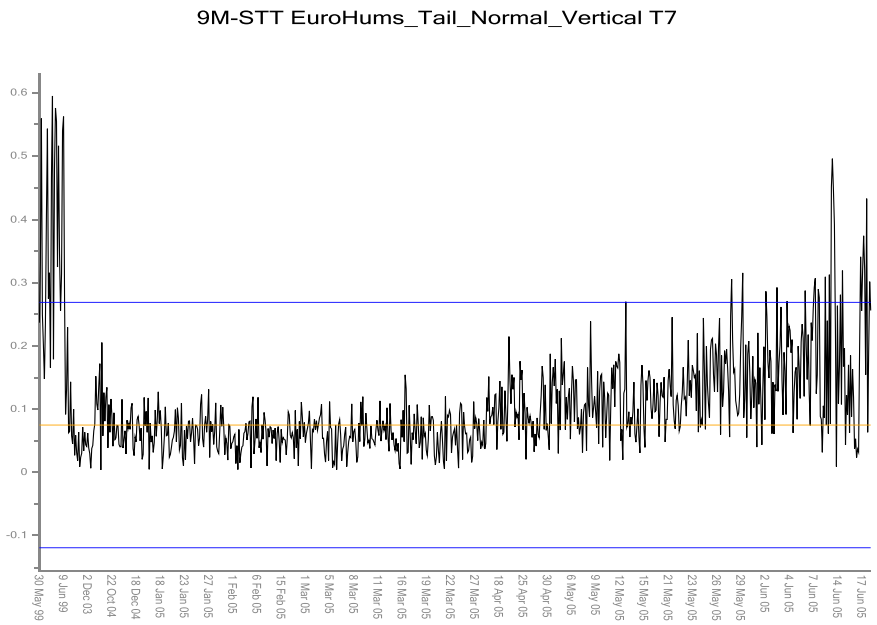

Figure 3-30: EuroHUMS™ Radial Vib 7T for Aircraft 9M-STT

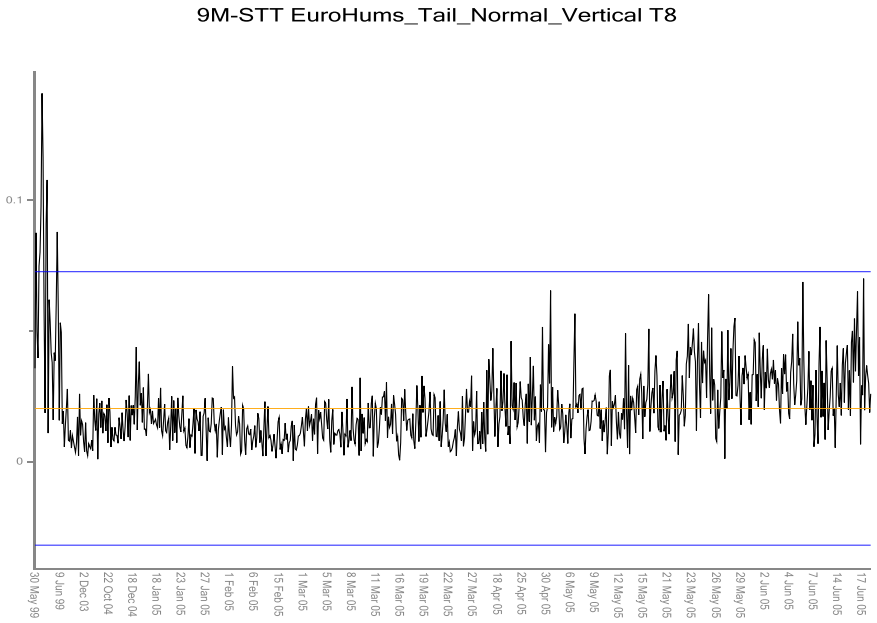

Figure 3-31: EuroHUMS™ Radial Vib 8T for Aircraft 9M-STT

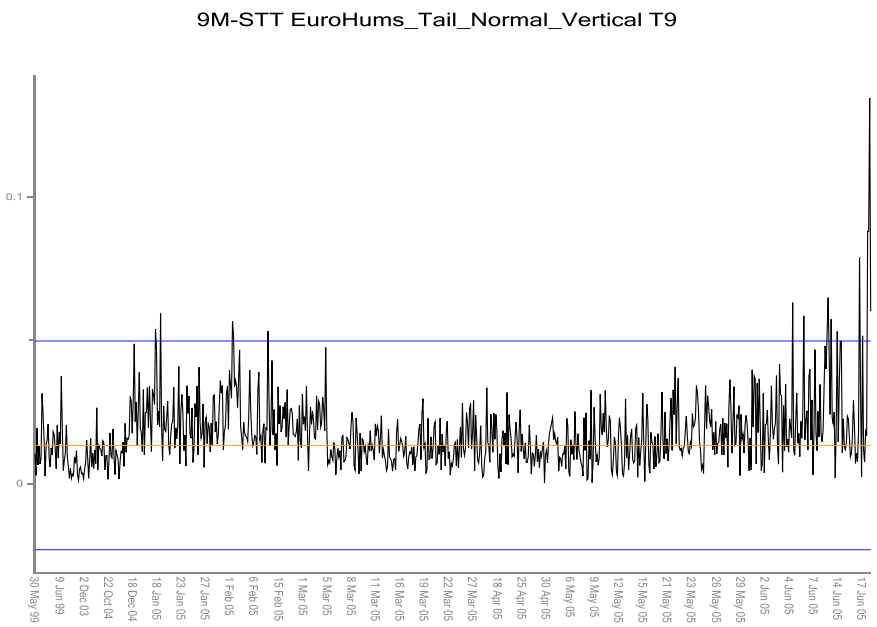

Figure 3-32: EuroHUMS™ Radial Vib 9T for Aircraft 9M-STT

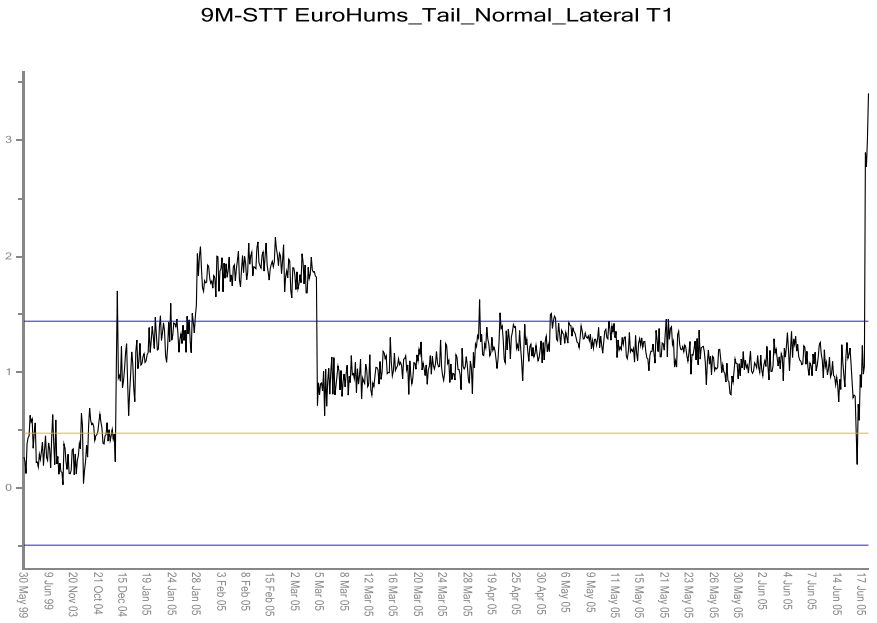

Figure 3-33: EuroHUMS™ Axial Vib 1T for Aircraft 9M-STT

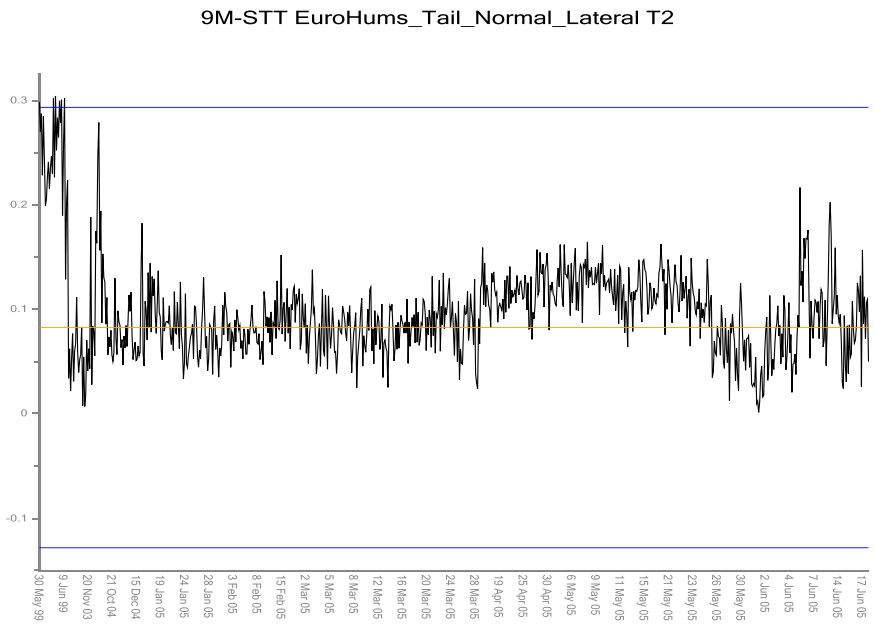

Figure 3-34: EuroHUMS™ Axial Vib 2T for Aircraft 9M-STT

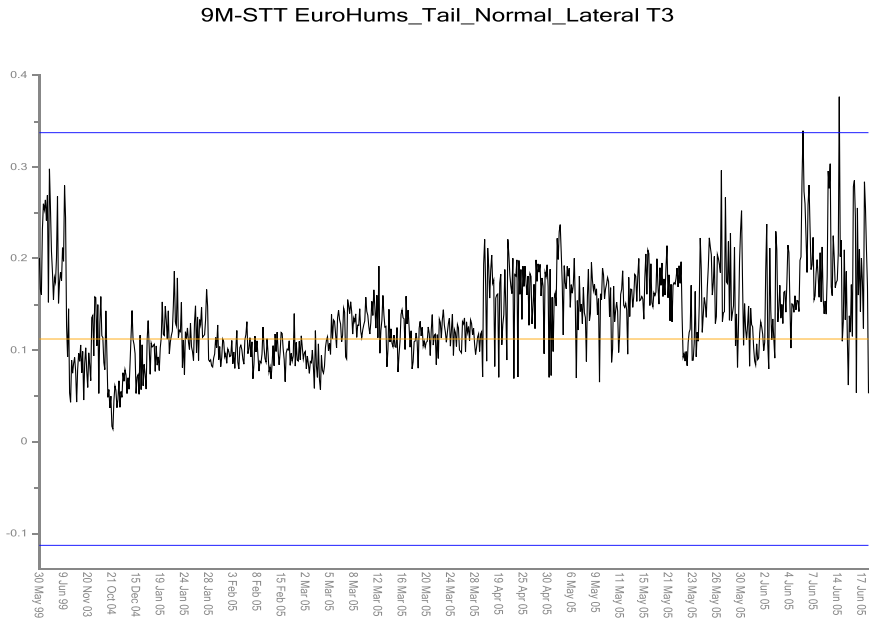

Figure 3-35: EuroHUMS™ Axial Vib 3T for Aircraft 9M-STT

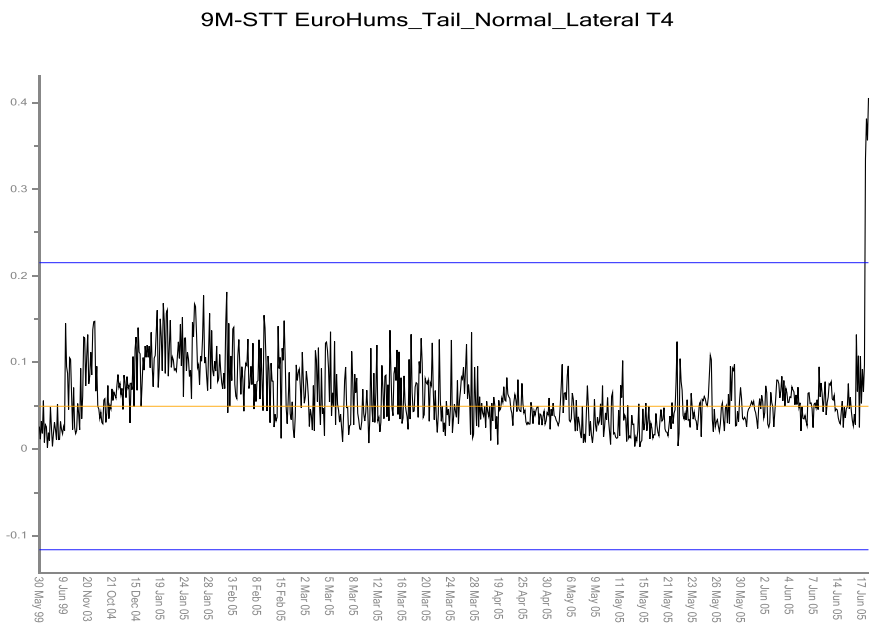

Figure 3-36: EuroHUMS™ Axial Vib 4T for Aircraft 9M-STT

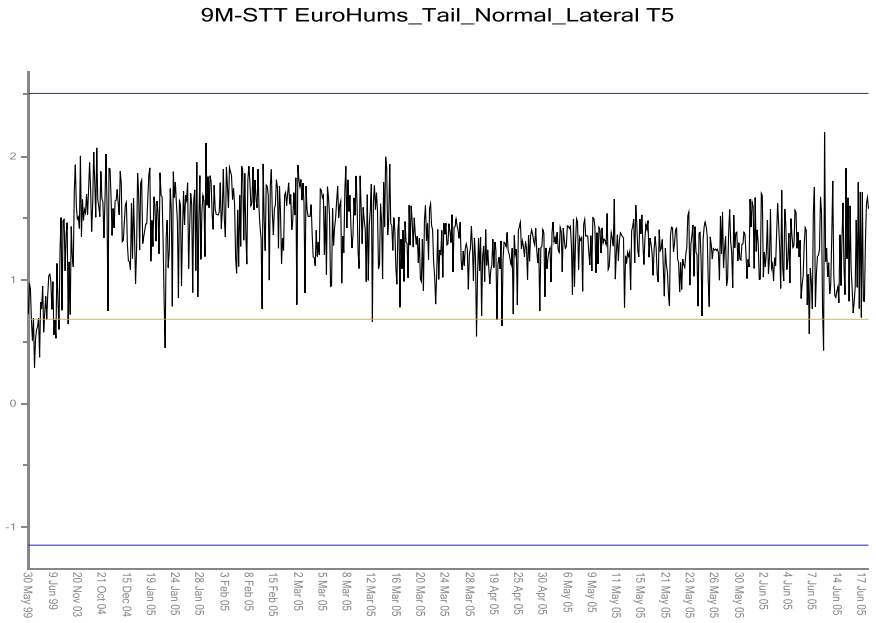

Figure 3-37: EuroHUMS™ Axial Vib 5T for Aircraft 9M-STT

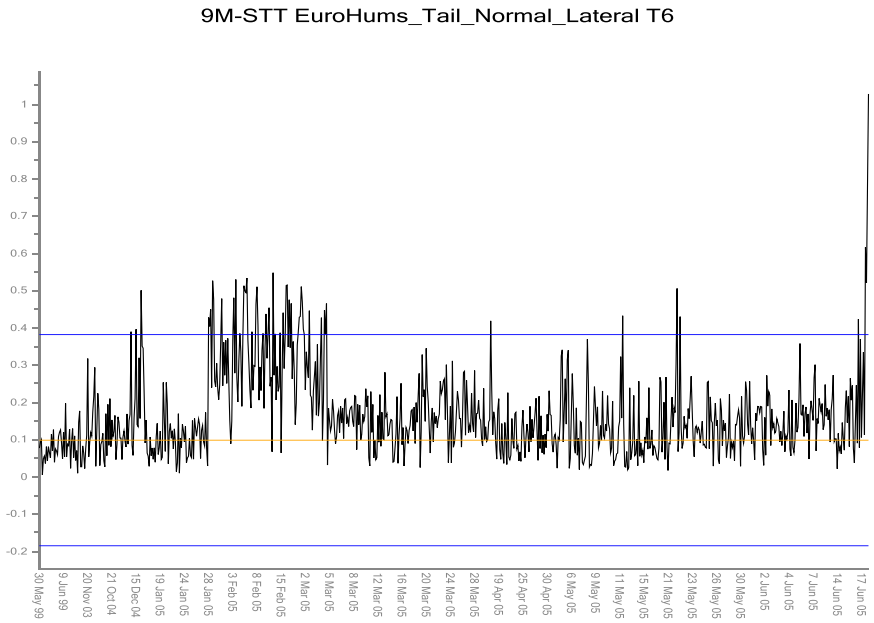

Figure 3-38: EuroHUMS™ Axial Vib 6T for Aircraft 9M-STT

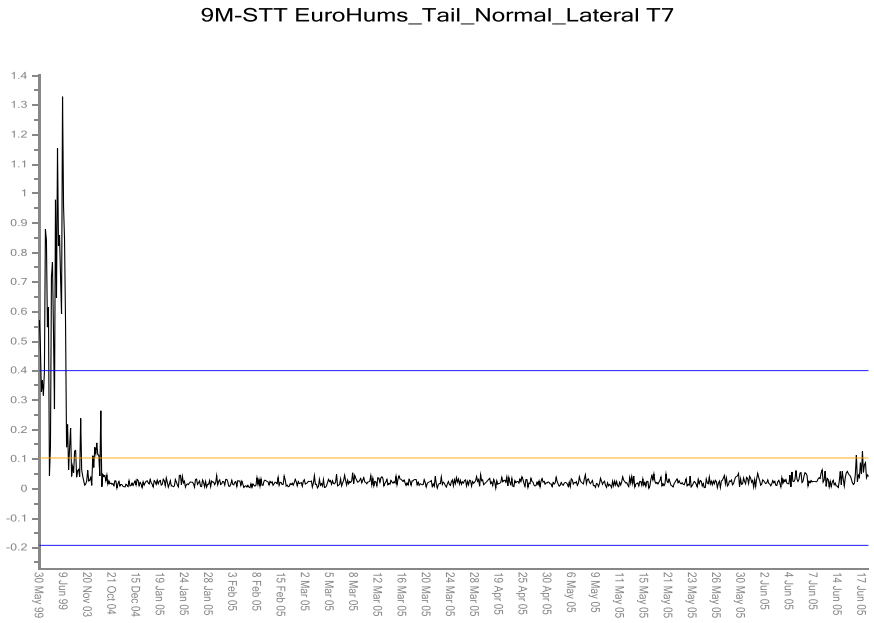

Figure 3-39: EuroHUMS™ Axial Vib 7T for Aircraft 9M-STT

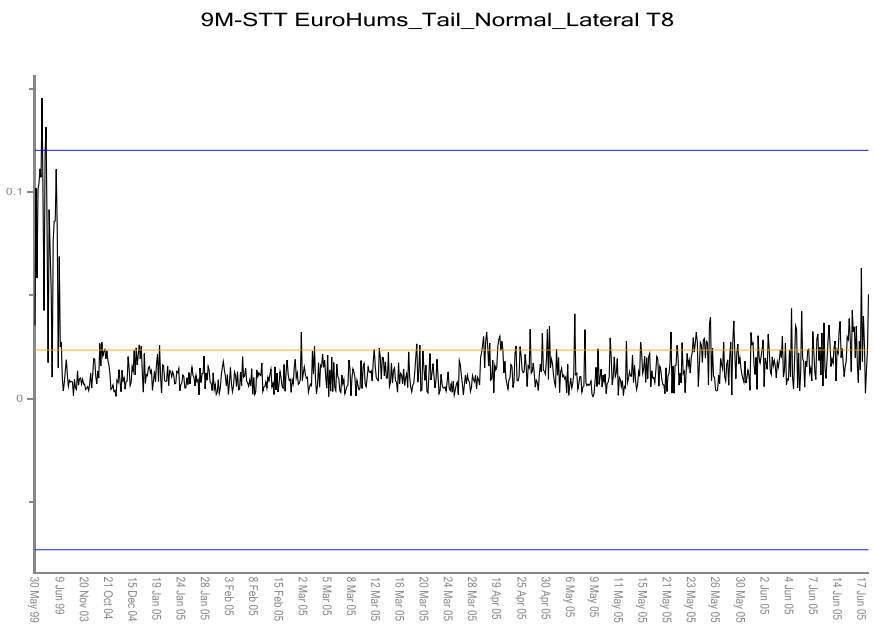

Figure 3-40: EuroHUMS™ Axial Vib 8T for Aircraft 9M-STT

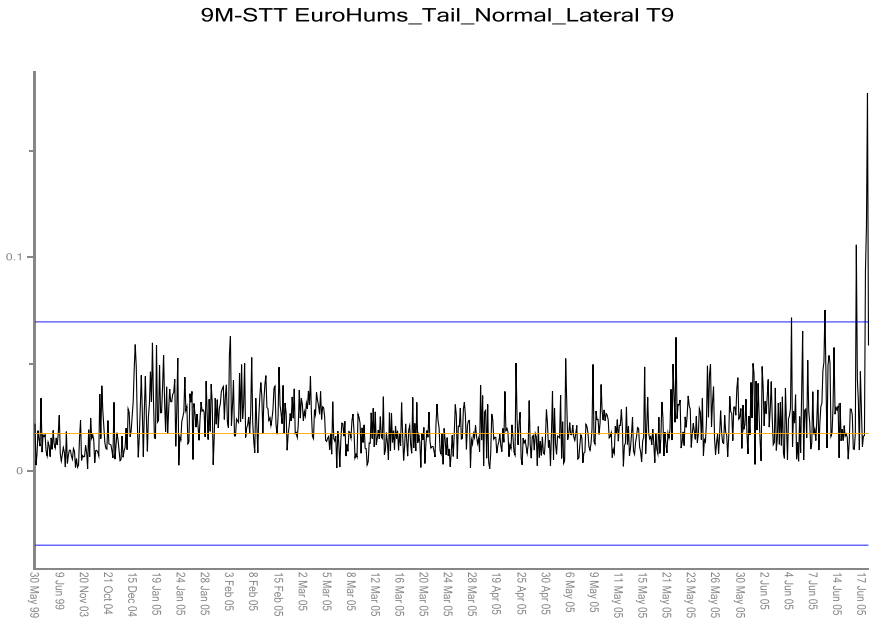

Figure 3-41: EuroHUMS™ Axial Vib 9T for Aircraft 9M-STT

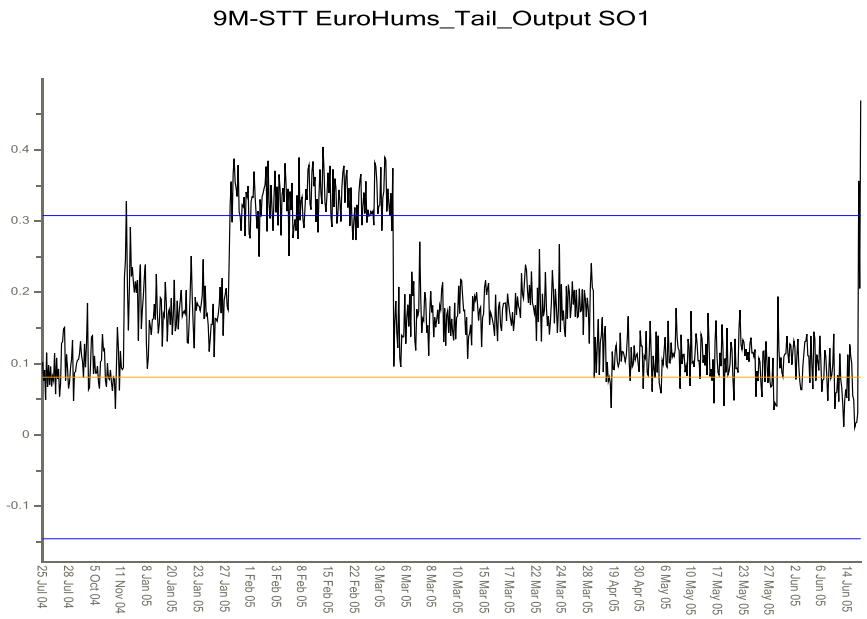

Figure 3-42: EuroHUMS™ Gearbox SO1 for Aircraft 9M-STT

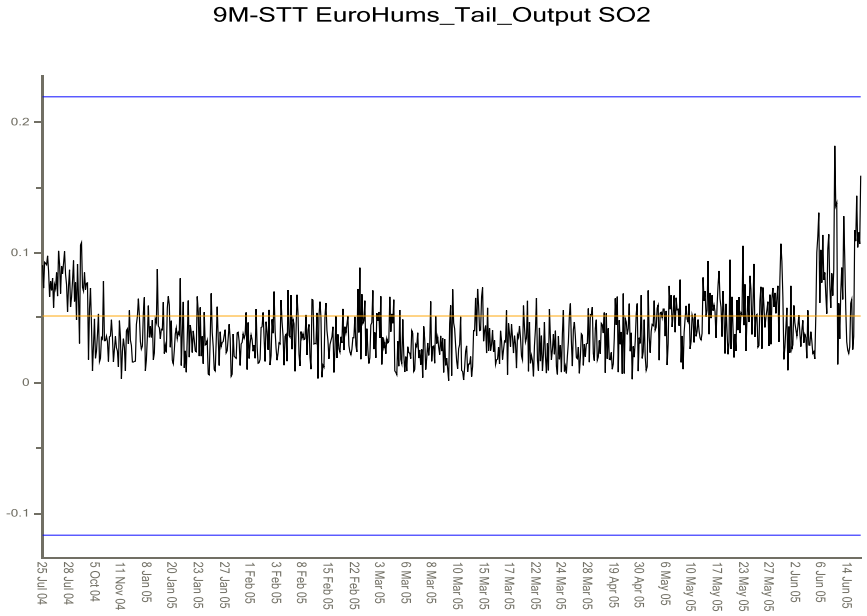

Figure 3-43: EuroHUMS™ Gearbox SO2 for Aircraft 9M-STT

Univariate AAD models were built for 1T, 4T and 6T radial as well as 1T, 4T and 6T axial vibration. Multivariate models were built using combinations of either the axial or radial vibration data. The models were built using data from the Cruise phase only. For each model, the Fitness Scores were normalised by the mean and standard deviation of the Fitness Score values calculated over all the acquisitions for all the aircraft. The minimum value for each aircraft was extracted and the values ranked in descending order of magnitude. The top 20 ranked orders of significance for the axial vibration models are given for all the aircraft in Table 3-4. The results for the corresponding radial vibration models are given in Table 3-5.

All models clearly responded to the accident data with significant Fitness Scores. The lowest ranked axial model was Axial 4T with a rank of 3. Models Axial 1T and Axial 1+6T were ranked 1. The remaining axial models were all ranked 2. In comparison the only radial model to be ranked 1 was Radial 6T. The lowest ranked radial model with a rank of 5 was Radial 1T. In general the axial models performed better at identifying the fault; the average rank for the axial models was 1.85 whilst the average rank for the radial models was 2.85. The multivariate models also performed better than the univariate models; the average rank for the univariate axial models was 2 whilst for the multivariate models the rank was 1.75. For the univariate radial models the average rank was 3.33 whilst for the multivariate models the average rank was 2.5. The highest ranked anomaly in most models is believed to be due to an instrumentation problem.

Radial and axial TR acquisitions were merged together, resulting in a loss of approximately 14% of the data, however no data related to the accident was lost. TR data was also merged with that from the TGB output. This resulted in a high proportion of the data being lost (approximately 60%). Because of the large amount of data lost by this merge, no anomaly models using TGB data were built. In this case, data fusion would need to be performed using diagnostic reasoning logic.

Three merged models were built; a four parameter model using axial 4T, axial 6T, radial 4T and radial 6T data (Both 46T), an eight parameter model using axial and radial 1T, 4T, 6T and 9T data (Both 1469T) and finally a two parameter model using axial 1T and radial 6T data. The normalised ranked results are shown in Table 3-6. The ranked results indicate that the two parameter model gave the greatest significance to the accident aircraft with a rank of 1 and a normalised minimum fitness score of 76.866 standard deviations below the mean; the next ranked value was 12 standard deviations below the mean. However, this result is somewhat artificial as the model has been somewhat contrived to illustrate the significance of the anomaly. The significance of the anomalous aircraft has been emphasised by using only the specific inputs which showed up as most significant in this particular case and would not be expected to be true generally. Nevertheless, the four parameter model gave a rank of 2 to the anomalous aircraft with a minimum normalised fitness score of 60 standard deviations below the mean. The eight parameter model ranked the accident aircraft 3 with a normalised fitness score of 38 standard deviations below the mean. However, with a PA threshold of 0.98 and a 2 out of 3 M out of N (MooN) alerting criteria (i.e. 2 out of 3 continuous points must be over the PA threshold to raise an alert), Aircraft 9M-STT raised an alert over the final 3 acquisitions. Only one other aircraft raised an alert with this threshold.

The trend detection algorithm was applied to the model outputs and identified clear trends on the accident aircraft, with the highest trend severities in all cases, with the exception of the Radial 1T and Radial 4T models; Aircraft 9M-STT was ranked 3 for the Radial 1T model and 2 for the Radial 4T model. The model with the highest severity was the eight parameter model Both 1469T. The trend algorithm results for

this model are shown in Table 3-7. The table shows all trends that were detected, i.e. trends were only detected in six out of the available 25 aircraft. It can be noted, however, the trend was only detected on the last two data points. An alternative trend detection approach was investigated, although it was difficult to improve detection time without identifying false trends due to data noise or spikes. To eliminate the effects of noise, it may be possible to fuse cruise model outputs with a MPOG model (where no response is observed in the accident case) to discriminate possible fault types.

Table 3-4: Ranked Orders of Significance for Minimum Fitness Score: EuroHUMS™ Axial Vibration Models

ID	Axial 1T	ID	Axial 4T	ID	Axial 6T	ID	Axial 14T	ID	Axial 16T	ID	Axial 46T	ID	Axial 146T
9M-STT	-32.615	AC-4	-99.822	AC-4	-15.558	AC-4	-48.679	9M-STT	-62.939	AC-4	-121.375	AC-4	-110.968
AC-1	-13.235	AC-17	-52.884	9M-STT	-14.535	9M-STT	-40.989	AC-4	-13.987	9M-STT	-44.959	9M-STT	-48.617
AC-2	-11.924	9M-STT	-28.808	AC-10	-10.530	AC-17	-24.488	AC-2	-10.572	AC-17	-30.336	AC-17	-25.535
AC-3	-8.346	AC-1	-13.880	AC-14	-10.030	AC-1	-17.212	AC-1	-8.650	AC-1	-9.507	AC-1	-9.752
AC-4	-7.473	AC-10	-6.673	AC-8	-7.197	AC-2	-8.587	AC-10	-7.573	AC-10	-7.697	AC-2	-7.091
AC-5	-5.791	AC-8	-6.427	AC-11	-6.611	AC-3	-6.018	AC-8	-6.622	AC-14	-6.167	AC-8	-6.538
AC-6	-4.679	AC-7	-5.754	AC-18	-5.359	AC-5	-5.404	AC-14	-6.298	AC-8	-6.111	AC-10	-6.259
AC-7	-3.838	AC-5	-5.663	AC-6	-4.898	AC-10	-3.349	AC-3	-5.948	AC-5	-5.001	AC-5	-5.739
AC-8	-3.562	AC-3	-4.790	AC-2	-4.600	AC-6	-3.109	AC-7	-5.177	AC-7	-4.414	AC-11	-4.862
AC-9	-2.786	AC-14	-4.564	AC-15	-4.049	AC-7	-2.971	AC-5	-5.134	AC-11	-4.169	AC-14	-4.474
AC-10	-2.669	AC-9	-3.848	AC-7	-3.974	AC-18	-2.904	AC-11	-4.975	AC-18	-4.062	AC-3	-4.207
AC-11	-2.653	AC-12	-3.287	AC-13	-3.797	AC-16	-2.846	AC-15	-4.441	AC-6	-3.789	AC-7	-3.637
AC-12	-2.386	AC-15	-3.206	AC-22	-3.775	AC-8	-2.654	AC-6	-3.876	AC-15	-3.645	AC-18	-3.443
AC-13	-2.356	AC-13	-2.167	AC-5	-3.465	AC-14	-2.439	AC-18	-3.084	AC-2	-3.490	AC-6	-3.014
AC-14	-2.319	AC-11	-2.009	AC-20	-3.062	AC-9	-2.370	AC-13	-2.867	AC-20	-3.067	AC-9	-2.949
AC-15	-2.293	AC-20	-1.904	AC-1	-2.520	AC-11	-2.085	AC-20	-2.739	AC-9	-2.775	AC-15	-2.567
AC-16	-2.216	AC-21	-1.546	AC-3	-1.670	AC-21	-2.050	AC-9	-2.595	AC-3	-2.460	AC-20	-2.351
AC-17	-2.166	AC-19	-1.506	AC-23	-1.643	AC-15	-1.937	AC-17	-2.244	AC-13	-2.429	AC-16	-2.083
AC-18	-2.154	AC-2	-1.486	AC-17	-1.634	AC-13	-1.639	AC-22	-2.175	AC-22	-1.977	AC-13	-2.050
AC-19	-2.094	AC-18	-1.291	AC-12	-1.591	AC-12	-1.606	AC-12	-1.839	AC-23	-1.799	AC-22	-1.770

Table 3-5: Ranked Orders of Significance for Minimum Fitness Score: EuroHUMS™ Radial Vibration Models

ID	Radial 1T	ID	Radial 4T	ID	Radial 6T	ID	Radial 14T	ID	Radial 16T	ID	Radial 46T	ID	Radial 146T
AC-24	-292.584	AC-17	-77.166	9M-STT	-111.481	AC-24	-387.718	AC-24	-289.432	AC-4	-70.043	AC-24	-267.003
AC-2	-14.407	AC-4	-74.900	AC-8	-25.200	AC-17	-44.134	9M-STT	-113.319	9M-STT	-52.477	9M-STT	-50.223
AC-12	-12.005	AC-1	-35.230	AC-14	-20.236	AC-4	-37.069	AC-8	-20.472	AC-17	-43.490	AC-17	-28.297
AC-4	-11.777	9M-STT	-28.933	AC-10	-18.351	9M-STT	-21.023	AC-4	-17.927	AC-1	-29.573	AC-4	-15.760
9M-STT	-10.114	AC-24	-8.274	AC-4	-17.528	AC-1	-15.271	AC-10	-16.517	AC-8	-11.003	AC-8	-13.415
AC-20	-6.846	AC-5	-8.222	AC-20	-17.305	AC-2	-12.819	AC-14	-15.589	AC-10	-7.229	AC-2	-12.263
AC-1	-6.538	AC-7	-5.704	AC-2	-11.858	AC-12	-10.410	AC-20	-13.261	AC-5	-6.772	AC-1	-9.805
AC-17	-6.442	AC-10	-5.568	AC-11	-9.723	AC-5	-4.989	AC-2	-10.953	AC-14	-5.686	AC-12	-8.884
AC-5	-6.226	AC-14	-4.712	AC-18	-5.541	AC-20	-4.964	AC-12	-8.322	AC-20	-5.036	AC-10	-8.097
AC-9	-5.867	AC-8	-4.616	AC-22	-4.023	AC-9	-4.279	AC-11	-7.092	AC-7	-4.910	AC-14	-6.869
AC-23	-4.906	AC-6	-3.882	AC-5	-3.917	AC-8	-3.928	AC-5	-6.407	AC-24	-4.471	AC-20	-6.361
AC-15	-4.765	AC-2	-3.480	AC-15	-3.606	AC-7	-3.880	AC-1	-4.911	AC-2	-4.200	AC-5	-4.646
AC-7	-4.653	AC-9	-3.104	AC-6	-3.390	AC-23	-3.847	AC-13	-4.732	AC-11	-3.640	AC-11	-4.177
AC-13	-4.593	AC-3	-2.825	AC-13	-3.193	AC-10	-3.629	AC-15	-4.633	AC-18	-3.194	AC-15	-3.578
AC-8	-4.387	AC-13	-2.533	AC-7	-2.533	AC-15	-3.604	AC-17	-4.261	AC-6	-2.959	AC-16	-3.405
AC-6	-4.001	AC-12	-2.425	AC-19	-1.946	AC-13	-3.588	AC-6	-4.112	AC-19	-2.925	AC-13	-3.309
AC-14	-3.695	AC-19	-2.109	AC-17	-1.911	AC-6	-3.583	AC-18	-3.750	AC-15	-2.577	AC-18	-3.300
AC-16	-2.967	AC-16	-2.052	AC-1	-1.808	AC-14	-3.486	AC-7	-3.585	AC-9	-2.550	AC-9	-3.181
AC-18	-2.838	AC-21	-1.694	AC-3	-1.183	AC-16	-2.889	AC-9	-3.584	AC-13	-2.109	AC-7	-3.134
AC-21	-2.572	AC-20	-1.603	AC-24	-1.134	AC-3	-2.219	AC-23	-2.860	AC-22	-1.993	AC-19	-2.389

Table 3-6: Ranked Orders of Significance for Minimum Fitness Score: EuroHUMS™ Combined Axial and Radial Vibration Models

ID	Both 46T	ID	Both 1469T	ID	Axial 1T + Radial 6T
AC-4	-82.392	AC-24	-178.248	9M-STT	-76.866
9M-STT	-60.596	AC-4	-62.526	AC-8	-12.134
AC-17	-39.875	9M-STT	-38.186	AC-4	-9.424
AC-8	-11.114	AC-17	-22.695	AC-2	-8.917
AC-1	-10.532	AC-1	-13.332	AC-1	-8.199
AC-10	-8.388	AC-6	-7.776	AC-14	-8.156
AC-14	-7.785	AC-8	-7.425	AC-10	-7.667
AC-7	-6.623	AC-14	-6.547	AC-20	-7.196
AC-24	-5.982	AC-10	-6.320	AC-5	-6.338
AC-5	-5.405	AC-12	-5.806	AC-11	-4.250
AC-20	-5.375	AC-2	-5.700	AC-3	-3.980
AC-11	-5.300	AC-9	-4.950	AC-7	-3.477
AC-15	-4.599	AC-7	-3.906	AC-15	-3.365
AC-2	-3.687	AC-11	-3.528	AC-6	-3.326
AC-6	-3.542	AC-20	-3.388	AC-18	-3.317
AC-18	-3.233	AC-15	-3.210	AC-17	-2.331
AC-19	-2.583	AC-5	-3.056	AC-22	-2.311
AC-23	-2.124	AC-3	-2.994	AC-13	-2.075
AC-13	-2.008	AC-18	-2.970	AC-9	-2.071
AC-12	-1.896	AC-13	-2.779	AC-16	-1.788

Table 3-7: Ranked Trend Detection Results for Model Both 1469T (no other trends were detected)

ID	Start Index	End Index	Min Fitness Score	Severity
9M-STT	701	702	-158.233	-29.509
AC-4	471	567	-269.760	-11.860
AC-17	647	832	-87.254	-7.116
AC-2	329	332	-9.383	-5.886
AC-8	1199	1245	-13.719	-4.110
AC-1	346	767	-22.629	-4.019

3.2.3 Super Puma, G-PUMH

The third incident case was for an IHUMS equipped Super Puma with a cracked flapping hinge retainer on one of the 5 TR blades. The HUMS database created for model building contained TR vibration data for 20 aircraft and TGB data for 30 aircraft. The data included TGB outputs SO1 and SO2 and 1T, 2T, 3T, 4T 5T and 10T radial vibration measurements in Cruise, Climb, Descent, 115 Knots 125 Knots, Hover and at MPOG. No axial vibration measurements were available, however the data set did include phase information.

As explained in Section 2.3.1, the available data for the incident on G-PUMH that occurred in 1995 was limited to plots of TGB output SO1, Figure 3-44, and composite TR vibration (i.e. measurements averaged over a number of different flights) for different flight regimes, Figure 3-45, published in the AAIB report (Reference [3]). During maintenance, just prior to the incident flight, it was discovered that the two TR airframe accelerometers had been crosswired and that the IHUMS TR lateral vibration was measuring in the radial plane and vice versa. Also, at the time of the incident, IHUMS hours lagged those of the aircraft logbook by some 72 hours. The composite graph in Figure 3-45 compares vibration levels observed 55 hours before the incident flight (13,975 IHUMS hours) to those observed at 14,017, 14,021 and 14,029 IHUMS airframe hours. This was before the accelerometer crosswiring was rectified and the TR balanced. The graph shows an increasing level of vibration in both the lateral and radial planes of the TR as time progressed. Because of the composite analysis implemented for RTB, the published TR incident data was insufficient to perform any meaningful TR analysis. The TR analysis in the IHUMS has been changed since that time, with only TR radial data now being recorded, but individual measurements being stored.

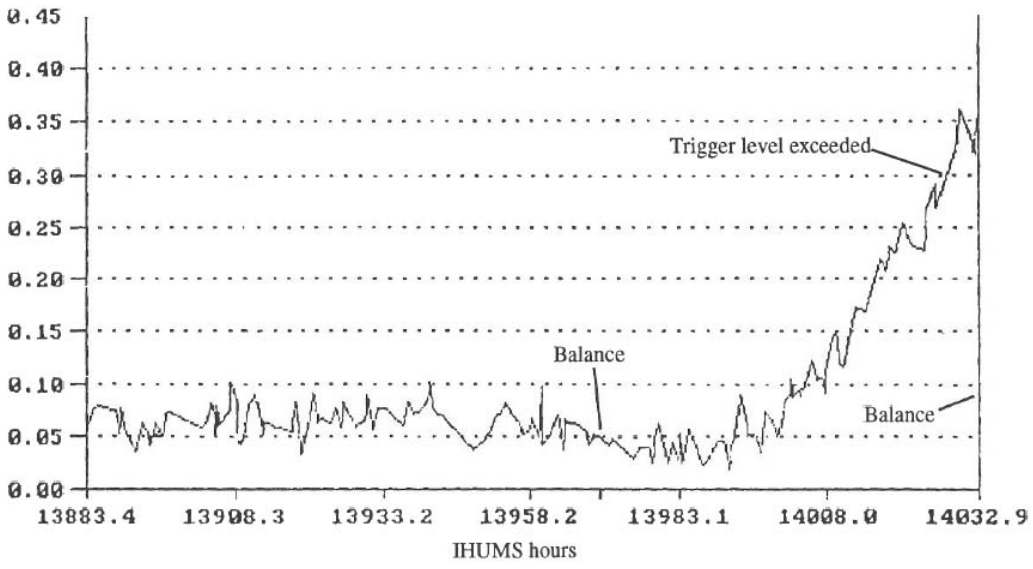

Figure 3-44: IHUMS Published Gearbox SO1 Output for Aircraft G-PUMH

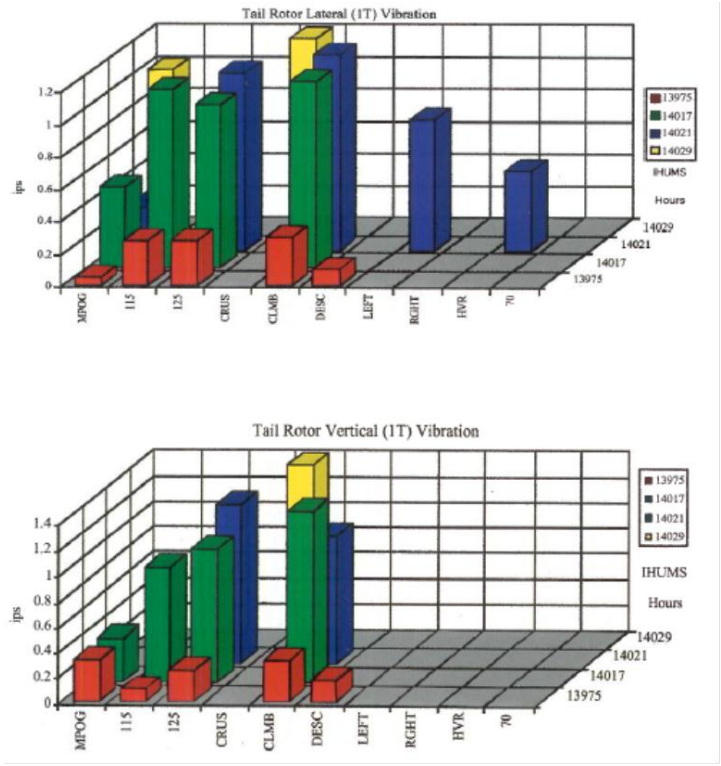

Figure 3-45: IHUMS Published Composite TR vibration for Aircraft G-PUMH

An anomaly model was built using the TGB output SO1 data. The reconstructed TGB SO1 data for aircraft G-PUMH is shown in Figure 3-46, the time history has a clear trend. The Fitness Score for the anomaly model output is shown in Figure 3-47. The accident aircraft was identified as anomalous, however there were some more extreme cases identified, mostly due to TR balance or instrumentation issues. The minimum normalised Fitness Score value was extracted for each Component Fit. The values were ranked and are shown in descending order of Fitness value in Table 3-8. The incident aircraft was ranked 10 out of 107 by Component Fit.

The trend detection algorithm was applied to the anomaly model FS and to the TGB output SO1. A clear trend was identified in the TGB SO1, giving the highest severity value of all the detected trends. All the trends detected ranked according to severity are shown in Table 3-9.

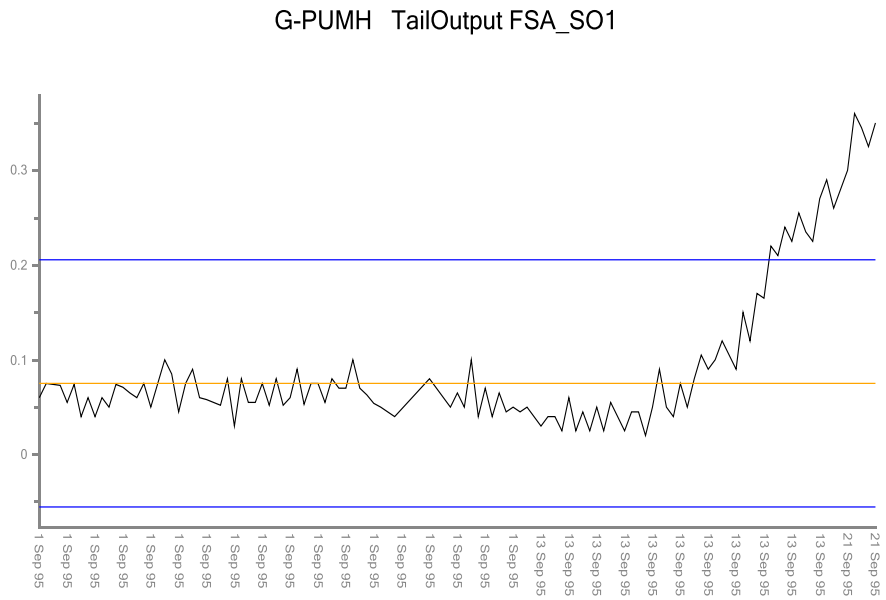

Figure 3-46: IHUMS Gearbox SO1 for Aircraft G-PUMH

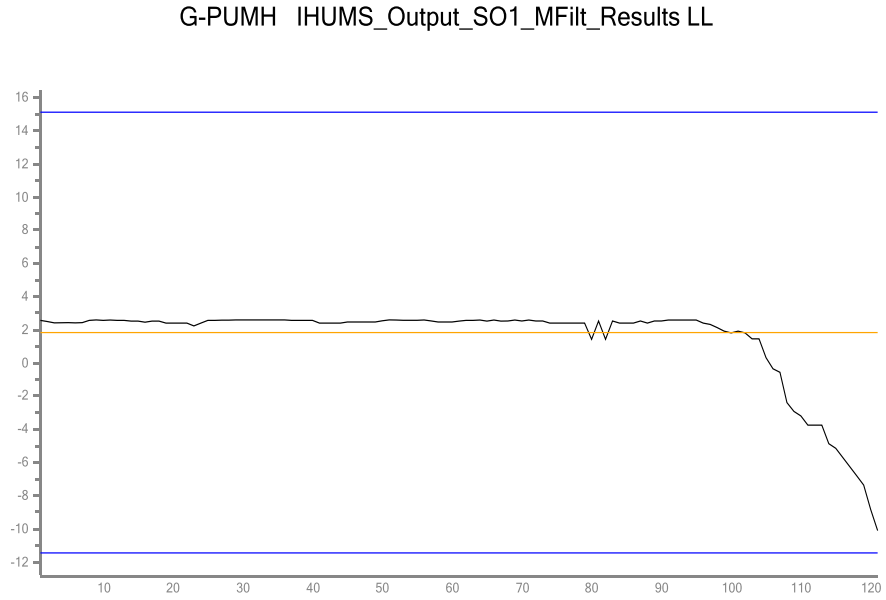

Figure 3-47: IHUMS Gearbox SO1 Anomaly Model Fitness Score for Aircraft G-PUMH

Table 3-8: Ranked Orders of Significance for Minimum Fitness Score: IHUMS TGB SO1 Model

Rank	Aircraft	CF	SO1	Rank	Aircraft	CF	SO1	Rank	Aircraft	CF	SO1	Rank	Aircraft	CF	SO1
1	G-BWMG	83	-180.971	28	G-BLPM	2	-1.251	55	G-BMCW	12	-0.753	82	G-PUMH	101	-0.466
2	G-BWZX	93	-61.813	29	G-TIGB	26	-1.223	56	G-BMCW	13	-0.737	83	G-BWWI	84	-0.442
3	G-TIGV	74	-11.201	30	G-TIGJ	48	-1.109	57	G-TIGC	32	-0.733	84	G-TIGV	76	-0.439
4	G-BLRY	7	-10.460	31	G-TIGL	50	-1.088	58	G-TIGF	39	-0.724	85	LN-OND	11	-0.385
5	G-TIGF	41	-7.212	32	G-TIGG	79	-1.084	59	G-BMCW	14	-0.720	86	G-TIGT	72	-0.377
6	G-TIGS	66	-6.074	33	G-TIGE	37	-1.053	60	G-BWZX	92	-0.718	87	G-BWWI	88	-0.344
7	G-BLPM	3	-3.625	34	G-TIGS	63	-0.976	61	G-BWZX	94	-0.704	88	G-PUMH	98	-0.330
8	G-TIGE	36	-3.269	35	G-BLXR	8	-0.962	62	G-BWMG	82	-0.692	89	G-BMCW	15	-0.258
9	G-TIGG	80	-2.808	36	G-BLXR	10	-0.960	63	G-TIGE	34	-0.692	90	G-PUMH	99	-0.235
10	G-PUMH	1	-2.696	37	G-BRXU	22	-0.948	64	G-TIGC	30	-0.675	91	G-TIGR	58	-0.164
11	G-BMCW	16	-2.600	38	G-TIGV	73	-0.947	65	G-BWMG	81	-0.669	92	G-TIGJ	45	-0.153
12	G-TIGM	52	-2.548	39	LN-OLC	107	-0.923	66	G-BWWI	86	-0.661	93	G-TIGL	49	-0.150
13	G-TIGS	65	-2.411	40	G-BWWI	87	-0.903	67	G-TIGJ	43	-0.660	94	G-TIGL	51	-0.124
14	G-TIGS	67	-2.048	41	G-TIGG	78	-0.902	68	G-TIGR	60	-0.649	95	G-TIGB	24	-0.101
15	G-TIGC	28	-1.978	42	G-PUMI	104	-0.890	69	G-TIGB	27	-0.647	96	LN-OBA	106	-0.073
16	G-BLPM	4	-1.973	43	G-TIGC	33	-0.864	70	G-TIGJ	44	-0.642	97	G-TIGC	29	-0.046
17	G-BWWI	89	-1.907	44	G-TIGO	54	-0.847	71	Scotia	96	-0.614	98	G-BWZX	91	-0.036
18	G-TIGF	42	-1.890	45	G-PUMH	102	-0.841	72	G-TIGF	40	-0.596	99	Scotia	97	-0.026
19	G-TIGR	57	-1.840	46	G-TIGT	70	-0.836	73	G-PUMH	100	-0.586	100	Scotia	95	-0.003
20	G-BWWI	90	-1.714	47	G-TIGC	31	-0.804	74	G-BWWI	85	-0.581	101	G-TIGB	23	0.030
21	G-BLXR	9	-1.663	48	G-BMCX	18	-0.804	75	G-TIGO	53	-0.575	102	G-BMCW	17	0.049
22	G-TIGF	38	-1.626	49	G-TIGT	69	-0.802	76	G-TIGT	71	-0.574	103	G-PUMI	103	0.073
23	G-TIGE	35	-1.516	50	G-TIGR	59	-0.797	77	G-TIGJ	46	-0.567	104	G-BLRY	6	0.107
24	G-TIGV	75	-1.464	51	G-TIGW	77	-0.793	78	G-BMCX	19	-0.566	105	G-TIGR	62	0.123
25	G-TIGJ	47	-1.458	52	G-TIGT	68	-0.786	79	G-TIGR	61	-0.557	106	G-TIGP	56	0.124
26	G-TIGO	55	-1.294	53	G-TIGS	64	-0.760	80	G-BRXU	20	-0.495	107	G-TIGB	25	0.129
27	G-BRXU	21	-1.285	54	G-PUMI	105	-0.754	81	G-BLRY	5	-0.470				

CF— Component Fit

Table 3-9: Ranked Trend Detection Results for TGB SO1 Model

ID	CF	Start Index	End Index	Min Fitness Score	Severity
G-PUMH	1	110	121	0.36	0.010086
G-TIGG	80	1579	1609	0.461187	0.003287
G-TIGO	55	1397	1451	0.391752	0.002034
G-BLXR	9	2359	2398	0.331605	0.001509
G-BLXR	10	908	1064	0.243502	0.000498
G-TIGR	60	1260	1321	0.169268	0.000375
G-TIGV	75	930	936	0.278288	0.000141

CF— Component Fit

An alternative trend algorithm was also applied to the TGB SO1 data. Due to limited resources the trend algorithm was only applied to the IHUMS dataset. After smoothing, the trend information was extracted by applying a 'moving median difference' algorithm; following each new acquisition, the median of the time history is re-calculated and subtracted from the newly acquired value to provide a normalised value. This technique reduces the impact of early post-installation trends, because the normalised value would gradually recover back to the median base line level. A trend model was built and the results were found to be very similar to the absolute model results. Such agreement is useful in indicating the significance of an alert and therefore the significance of a possible fault. For example, if trend data is anomalous with respect to the fleet the significance of this can be affected by whether the data is also anomalous at the fleet absolute level. If the data is not anomalous at the fleet absolute level then only an increasing trend has been detected but it is known that the actual levels of vibration are not outside fleet norms. Conversely, any potential fault would be expected to be more significant if an abnormal trend is developing and the values within that trend are also anomalous with respect to the fleet. The similarity of the trend and absolute model results is therefore indicative of the significance of the faults identified. Therefore a quick exercise was conducted to quantify the similarity of the results.

The minimum normalised Fitness Score value was extracted for each Component Fit and a rank was calculated. The values were compared with the rankings given by the absolute model (Table 3-8) and are shown in Figure 3-48. The figure shows a high degree of correlation between the two sets of results; the ranked correlation over all 51 aircraft was 0.886; ranked correlation is a more robust statistic than calculating the correlation between Fitness Score values. A high ranked correlation is indicative of a genuine linear relationship whereas a single very low Fitness Score for one of the aircraft results could lead to high correlation between Fitness Scores when no linear relationship exists.

The running correlation is shown in Figure 3-49. At each point *n* the running correlation is the correlation calculated over the *n* highest ranked aircraft when the data is ordered by the rankings of the absolute model. The ranked correlation is a single statistic expressed for one instance of the dataset available. Additional results for other aircraft Component Fits may or may not significantly affect the results although this cannot be known from a single statistic. If there are a large number of aircraft with low levels of Fitness Score significance variations due to, for example, noise, this can greatly affect the ranking orders across different models. This could

mask high levels of agreement between models on the highest ranked aircraft (and most significant anomalies) as the correlation between models over a large number of aircraft would tend to zero.

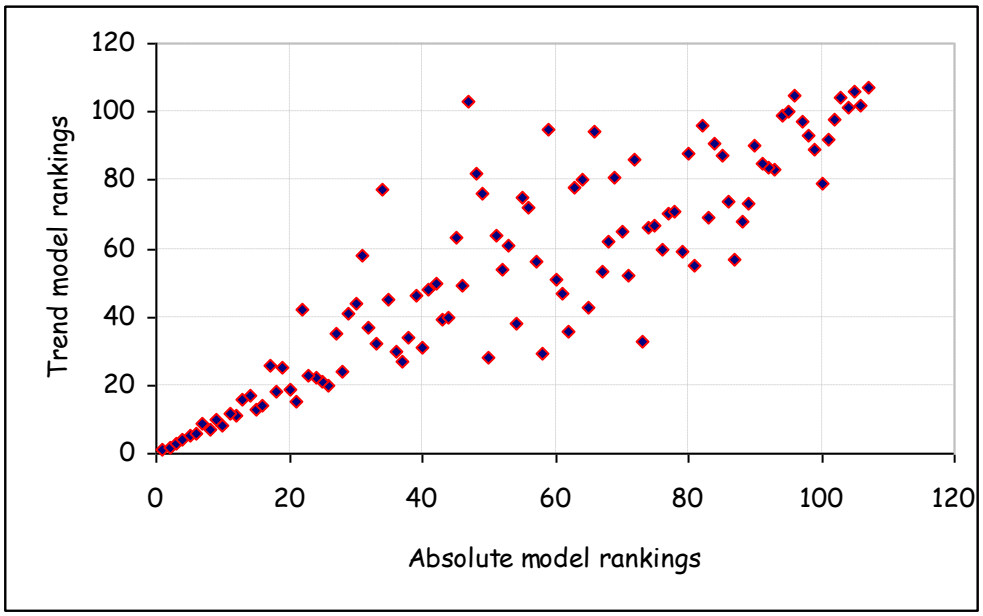

Figure 3-48: IHUMS Gearbox SO1 Absolute Model Rankings vs. Trend Model Rankings

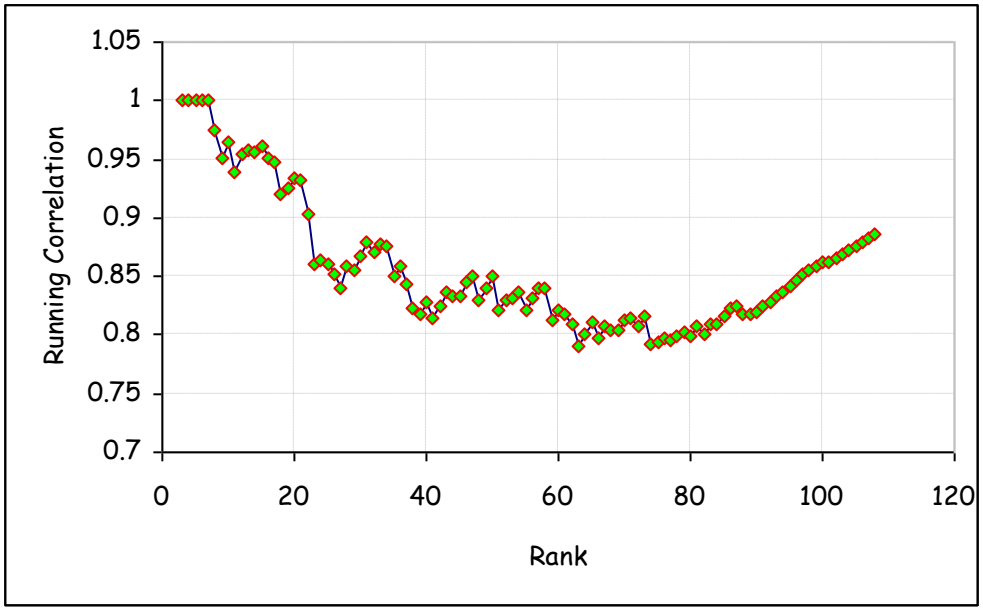

Figure 3-49: IHUMS Gearbox SO1 Running Rank Correlation between Absolute Model Rankings and Trend Model Rankings

Therefore a running ranked correlation will give an indication of the agreement between the models of the ranked orders starting with the most significant aircraft (with respect to levels of the anomalies). It will also give an indication of the depth (number of aircraft) to which the agreement is held, i.e. the number of ranked aircraft before the relationship in model rankings becomes random. The variability of the running ranked correlation between ranks is also an indicator of the level of agreement between models over different numbers of aircraft; high variability indicating that high correlations are not significant but simply due to chance. Table 3-10 gives the results of the running correlation for the top 20 aircraft ranked by the absolute model rankings. The figure and the table show that for the highest ranked aircraft, i.e. the most significant anomalous aircraft (as indicated by low minimum Fitness Score values) the rank correlation between the two models is very high; the rank correlation is greater than 0.95 over all the top 15 ranked aircraft. This indicates that the results of the trend model and the absolute model are very similar and highlights the significance of the anomalies identified.

Table 3-10: IHUMS Gearbox SO1 Running Rank Correlation between Absolute Model Rankings and Trend Model Rankings: Top 20 Aircraft Ranked by Absolute Model

Absolute Model			Trend Model			Running Correlation
Rank	Aircraft	CF	Rank	Aircraft	CF	
1	G-BWMG	83	1	G-BWMG	83	
2	G-BWZX	93	2	G-BWZX	93	1
3	G-TIGV	74	3	G-TIGV	74	1
4	G-BLRY	7	4	G-BLRY	7	1
5	G-TIGF	41	5	G-TIGF	41	1
6	G-TIGS	66	6	G-TIGS	66	1
7	G-BLPM	3	9	G-BLPM	3	0.975017
8	G-TIGE	36	7	G-TIGE	36	0.950437
9	G-TIGG	80	10	G-TIGG	80	0.965394
10	G-PUMH	1	8	G-PUMH	1	0.939394
11	G-BMCW	16	12	G-BMCW	16	0.953821
12	G-TIGM	52	11	G-TIGM	52	0.958042
13	G-TIGS	65	16	G-TIGS	65	0.955909
14	G-TIGS	67	17	G-TIGS	67	0.962012
15	G-TIGC	28	13	G-TIGC	28	0.951112
16	G-BLPM	4	14	G-BLPM	4	0.947645
17	G-BWWI	89	26	G-BWWI	89	0.919631
18	G-TIGF	42	18	G-TIGF	42	0.924584
19	G-TIGR	57	25	G-TIGR	57	0.934069
20	G-BWWI	90	19	G-BWWI	90	0.931935

4 Maintenance data analysis

4.1 Bristow IHUMS data

The aim of this study was to, where possible, correlate anomaly model outputs with TR faults and maintenance actions recorded in Bristow's 332L maintenance database.

All the TR data analysis was based on the IHUMS Cruise flight regime database, which contained 11,616 TR acquisitions. The maintenance data were aligned with these TR data acquisitions - an example is shown in Table 4-1. The data were aligned such that a maintenance action was associated with the closest acquisition following the maintenance action; the table shows that more than one maintenance action could be associated with a single acquisition. Of the 471 listed TR maintenance actions 16 actions were not included because there was no associated tail number in the TR database. Maintenance actions that fell outside the acquisition periods for each Component Fit listed in the TR database tables were not included; this lead to approximately 106 maintenance actions being excluded. In addition, a time limit of 31 days (1 month) was placed on the maximum difference between a maintenance action and the last acquisition. This caveat excluded approximately 19 maintenance actions. Therefore, out of 471 maintenance actions about 140 were not associated with any acquisitions in the TR harmonics database.

The table also shows an additional derived parameter called the 'Life number'. This parameter is an integer valued parameter that was initialised at the start of each new Component Fit, then incremented each time a maintenance action was performed. It was used to help visualise when maintenance occurred during acquisition periods. It provides a guide that can be used for associating any maintenance actions with trends in TR harmonics and also indicates the level of TR maintenance. It can be noted that when separate maintenance actions are associated with a single acquisition date the life number was only incremented once: the life number does not give any indication of the type or level of maintenance performed so multiple maintenance actions were grouped as a single maintenance period.

Figure 4-1 shows the 1T harmonic acquisitions for Component Fit 47 given in the Cruise database. The figure also shows the life number and shows that 6 maintenance actions were performed during the acquisition period. The maintenance actions carried out included identifying worn pitch link, sleeve and spindle failures and TR balances. Some interesting characteristics were observed in the behaviour of different harmonics for many Component Fits with respect to maintenance actions, as described below.

Figure 4-1 shows that there is a period of fairly intense maintenance activity with four separate maintenance actions performed over a ten day period. There is an increase in the amplitude of 1T vibrations following the first maintenance action. A trend of increasing 1T amplitude develops following the second maintenance action that occurs three days later. This trend is reversed following the third maintenance action, which occurs five days after the second action, and continues after the fourth maintenance action. These maintenance actions could affect the amplitudes of 1T vibration either by making adjustments or replacing damaged\failed components, or simply by disturbing components to achieve access for other maintenance. However, the fifth maintenance action, which occurred ten days after the fourth action, does not appear to influence the mean or variance of the 1T vibration. Similarly, the sixth maintenance action, occurring a month after the fifth action, does not affect the

levels of 1T vibration. In these cases it may be that the action performed would not influence the performance of the TR. Alternatively, the maintenance action details that worn pitch links were observed but does not indicate whether any action was performed to rectify the problem, or indicate the level of wear found.

The figure also shows another feature, where after sequence number 106 (date 27/10/06) a step change in the mean level of 1T vibration can be seen. However, there is no recorded maintenance action around this date to indicate a fault had occurred and was rectified, or that the act of performing a maintenance action lead to a change in vibration levels. It is possible that daily checks, such as TR greasing (recorded separately under routine maintenance), could affect recorded TR vibration levels.

Table 4-1: Extract Example of Maintenance Actions Aligned with Acquisitions and Creation of "Life" Line

Registration	Component Fit ID	Sequence	Date	Number of associated maintenance records	LIFE number	Maintenance action description for first maintenance action	Date of first maintenance action	Maintenance action description for second maintenance action	Date of second maintenance action
G-BMCW	16	351	18/05/2007	0	9				
G-BMCW	16	373	06/07/2007	0	9				
G-BMCW	16	374	09/07/2007	2	10	PMC Creation	08/07/2007	5 Pitch change links worn	07/07/2007
G-BMCW	16	375	11/07/2007	0	10				
G-BMCW	16	391	14/08/2007	0	10				
G-BMCW	16	393	16/08/2007	0	10				
G-BMCW	16	394	27/08/2007	2	11	T/R Spider end cap disturbed	21/08/2007	T/R Bellows damaged	18/08/2007
G-BMCW	16	395	27/08/2007	0	11				
G-BMCW	16	401	04/09/2007	0	11				
G-BMCW	16	402	05/09/2007	0	11				
G-BMCW	16	403	08/09/2007	0	11				
G-BMCW	16	404	11/09/2007	0	11				
G-BMCW	16	405	12/09/2007	1	12	Red T/R bearing worn.	11/09/2007		
G-BMCW	16	406	12/09/2007	0	12				
G-BMCW	16	417	03/10/2007	0	12				
G-BMCW	16	418	09/10/2007	1	13	RTB Adjustments	06/10/2007		
G-BMCW	16	419	10/10/2007	0	13				
G-BMCW	16	428	23/10/2007	0	13				

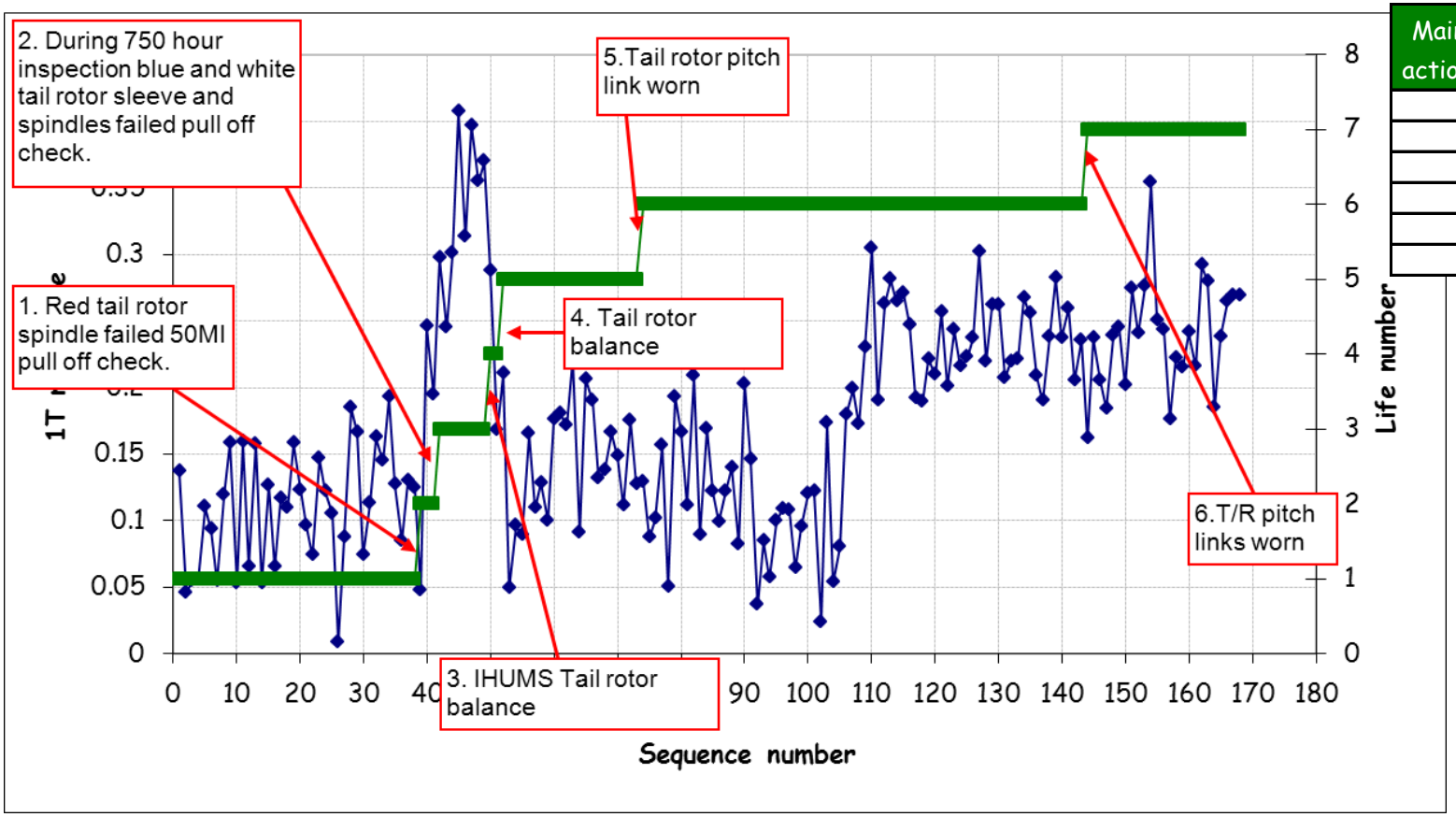

Maintenance action number	Maintenance action date
1	21/09/2006 01:16
2	24/09/2006 19:21
3	29/09/2006 07:55
4	30/09/2006 12:59
5	10/10/2006 23:05
6	09/11/2006 00:35

Figure 4-1: Example of Maintenance Action Indicator Line (Life Line) and Corresponding 1T Amplitude for Component Fit 47

Further investigation was carried out into the effects of maintenance actions on the harmonic responses by visually scanning the data. Some interesting examples are displayed in Figure 4-2 through Figure 4-10 for aircraft G-TIGE. The figures also show the fleet mean values (yellow line) and fleet 3SD bands (blue lines) to give an indication of the levels of vibration displayed by G-TIGE with respect to the rest of the fleet. Corresponding maintenance actions are shown in Table 4-2 through Table 4-4.

Figure 4-2 shows the 2T harmonic for aircraft G-TIGE; Figure 4-3 shows the corresponding 3T vibration and Figure 4-4 shows the 4T vibration. Over-laid on the charts are five lines indicating significant features. The data trends up prior to Feature 1. Significant downward steps in 3T and 4T are observed at this point. A small downward step may be observed in the 2T data, although there is little effect on the data trend. After Feature 1, 3T resumes trending up whilst 2T also continues to trend. No such trend is observed in 4T. At Feature 2, 2T and 3T step down again but no step is observed in 4T. In all the vibration harmonics shown the data then maintains constant mean amplitude levels until at Feature 3 an upward step is observed in 3T; no step is observed in 2T or 4T. Shortly after however, at Feature 4 upward steps are noted in the 2T and 4T vibration but not in 3T. Slight upward trends are observed (more apparent in the 2T vibration) before, at Feature 5, all harmonics demonstrate a downward step. Cross correlating these features with maintenance actions shown in Table 4-2 indicates that maintenance occurred at Feature 1, Feature 2 and Feature 5, and may account for the steps in the vibration amplitudes observed. No maintenance listing was available to account for the steps in the data at Feature 3 and Feature 4. Nevertheless, the maintenance actions themselves do not account for why a step may be observed in one or more harmonics.

Similar behaviour was observed for the other aircraft indicating this effect is quite common. Figure 4-5 shows the 2T vibration for aircraft G-TIGF from the Cruise database. Figure 4-6 shows the corresponding 3T vibration and Figure 4-7 shows the gearbox SO1 vibration. Both figures also show the fleet mean values (yellow line) and fleet 3SD bands (blue lines). The maintenance actions for the period are listed in Table 4-3. The figures show that similar steps in the data are also observed in the gearbox data that correspond with features in the TR sensor data. Three of the five features identified may be associated with maintenance actions, however, not every data step can be directly linked to maintenance.

Figure 4-8 shows 2T for the aircraft G-TIGC. Figure 4-9 shows the corresponding 4T harmonic and Figure 4-10 shows 5T. Again, the fleet mean values (yellow line) and fleet 3SD bands (blue lines) are shown on the figures. The maintenance records for the period are shown in Table 4-4. Similar behaviour is observed.

It is noted that the majority of maintenance actions over these periods are related to the flapping hinge.

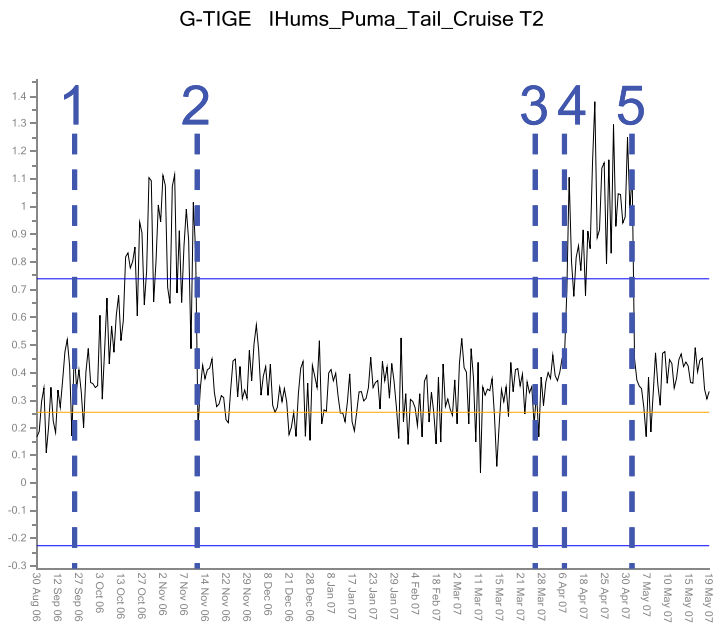

Figure 4-2: Maintenance Actions on G-TIGE 2T IHUMS Cruise Database

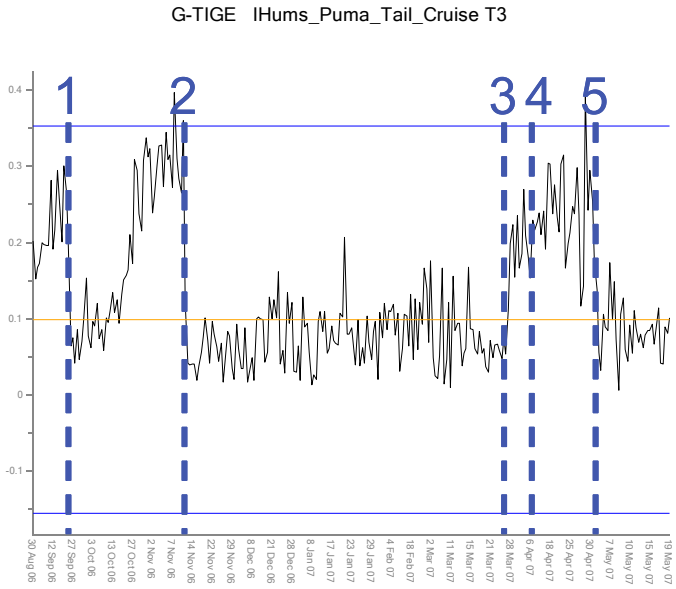

Figure 4-3: Maintenance Actions on G-TIGE 3T IHUMS Cruise Database

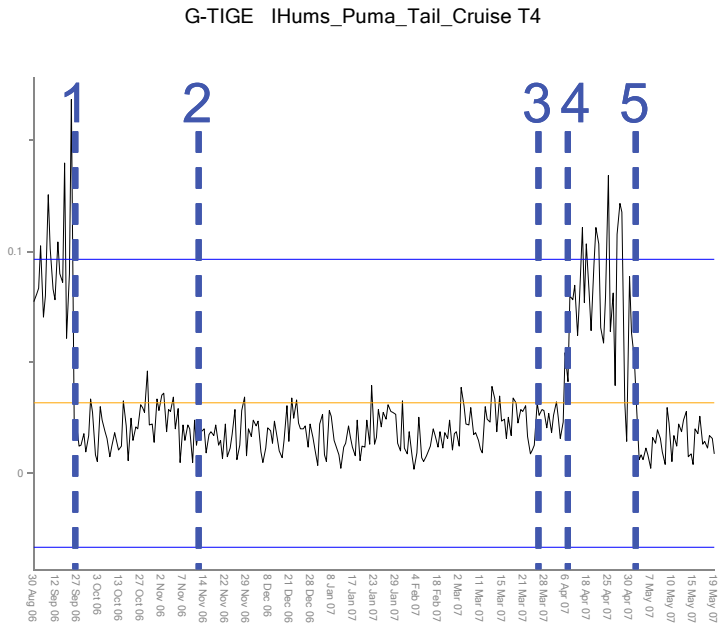

Figure 4-4: Maintenance Actions on G-TIGE 4T IHUMS Cruise Database

Table 4-2: Maintenance Actions for Identified Features of Aircraft G-TIGE

Feature	Date	Maintenance Action
1	20-27 Sep 06	Blue ,yellow and black tail rotor sleeve and spindle flapping hinge bearings worn)
2	10-13 Nov 06	(Blue and black flapping hinge bearings worn)
3	27-28 Mar 07	None listed
4	09-12 Apr 07	None listed
5	01-03 May 07	(Pilot Reports Vibration on tail rotor Needle bearings and Inner race found worn on Black and Yellow tail rotor hub)

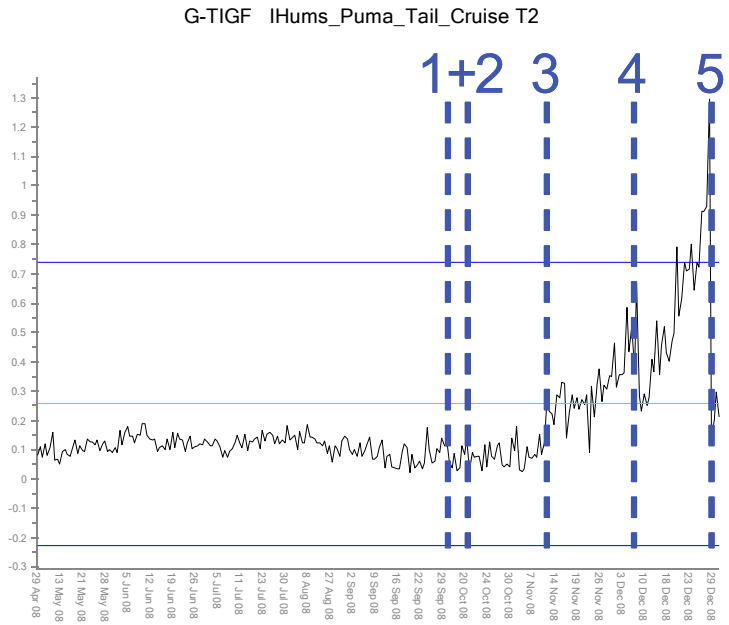

Figure 4-5: Maintenance Actions on G-TIGF 2T IHUMS Cruise Database

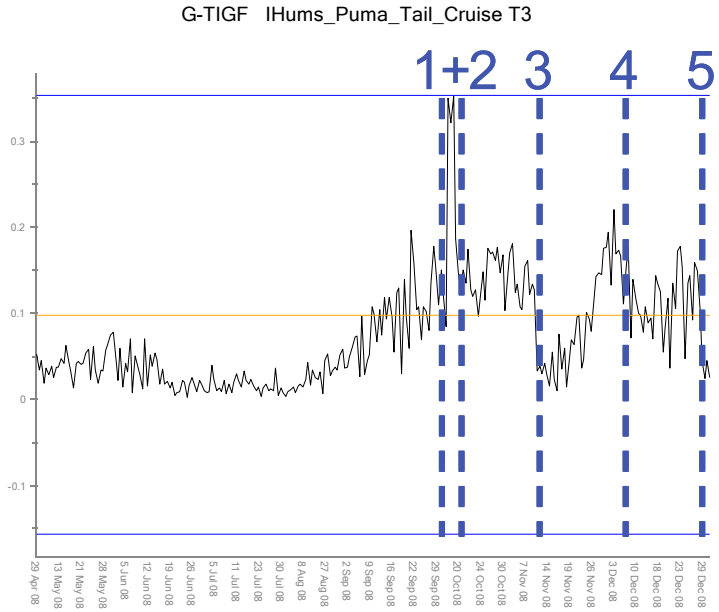

Figure 4-6: Maintenance Actions on G-TIGF 3T IHUMS Cruise Database

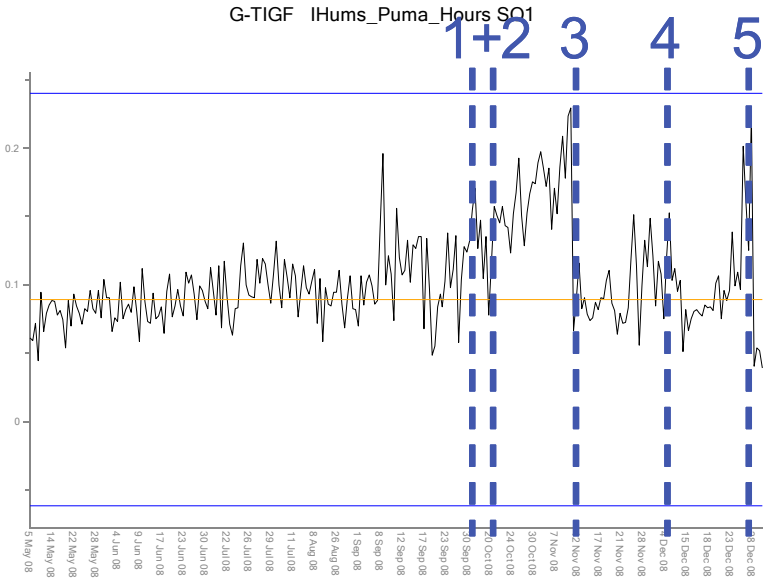

Figure 4-7: Maintenance Actions on G-TIGF SO1 IHUMS Gearbox Database

Table 4-3: Maintenance Actions for Identified features of Aircraft G-TIGF

Feature	Date	Maintenance Action
1	01-16 Oct 08	None listed
2	17-20 Oct 08	None listed
3	11-12 Nov 08	Blue T/R flapping hinge bearings worn
4	05-09 Dec 08	Red Tail Rotor flapping hinge bearing inner race worn
5	28-29 Dec 08	Red TR flapping hinge brinelled

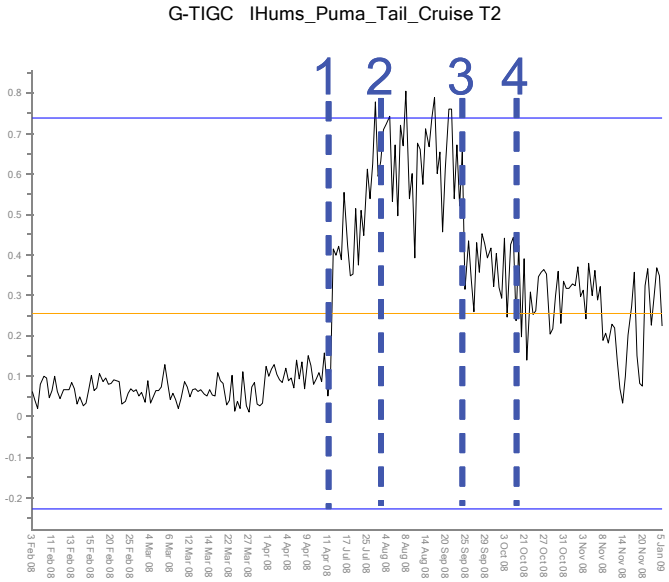

Figure 4-8: Maintenance Actions on G-TIGC 2T IHUMS Cruise Database

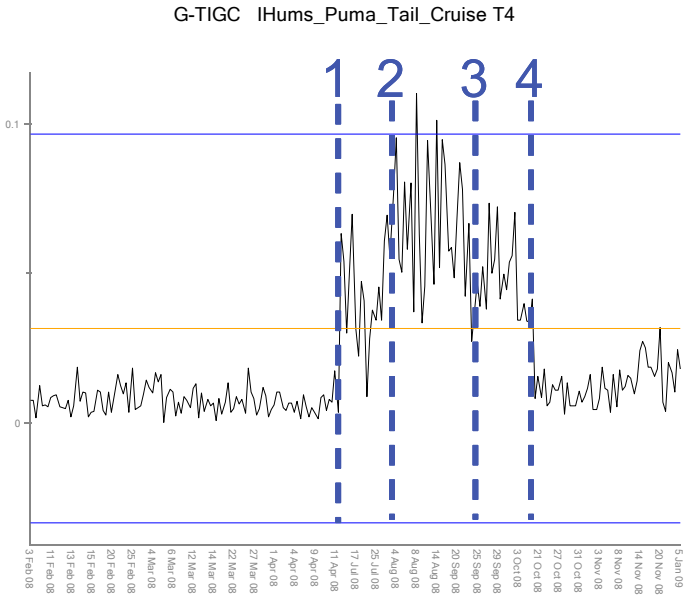

Figure 4-9: Maintenance Actions on G-TIGC 4T IHUMS Cruise Database

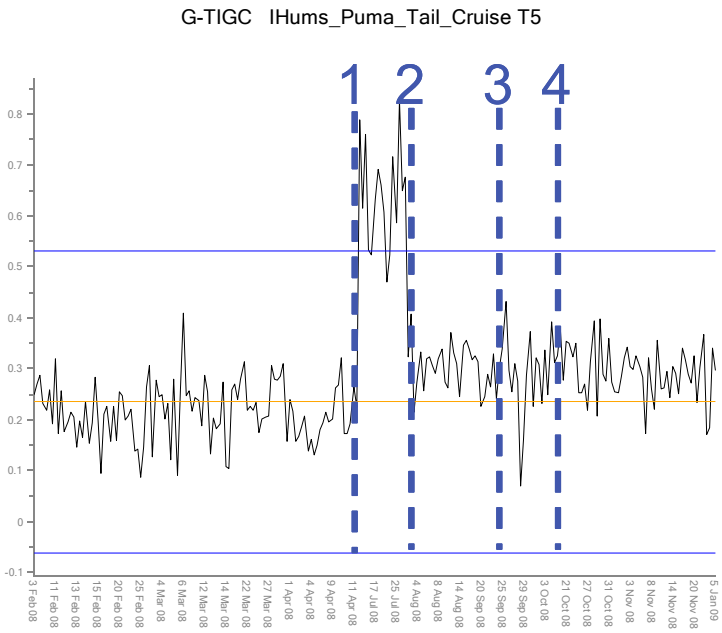

Figure 4-10: Maintenance Actions on G-TIGC 5T IHUMS Cruise Database

Table 4-4: Maintenance Actions for Identified Features of Aircraft G-TIGC

Feature	Date	Maintenance Action
1	14 Apr–16 Jul 08	None listed
2	29 Jul–04 Aug 08	None listed
3	23-25 Sep 08	Yellow tail rotor flapping hinge bearings worn. All tail rotor pitch links worn beyond limits
4	06-16 Oct 08	Black and White tail rotor flapping hinge bearings found worn on 750 hr inspection. Spider bearing axial play at maximum limit

4.2 Anomaly models incorporating phase

The IHUMS data records both amplitude and phase for 1T, 2T, 3T, 4T, 5T and 10T harmonics of the radial TR vibration. The purpose of this analysis was to ascertain whether the phase information provided any additional useful information that could be incorporated in the anomaly models for fault detection.

4.2.1 Clustering of Component Fit lives

Figure 4-11 shows the 1T vibration for Component Fit 76. The right hand chart displays the vibration amplitude as a function of sequence number (chronologically ordered) together with the life line indicating when a maintenance action had been performed; although there appears to be some trends in the data where mean amplitude levels can appear to be increasing and decreasing over time there appears to be no strong correlation between 1T vibration amplitude trends and a maintenance action. Similar observations are noted for Component Fit 71, shown in Figure 4-12.

The left hand charts for each of the Component Fits shows the vibration amplitude and phase data plotted in polar coordinates. The data are coloured by their life value. Each life appears as a nearly circular cluster of points centred on a position in the amplitude/phase space. The principle effect of maintenance on the vibration is to modify the position of cluster centres in the amplitude/phase space.

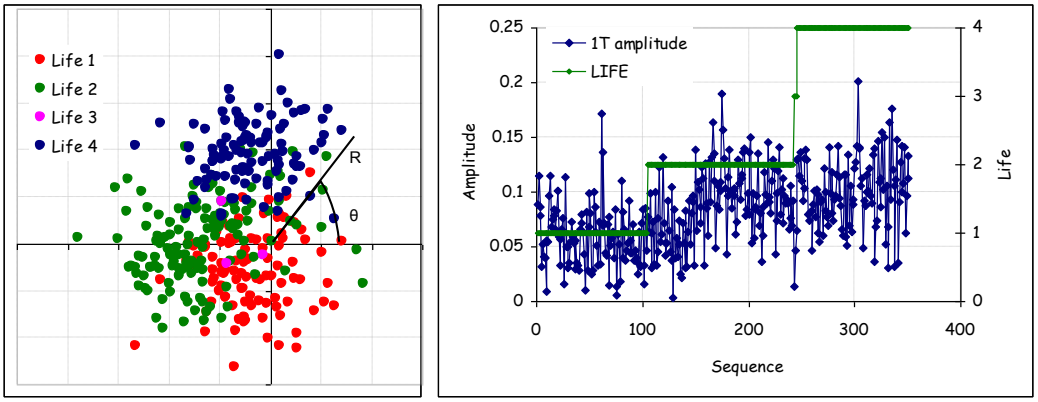

Figure 4-11: Component Fit 76 1T Amplitude and Phase

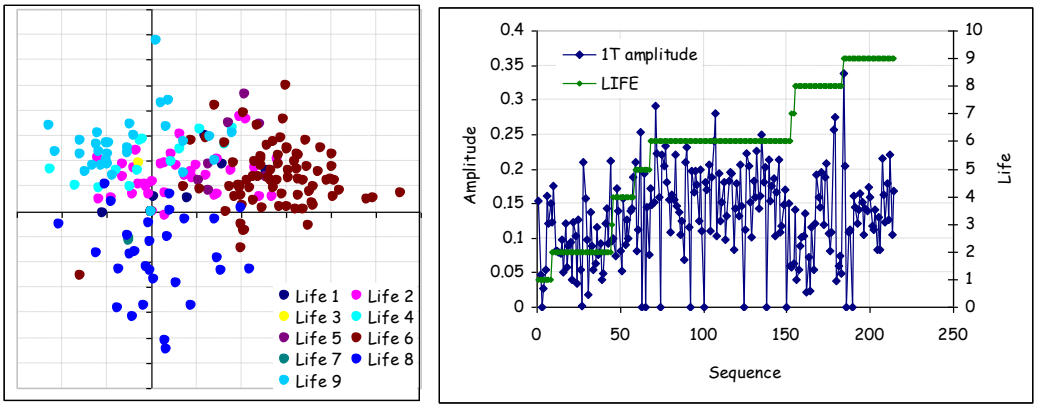

Figure 4-12: Component Fit 76 1T Amplitude and Phase

The separation between the clusters for different lives would appear to indicate that better results may be obtained by taking this into account in the anomaly models. However, many Component Fits did not have any clear separation between clusters for different lives as shown in Figure 4-13. No significant advantage was obtained by targeting individual lives in the anomaly model instead of the Component Fits themselves.

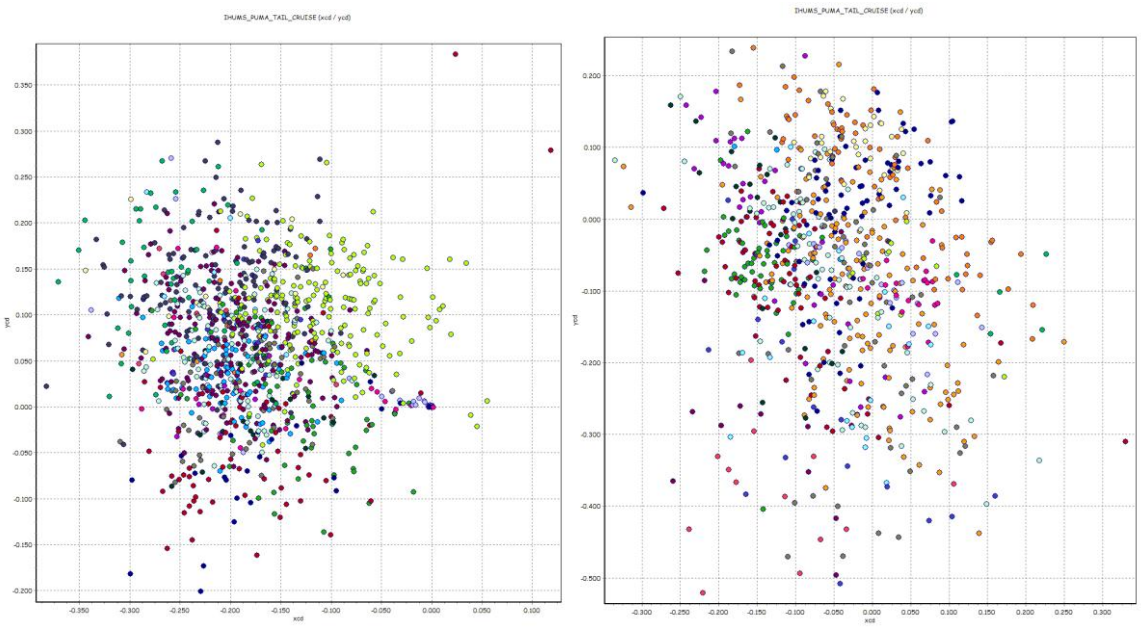

Figure 4-13: Component Fit 16 and Component Fit 66 1T Amplitude and Phase (Data are coloured according to their life value)

4.2.2 Linear tracks and vector differences

The 10T amplitude for Component Fit 41 is shown in Figure 4-14. The figure shows significant trends in the amplitude values. Some of the shifts appear to coincide with maintenance actions however it can also be noted that a significant amount of TR maintenance was performed during the acquisition period for this Component Fit. An alternative view of the data that incorporates the phase information is shown in Figure 4-15. The figure shows how, in this case, the recorded vibration forms a ring in the amplitude/phase space.

There is the potential for a developing fault to cause changes in either or both the amplitude and phase values such that a fault may be characterised by the acquisition values moving across the amplitude/phase space, i.e. a fault may not just be detected by changes in amplitude values. A potential illustration of this effect is given by examination of some of the individual lifetimes of Component Fit 41 10T vibration.

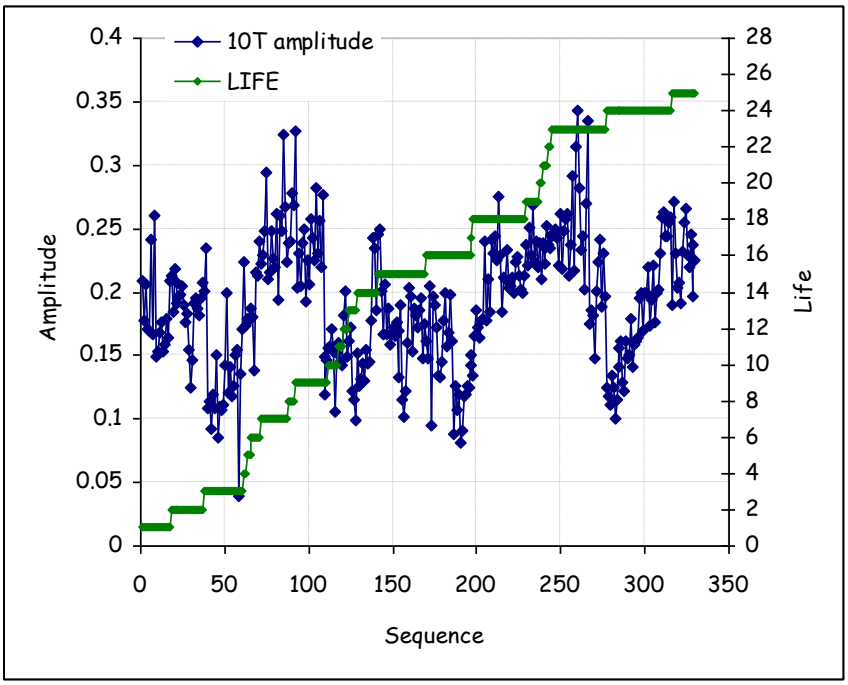

Figure 4-14: Component Fit 41 10T Amplitude

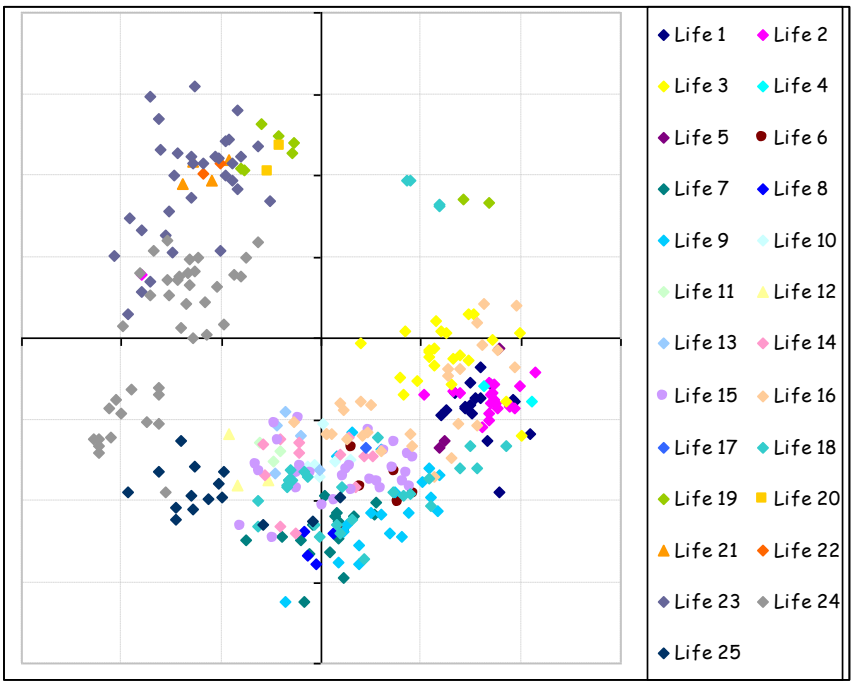

Figure 4-15: Component Fit 41 10T Amplitude and Phase

Figure 4-16 shows the amplitude/phase data with the addition of a line between successive acquisition values to indicate the order in which the acquisitions were taken. The figure shows that generally a fairly random pattern evolves for the distribution of points over each lifetime. However, Life 2 and Life 24 for this data illustrate some interesting points. The acquisitions for these lives are highlighted in Figure 4-17.

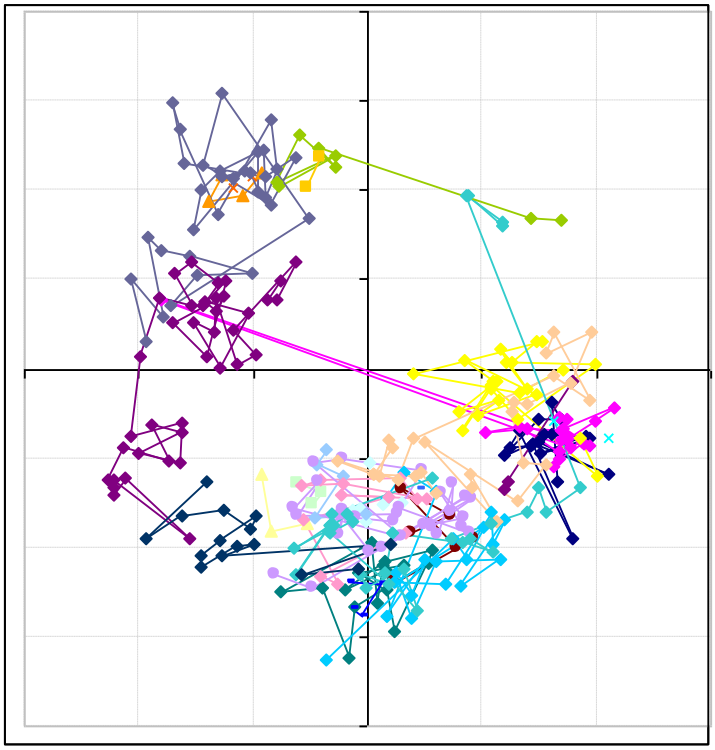

Figure 4-16: Component Fit 41 10T Amplitude and Phase Tracking Acquisitions

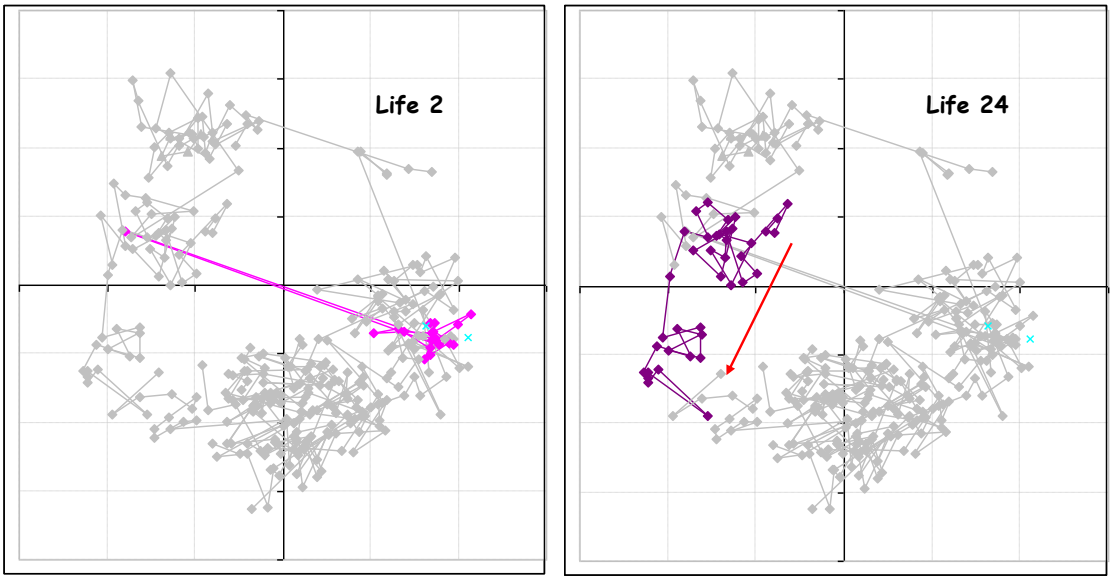

Figure 4-17: Component Fit 41 10T Amplitude and Phase Tracking Acquisitions Through Individual Lifetimes

During Life 2 it can be observed that one acquisition had a significantly different phase value although its amplitude was not abnormal and in fact lay within the cluster of values associated with a different life time. In this case the phase difference between the abnormal value and the mean phase value for the cluster of points included in the same lifetime was of the order of 180 degrees and indicates that the error was more likely an instrumentation fault. Nevertheless, one strategy was to calculate the vector differences between acquisitions and use the magnitude of the vector differences as inputs to anomaly models derived for each harmonic. The magnitudes of vector differences for Component Fit 41 10T vibration are shown in Figure 4-18. The figure also highlights the acquisitions recorded during Life 2. The large magnitude vector differences caused by the anomalous point are clearly observed as the data jumps from the cluster of Life2 values to the anomalous point and back to the cluster again.

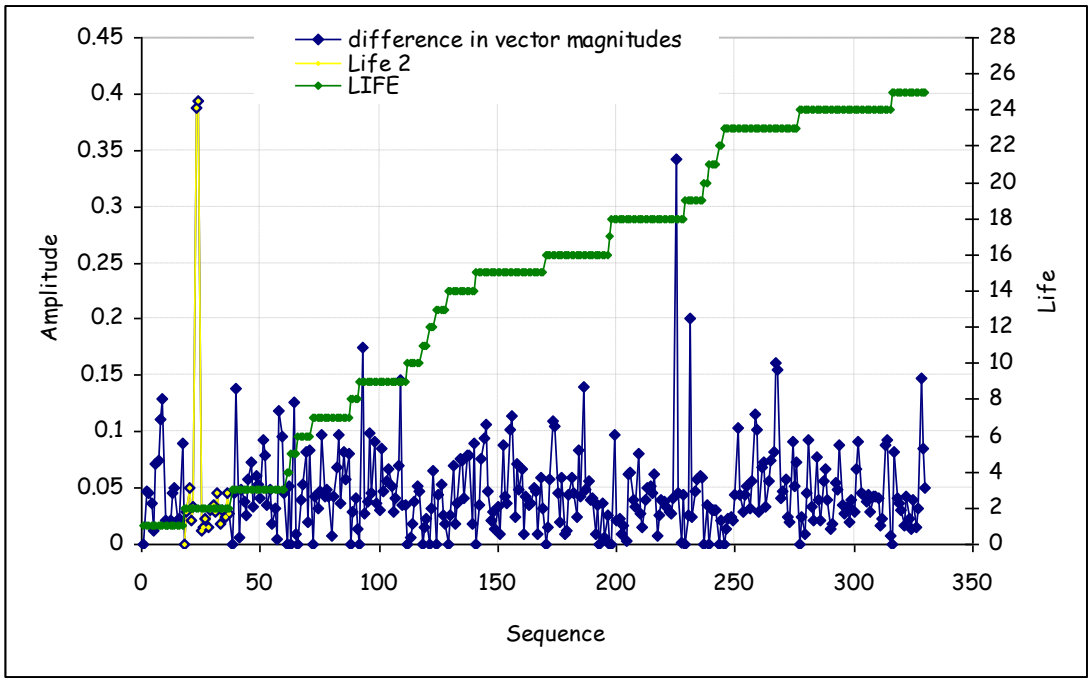

Figure 4-18: Component Fit 41 10T Differences in Vector Magnitudes

Lifetime 24 illustrates how values could move across the amplitude/phase space in a defined track over a life period, which may indicate the presence of an anomaly. An algorithm was developed to identify any linear tracks that developed in the data. The algorithm worked by taking each successive acquisition and comparing it to the current track by measuring the perpendicular distance from the point to the linear trend line that characterised the points making up the track. If the distance was within a prescribed number of standard deviations the point was added to the track and the linear trend line updated. If the point was outside the track it was used to generate a new linear track. The lengths of the linear tracks identified were calculated after each acquisition and were used as inputs to another anomaly model. The linear track lengths for Component Fit 41 10T vibration are shown in Figure 4-19. The figure also highlights the acquisitions recorded during Life 24. Although a linear track of reasonable length is seen to develop, the largest linear track is in fact associated with the anomalous point in Life 2. Comparisons between linear track length and the magnitude of vector differences over a number of Component Fits

indicated that track length was dominated by the larger magnitude of vector differences that appeared in a life period; the track length traces appeared as a "smoothed" version of the magnitude of vector difference traces. In addition, anomalies indicated by the anomaly models did not show any strong correlations with the maintenance data. No advantage was therefore seen in developing the linear tracking method and no further work was performed.

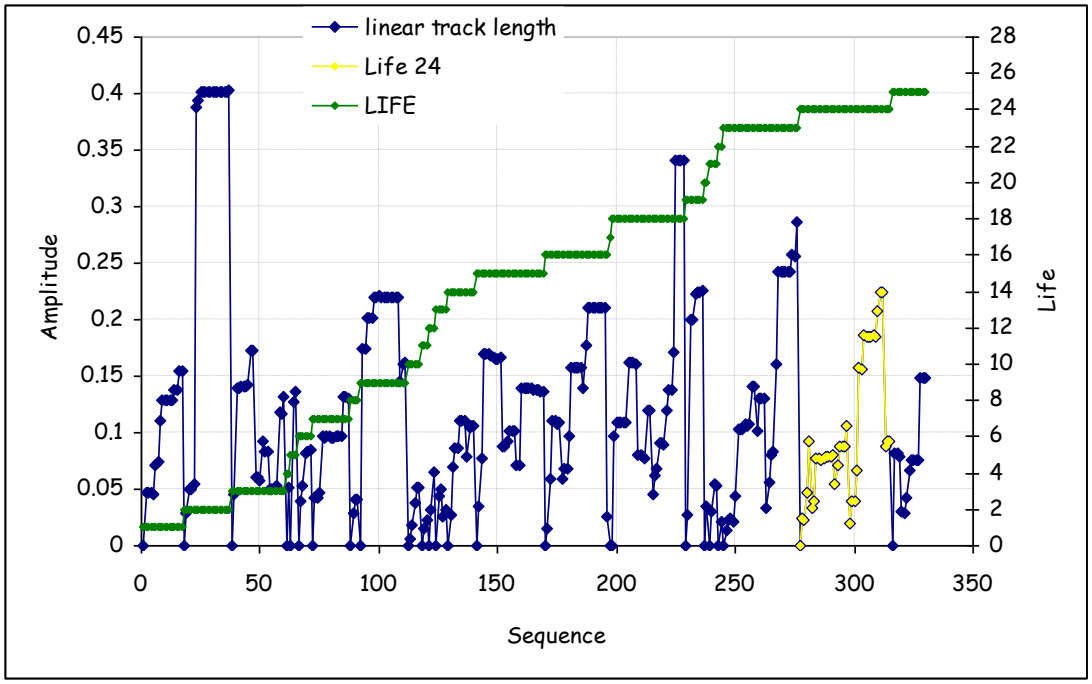

Figure 4-19: Component Fit 41 10T Linear Track Length

For comparison, an anomaly model was constructed using the polar values of the vibration amplitude and phase data for each of the harmonics. These models were the simplest to visualise physically as they are just the position of the acquisitions on the amplitude/phase space. The results were compared with the Fitness Score values for the anomaly models built using the vector differences. A typical result is shown for Component Fit 41 in Figure 4-20. The anomaly models for the vector difference parameters typically showed stronger anomalies (lower Fitness Score values) than using the polar values, however, where a feature was significant in the vector difference models it was typically significant in the polar models. From Figure 4-20 significant Fitness Score values can be seen to start around sequence number 90 and continue to sequence number 110. Following this were a large number of maintenance actions. The maintenance performed at this time is listed in Table 4-5 and indicates a wide range of TR maintenance actions including identifying worn pitch links, flap hinges and spindles.

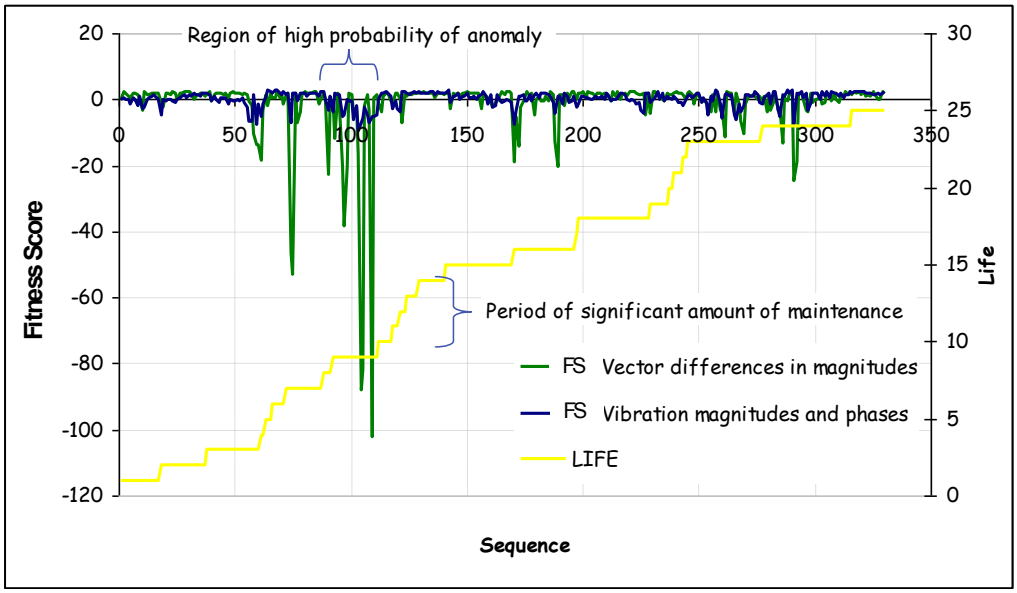

Figure 4-20: Component Fit 41 1T Differences in Vector Magnitudes

Table 4-5: Maintenance Actions Performed after Significant Fitness Score Values

Sequence	Date	Maintenance Action
92	06/01/2007	Spider end cap disturbed to facilitate 250 bearing inspection. This LBE is for PMC creation only.
112	30/01/2007	Tail Rotor IHUMS RTB's required
118	05/03/2007	Red tail rotor flapping hinge bearing shows signs of being worn.
121	07/03/2007	Pitch change bearings and links worn
124	26/03/2007	t/r blue sleeve and spindle timex
129	31/03/2007	Spider end cap removed to facilitate SB 05-29
141	12/04/2007	White & Blue T/R sleeve & Spindles failed 50 Pull off check

The magnitudes of the vector differences for the 1T harmonic are shown in Figure 4-21 for Component Fit 41; the corresponding 1T amplitudes are shown in Figure 4-22. Highlighted is the region that generated the significant Fitness Score values identified above. Some degree of similarity can be seen between the two figures. Trends can be seen in the graphs of both increasing vector differences and increasing IT amplitude; high values for the magnitude of vector differences coincide with high 1T amplitude values and generate the significant Fitness Score values observed.

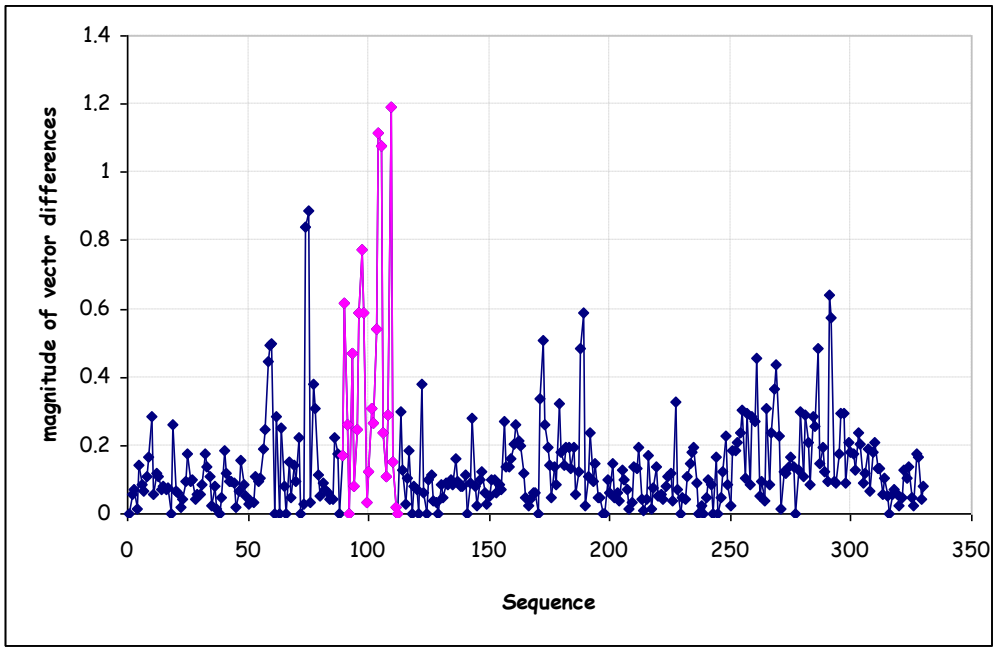

Figure 4-21: Component Fit 41 1T Magnitude of Vector Differences

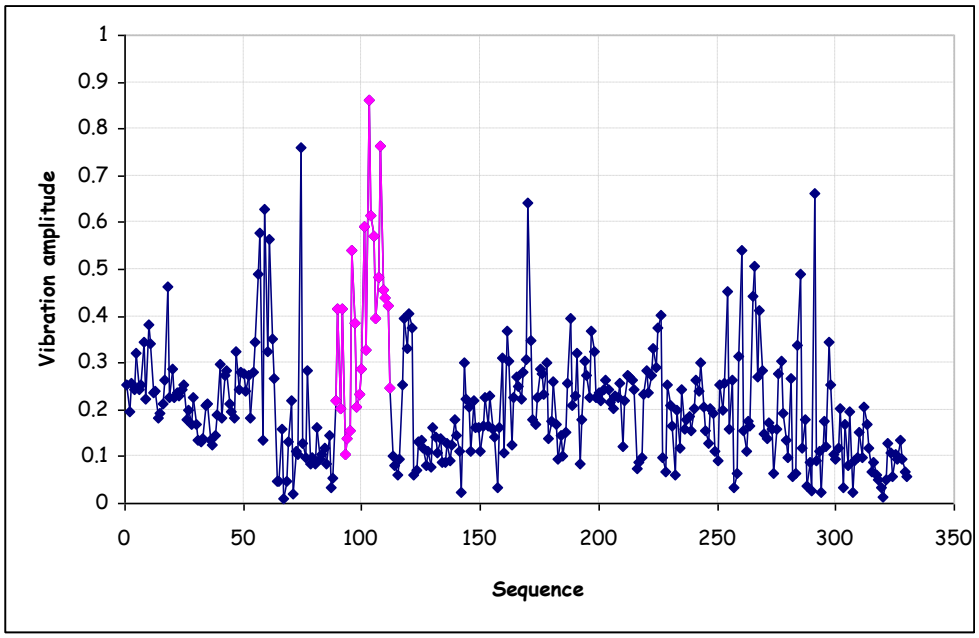

Figure 4-22: Component Fit 41 1T Amplitudes

The data for this Component Fit has also been plotted in polar coordinates to show the amplitude and phase information in Figure 4-23. The highlighted data points correspond to the points indicated above that generated significant Fitness Score values. The figure also shows the tracking line between successive points in the highlighted region. It can be observed that the points do not concentrate in any one part of the amplitude/phase space or appear to move across the amplitude/phase space in any defined order; the points, with regard to their phase distribution, essentially appear random. In this case successive large amplitude values (large

radius on the chart) will automatically lead to large magnitudes for the vector differences as the points appear to have random phase values. This accounts for the similarity between the magnitudes of the vector differences and the harmonic amplitudes observed. For this reason using magnitudes of vector differences as anomaly model inputs was not pursued further.

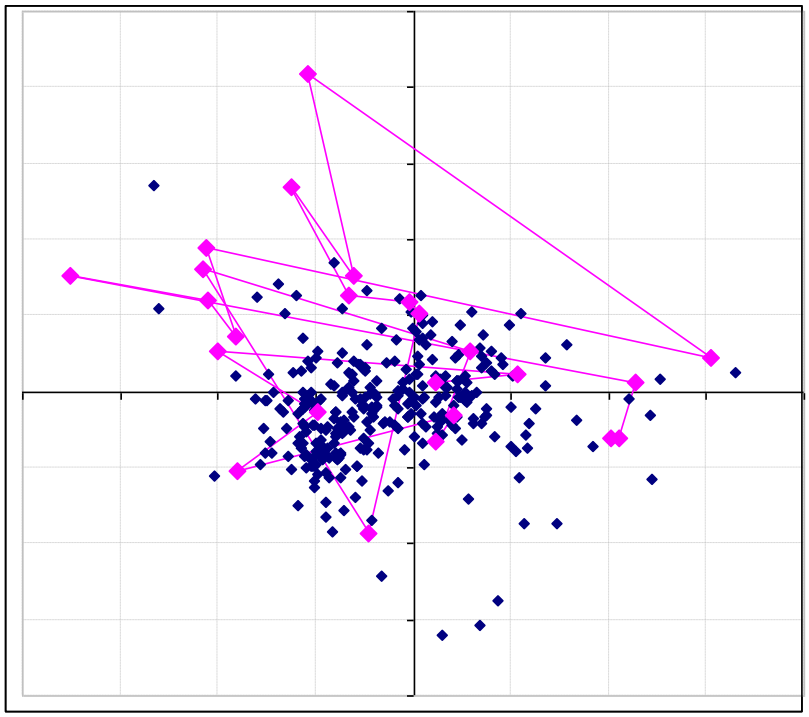

Figure 4-23: Component Fit 41 1T Amplitudes and Phases

4.2.3 Fitness Score values dominated by amplitude values only

The anomaly model based on the polar coordinates of the 1T amplitude/phase information was used to generate predictions for the Component Fits. An extract of the Fitness Score values is shown in Figure 4-24 together with the (negative) 1T amplitudes. Strong correlation was observed between the two traces. Measured over all 11,616 acquisitions of the Cruise dataset a correlation of 0.86 was obtained. This indicates that the phase information has very little influence in the anomaly model output; the outputs are dominated by the amplitude values alone. This can also be deduced from the typically circular clusters observed when the amplitude/phase data are plotted as a polar chart and the observation that successive acquisitions appear to have random angular positions. In this case the likelihood of an anomaly will increase simply as a function of its distance from the centre of the cluster (radius) and not a function of its angular position with the cluster. Since the radial distance equates to the harmonic amplitude and phase to the angular position it indicates that phase will have little influence on the anomaly model outputs. No further use was made of phase information in the work.

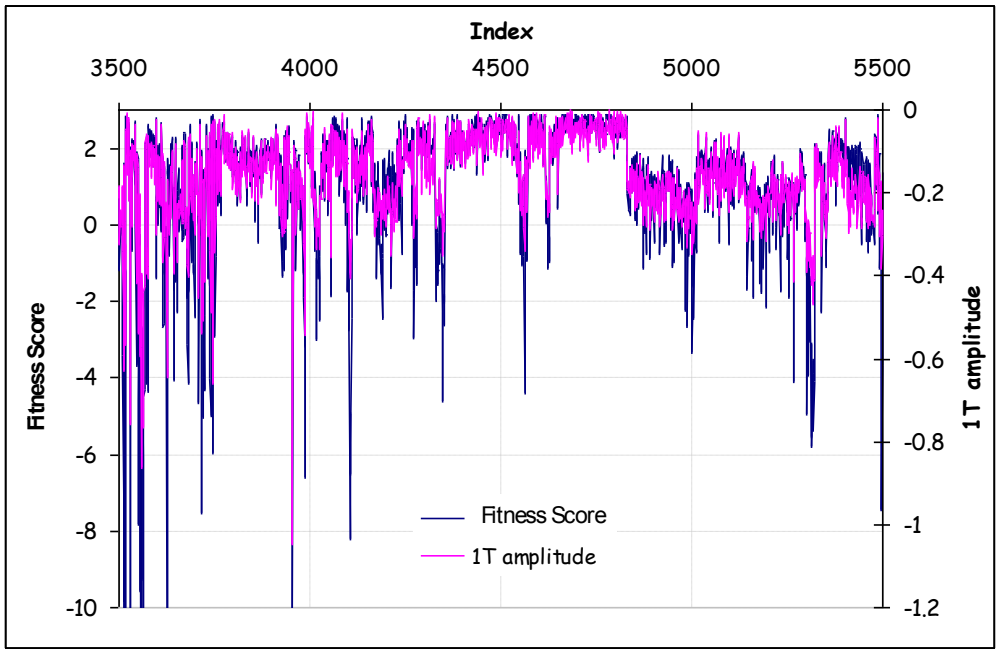

Figure 4-24: Extract of (negative) 1T Amplitudes and Fitness Score Values

4.3 Anomaly models using different input harmonics

4.3.1 Data processing techniques used

Analysis was performed to investigate the most suitable combination of inputs that identify anomalies. A 5 point median filter was used in accordance with common practice when processing CI's. The following anomaly models were constructed using the Cruise database:

- Separate models built on 1,2,3,4 and 5T Radial
- Other models built on the following combinations:
  - 1,2,3,4,5T
  - 2,3,4,5T
  - 2,4,5T
  - 2,3,4T

The models were used to identify anomalies by using the model probability of anomaly outputs. Abnormalities that had a probability greater than 0.9 were extracted for each aircraft Component Fit. The start\end period of a continuous alert was identified and the maintenance database interrogated to link anomalies with maintenance actions.

It was concluded that the most effective approach was to combine multiple harmonics into a single model to provide general fault detection; maintaining a separate 1T model remains useful to identify balance issues. The results for the 1T model are shown in Table 4-6. The results for the combined 2T, 3T and 4T model are shown in Table 4-7. The tables show details of the aircraft Component Fit (ComponentFitId, Sequence and Registration), the date of the alert and details of the alert including Probability of Anomaly to indicate the confidence in the alert together with the Fitness Score combined with the maintenance action (if available) detailed

in the maintenance database that corresponded most closely with the alert. Table 4-7 also includes an “Alerts in Individual Harmonics” column. This shows any individual harmonic models that alerted at the same time as the combined 2T, 3T and 4T model. For example, Row 1 shows that on 29/10/2007 the 1T, 3T, 4T and 5T individual models (four models) were alerting together with the 2T, 3T and 4T combined model (one model). Twelve anomaly alerts were identified by the 1T model with 7 alerts being associated with maintenance actions. Eighteen anomaly alerts were identified by the combined model with 15 alerts being able to be associated with maintenance actions. This represents a high proportion and indicates that anomaly models using combined harmonic inputs are effective at identifying potential faults.

Table 4-6: IHUMS Tail Rotor Model Alerts 1T Radial Model

Component Fit ID	Sequence	Date	Registration	Fitness Score (FS)	Probability of Anomaly (PA)	Maintenance Action
3	102	03/03/2007	G-BLPM	-7.15142	0.9438354	Yellow and Blue flapping bearings worn. Red blade removed for access.
4	4	05/04/2007	G-BLPM	-5.891846	0.919758	Maintenance requirement, Tail rotor balance to be carried out.
16	434	25/10/2007	G-BMCW	-6.316968	0.9295227	BLUE BLACK WHITE T/R S/SPINDLE FAILED PULL OFF CHECK SPINDLR TO BE REPLACED,
41	61	14/11/2006	G-TIGF	-15.67309	0.9854285	IHUMS Tail rotor RTB requirements
41	113	01/02/2007	G-TIGF	-6.810799	0.9386261	Tail Rotor IHUMS RTB's required
41	269	15/10/2007	G-TIGF	-6.409599	0.931393	? Spikes
42	172	20/10/2008	G-TIGF	-9.111687	0.9634778	? Spike
55	492	29/12/2007	G-TIGO	-5.662749	0.9135376	? Trend but no maint data (dec 08)
75	238	29/01/2007	G-TIGV	-11.38692	0.9751208	? But TAIL ROTOR BLADE swap seems to cause alert
89	412	26/03/2007	G-BWWI	-14.05487	0.9825414	long high period starts with TAIL ROTOR BLACK SLEEVE AND SPINDLE ASSY. FAILED 50HR. PULL-OFF CHECK.
89	414	27/03/2007	G-BWWI	-14.05487	0.9825414	TAIL ROTOR G.BOX - Suspect cause of high tail rotor vibration.
107	98	05/06/2007	LN-OLC	-9.560049	0.9664071	? Trend but no maint data (Jun 07)

Table 4-7: IHUMS Tail Rotor Model Alerts 2T, 3T & 4T Radial Model

Component Fit ID	Sequence	Date	Registration	Fitness Score (FS)	Probability of Anomaly (PA)	Alerts in Individual Harmonics	Maintenance Action
16	436	29/10/2007	G-BMCW	-7.929957	0.9516584	1, 3, 4 & 5	BLUE BLACK WHITE T/R S/SPINDLE FAILED PULL OFF CHECK SPINDLR TO BE REPLACED,
33	153	23/09/2008	G-TIGC	-5.841379	0.9107861	4	Yellow tail rotor flapping hinge bearings worn (also later Black and White tail rotor flapping hinge bearings found worn on 750 hr inspection)
36	18	27/09/2006	G-TIGE	-16.31388	0.989189	3 & 4	Blue ,yellow and black tail rotor sleeve and spindle flapping hinge bearings worn.
36	71	13/11/2006	G-TIGE	-9.405784	0.9659137	2 & 3	blue and black flapping hinge bearings worn
36	258	03/05/2007	G-TIGE	-20.46608	0.9933012	2, 3 & 4	Pilot Reports Vibration on tail rotor Needle bearings and Inner race found worn on Black and Yellow tail rotor hub assy.
37	69	06/07/2007	G-TIGE	-6.683832	0.9317327	4	part of: Found during the 50 MI pull of check the RED TRB sleeve spindle bearing to high. (approx. 8 Lbs) Also a lot of brinelling on RED sleeve. Replace
37	627	04/11/2008	G-TIGE	-7.150917	0.940396	3 & 4	Blue T/R flapping hinge bearing worn.
42	172	20/10/2008	G-TIGF	-24.97542	0.9956075	-	? short period
42	272	30/12/2008	G-TIGF	-9.24098	0.964651	2	Red TR flapping hinge brinelled
48	344	30/04/2008	G-TIGJ	-13.83395	0.9847144	3	Yellow tail rotor flapping hinge bearing req. replacement. Blue sleeve and spindle on TRH req. replacement. Found during 50 hr insp.
48	402	21/07/2008	G-TIGJ	-23.97768	0.9952105	3	TR White flapping bearing U/S.

Component Fit ID	Sequence	Date	Registration	Fitness Score (FS)	Probability of Anomaly (PA)	Alerts in Individual Harmonics	Maintenance Action
66	20	15/09/2006	G-TIGS	-28.91406	0.9967821	2 & 3	Red tail rotor flapping hinge bearing found to be stiff and notchy
66	91	30/10/2006	G-TIGS	-6.289216	0.9229196	3	Daily inspection, following tail rotor pitch links found u/s, bearings worn.
66	441	17/04/2007	G-TIGS	-5.865495	0.9115072	3	BLUE AND YELLOW TAIL ROTOR PITCH LINKS TO BE REPLACED BEARINGS WORN.
66	1011	06/05/2008	G-TIGS	-8.273859	0.9556646	-	? Very noisy with drop outs
67	9	22/09/2008	G-TIGS	-15.24505	0.9875329	3	IHUMS showing excessive vibrations from tail rotor.
67	30	17/10/2008	G-TIGS	-7.090832	0.9393739	3	? Poss missing maint
80	87	17/11/2008	G-TIGG	-11.10766	0.975835	2 & 3	Blue sleeve/spindle bearings worn. Red and black flapping hinge bearings worn.
83	1	13/02/2008	G-BWMG	-9.855365	0.9690419	-	? First point. Very little data
89	104	25/10/2006	G-BWWI	-6.39331	0.9253971	2	red tail rotor flapping hinge brg worn
89	300	23/01/2007	G-BWWI	-6.201467	0.9207379	1 & 4	Caused by: TAIL ROTOR BLACK SLEEVE AND SPINDLE ASSY. FAILED 50HR. PULL-OFF CHECK.
93	759	29/10/2007	G-BWZX	-5.81036	0.909846	3	Trending until end of fit (gearbox due overhaul)

4.4 Anomaly models incorporating trend analysis

4.4.1 Data processing techniques used

Analysis was performed to investigate processing techniques that improve the visibility of data features and reduce the effects of noise. An illustration of the data processing techniques investigated is shown in Figure 4-25. As a control models were also built using the unprocessed harmonic magnitudes. It was expected that due to the levels of noise observed in the data a significant number of alerts would be generated that did not relate to an actual anomaly. In this analysis work has focused mainly on Cruise database.

A Savitzky-Golay (SG) filter using a 20 point second order filter was used to preserve any trends in the data whilst eliminating any localised variations that are likely to be due mainly to noise; unlike filters such as window averaging the Savitzky-Golay filters are effective at preserving the amplitudes of underlying narrow width features and should therefore be effective at preserving short term trends whilst eliminating high levels of noise, Figure 4-25b.

A disadvantage of the smoothing filter, however, is the natural tendency to smooth step changes in the data. An alternative approach that would preserve any step changes but extract trends in the data was to use linear regression to track trends in the data. Similar to the tracking algorithm developed in the previous section the algorithm worked by taking each successive acquisition and comparing it to the current trend by measuring the perpendicular distance from the point to the linear trend line that characterised the trend. If the distance was within a prescribed number of standard deviations the point was added to the trend and the linear trend line updated. If the point was outside the trend it was used to generate a new linear trend, Figure 4-25c. A trend anomaly model was developed from this process by measuring the difference between each point in the trended data and the median of the proceeding points. It was assumed for this analysis that any maintenance action performed would return the TR to a healthy state. Therefore after each lifetime the number of points used to calculate a median value was reset (zeroed). This had the effect of taking into account any jumps in the amplitude values that followed a maintenance action and effectively normalised the data.

To enable identification of the ability of the different models to identify faults based on the individual TR harmonics, separate anomaly models were constructed for each harmonic.

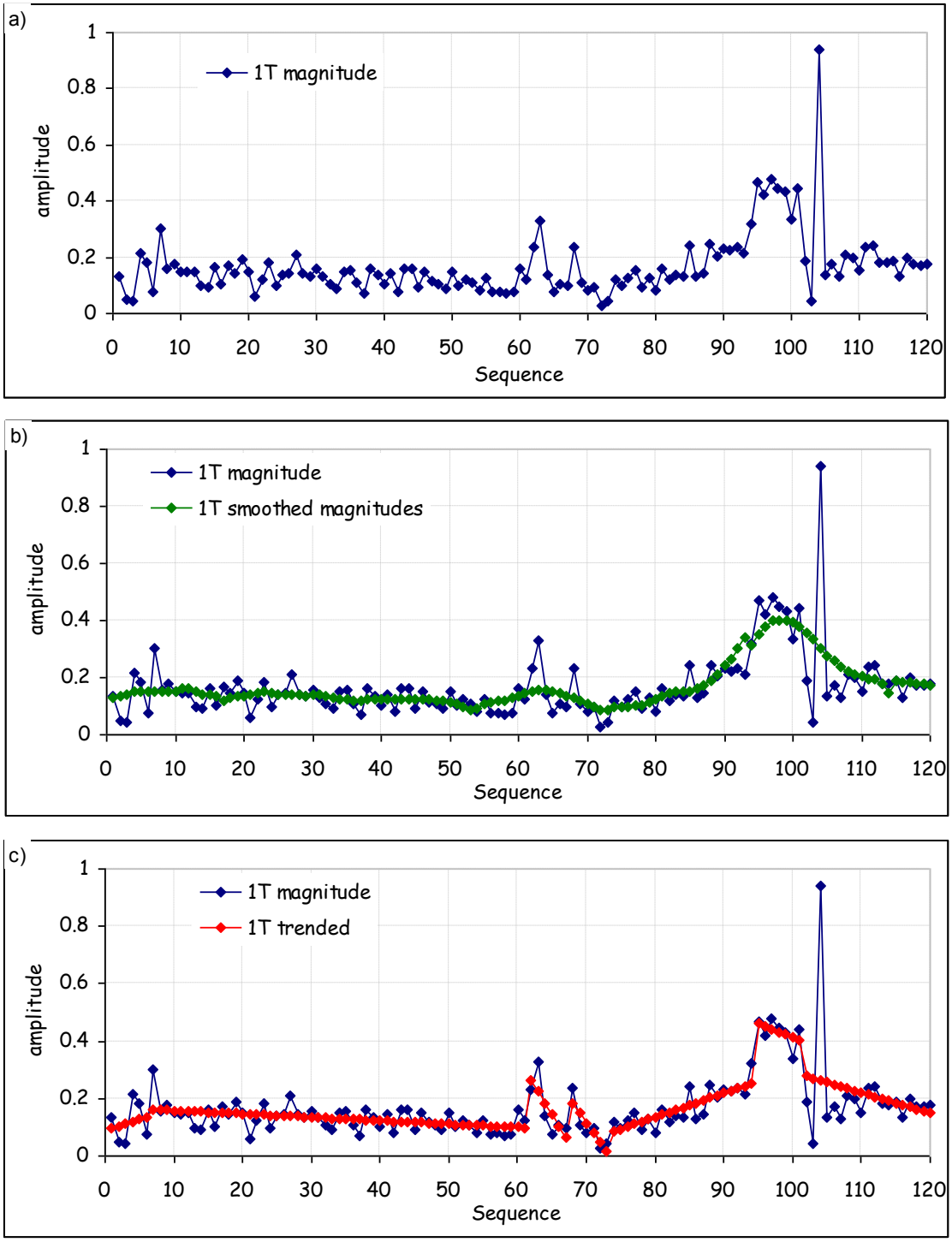

Figure 4-25: Trending Component Fit Amplitudes

4.4.2 Trend models

Separate anomaly models were constructed for each individual harmonic for the Cruise flight condition using the harmonic amplitudes, the SG smoothed amplitudes and the trended amplitude data. The following charts show both the PA parameter and an Alert parameter. The Alert parameter was derived by filtering the PA parameter such that to be considered as an alert the PA must exceed a specified threshold for at least 3 out 4 continuous points. For each alert the maintenance database was interrogated and the next maintenance action following the alert within a 1 month window was extracted. In some cases there was no additional maintenance performed within a month of an alert. The number of days between the alert and the identified maintenance action was also recorded. Maintenance that occurred more than a few days after the alert would not be considered as triggered by the identified anomaly.

4.4.2.1 Anomaly model using the harmonic amplitudes

The alerts for the 1T, 2T and 3T harmonics across all 11,616 TR acquisitions in the Cruise dataset are shown in Figure 4-26. The charts show both the PA parameter and the filtered alerts. The corresponding 4T, 5T and 10T harmonics are shown in Figure 4-27. The 1T model generated a total of 20 alerts. The alerts and corresponding maintenance (within a 1 month window) are shown in Table 4-8. The alerts were compared with results described in Section 4.3.1 using the 5-point median filter, Table 4-6. While a number of additional anomalies were identified, all the anomalies identified in were identified using the raw amplitudes. The low number of additional anomalies would indicate that the use of a median filter in this case had little effect on the results and that the noise in the data is more complicated than 1 or 2 point spikes. No correlation between alerts of the individual harmonics was observed when they were visually compared. Overall, as expected the number of significant PA values was much greater than the number of extracted alerts because most of the high PA values were caused by individual spikes in the data due to noise. However, the 3T harmonic unusually generates just a single alert. The reasons for this are unclear and no further explanation can be offered.

The results of the individual harmonics were combined by taking at each acquisition the maximum PA value of any of the harmonic data. The alert filtering algorithm was then applied to the combined PA parameter to generate a combined alert parameter. The combined model generated a total of 74 alerts. The alerts and corresponding maintenance are shown in Table 4-9. 42 of the alerts could be associated with any maintenance action of which only 32 occurred less than 10 days after the alert.

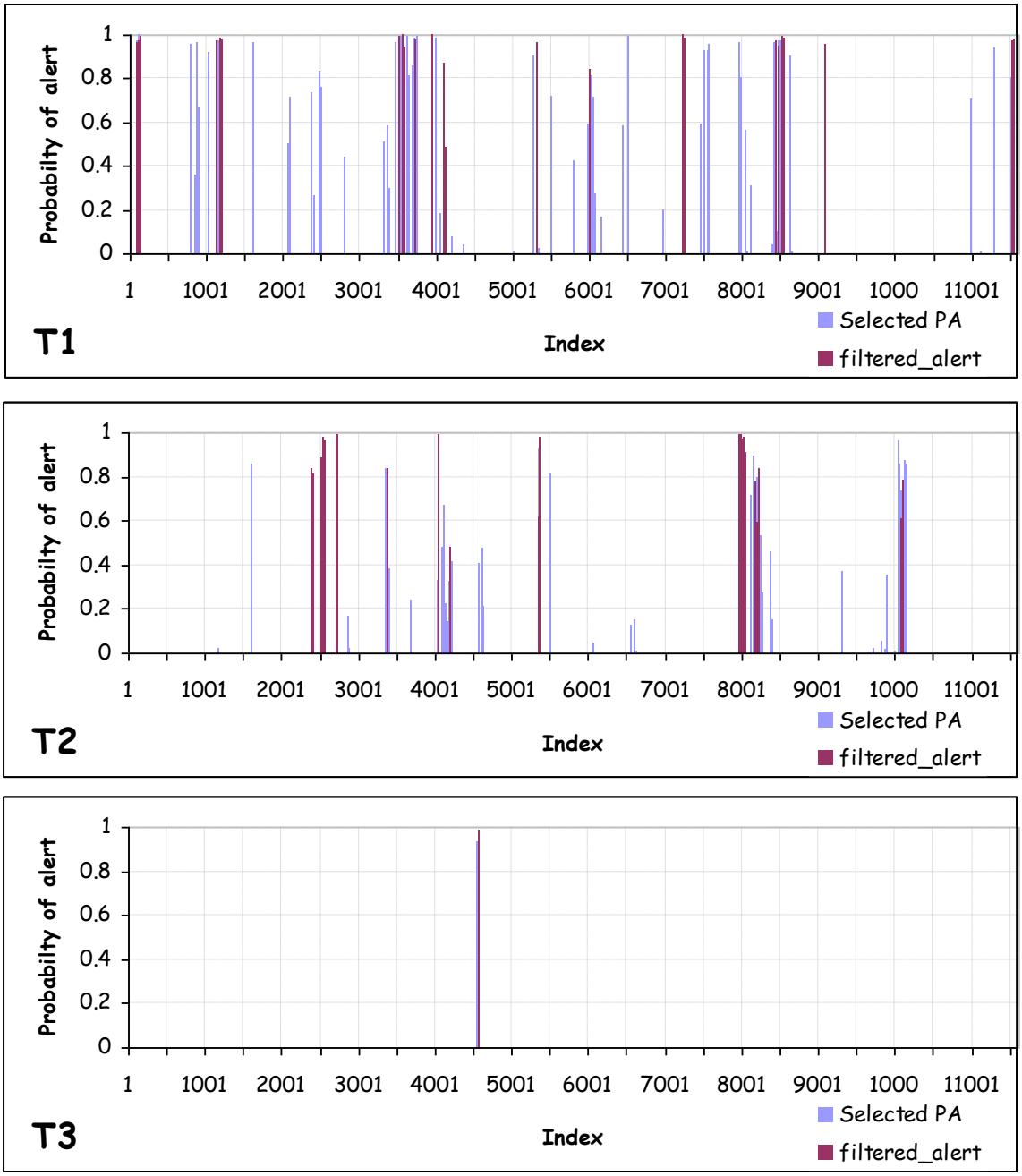

Figure 4-26: Alerts for 1/2/3T Harmonics from Amplitude Anomaly Model

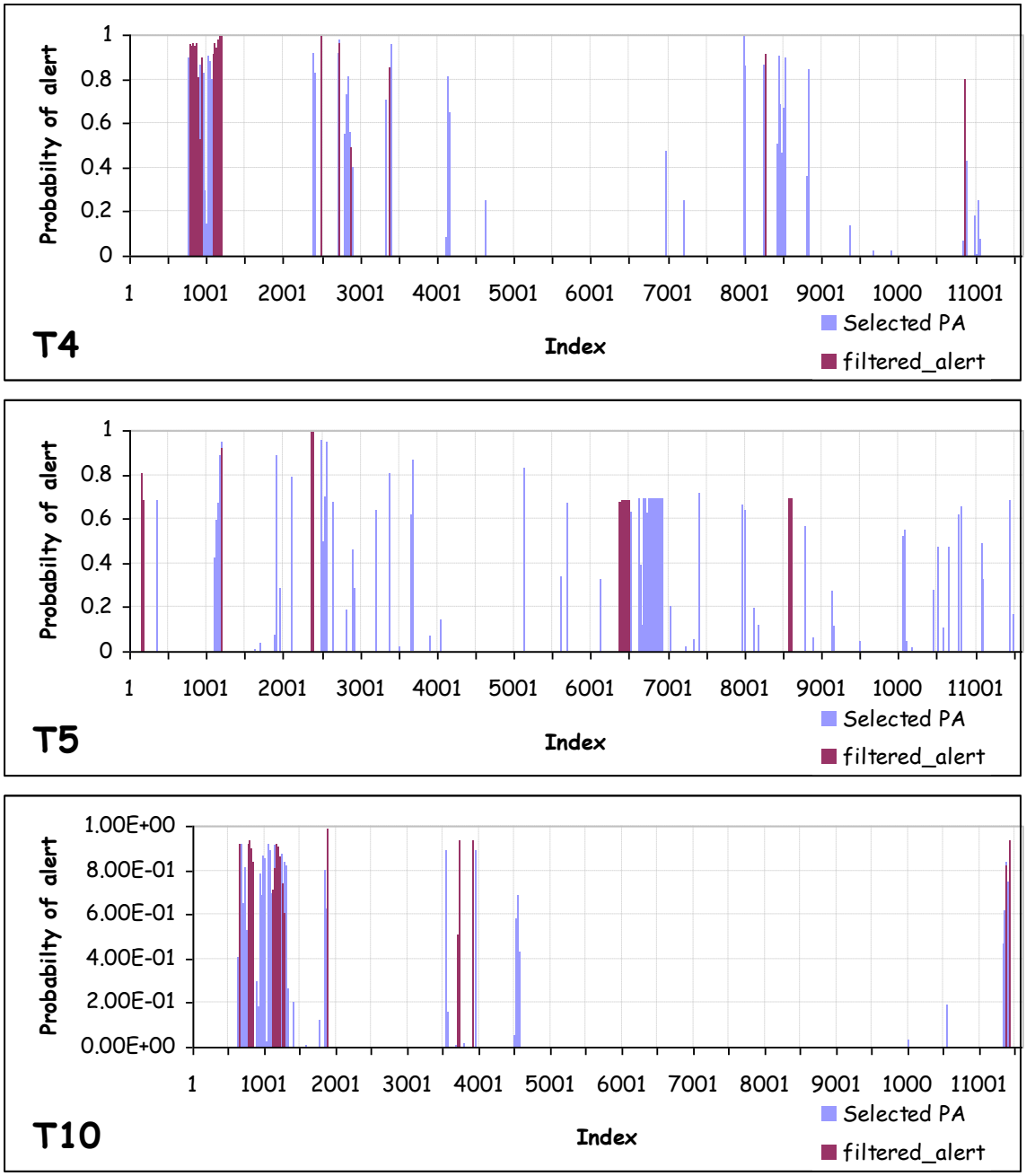

Figure 4-27: Alerts for 4/5/6T Harmonics from Amplitude Anomaly Models

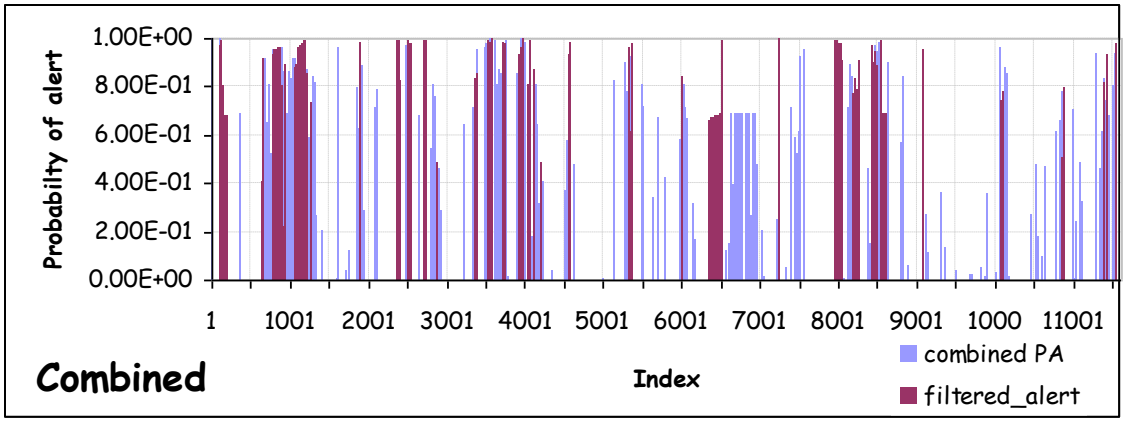

Figure 4-28: Combined Alerts for 1/2/3/4/5/6T Harmonics from Amplitude Anomaly Models

Table 4-8: Alerts and Associated Maintenance Actions 1T Harmonic, Anomaly Model Derived from Raw Harmonic Amplitudes

Registration	ComponentFitID	Sequence	Date	Number of associated maintenance records	Maintenance action description for first maintenance action	Maintenance action description for second maintenance action	Maintenance action description for third maintenance action	alert_time	alert_index	Maintenance_lag (days)
G-BLPM	3	105	07/03/2007	1	Yell & Blu. Flapping brngs. worn.			03/03/2007	102	4
G-BLPM	4	5	06/04/2007	1	Tail Rotor Balance			05/04/2007	124	1
G-BMCW	16	374	09/07/2007	2	PMC Creation	5 Pitch change links worn		15/06/2007	1129	24
G-BMCW	16	405	12/09/2007	1	Red T/R bearing worn.			04/09/2007	1166	8
G-BMCW	16	419	10/10/2007	0				10/10/2007	1184	0
G-BMCW	16	435	27/10/2007	3	50hr INSP.	50hr INSPECTION	50hr INSP	25/10/2007	1199	2
G-TIGF	41	63	15/11/2006	1	RTB'S required on Tail rotor			14/11/2006	3516	1
G-TIGF	41	112	30/01/2007	1	IHUMS T/R RTB's			30/01/2007	3566	0
G-TIGF	41	124	26/03/2007	1	blue sleeve and spindle timex			08/03/2007	3576	18
G-TIGF	41	277	31/10/2007	1	T/R spider bearing replaced			15/10/2007	3723	16
G-TIGF	42	193	03/11/2008	1	Tail rotor pitch links.			19/10/2008	3955	15
G-TIGJ	47	50	30/09/2006	1	IHUMS TAIL ROTOR BALANCE			30/09/2006	4108	0

Registration	ComponentFitID	Sequence	Date	Number of associated maintenance records	Maintenance action description for first maintenance action	Maintenance action description for second maintenance action	Maintenance action description for third maintenance action	alert_time	alert_index	Maintenance_lag (days)
G-TIGO	55	492	29/12/2007	0				29/12/2007	5320	0
G-TIGS	66	705	06/09/2007	0				06/09/2007	6006	0
G-TIGV	75	298	26/01/2007	0				26/01/2007	7230	0
G-BWWI	89	318	30/01/2007	1	IHUMS ADJUSTMENT REQUIRED			28/01/2007	8429	2
G-BWWI	89	359	19/02/2007	3	High T/R vertical balance (IHUMS)	Tail rotor pitch links	Tail rotor balance	15/02/2007	8468	4
G-BWWI	89	413	27/03/2007	0				27/03/2007	8528	0
G-BWWI	90	550	25/04/2008	1	IHUMS warning			23/04/2008	9078	2
LN-OLC	107	98	05/06/2007	0				05/06/2007	11546	0

Table 4-9: Alerts and Associated Maintenance Actions Combined 1T/2T/3T/4T/5T/10T Harmonics, Anomaly Models Derived from Individual Raw Harmonic Amplitudes

Registration	ComponentFitID	Sequence	Date	Number of associated maintenance records	Maintenance action description for first maintenance action	Maintenance action description for second maintenance action	Maintenance action description for third maintenance action	alert_time	alert_index	Maintenance_lag (days)
G-BLPM	3	105	07/03/2007	1	Yell & Blu. Flapping brngs. worn.			03/03/2007	102	4
G-BLPM	4	5	06/04/2007	1	Tail rotor Balance			05/04/2007	124	1
G-BLPM	4	31	03/05/2007	0				03/05/2007	151	0
G-BLPM	4	55	05/06/2007	1	tail rotor boot torn			05/06/2007	175	0
G-BMCW	14	16	09/08/2005	0				09/08/2005	645	0
G-BMCW	14	25	12/08/2005	0				12/08/2005	654	0
G-BMCW	16	65	20/10/2006	1	4 TR Pitch links worn			16/10/2006	818	4
G-BMCW	16	93	04/11/2006	0				04/11/2006	858	0
G-BMCW	16	119	21/11/2006	0				21/11/2006	884	0
G-BMCW	16	134	30/11/2006	0				30/11/2006	899	0
G-BMCW	16	193	08/01/2007	1	Red t/r pitch link			27/12/2006	937	12
G-BMCW	16	277	05/03/2007	0				05/03/2007	1042	0

Registration	ComponentFitID	Sequence	Date	Number of associated maintenance records	Maintenance action description for first maintenance action	Maintenance action description for second maintenance action	Maintenance action description for third maintenance action	alert_time	alert_index	Maintenance_lag (days)
G-BMCW	16	315	03/04/2007	1	%x T/R. pitch links worn.			28/03/2007	1075	6
G-BMCW	16	317	04/04/2007	0				04/04/2007	1082	0
G-BMCW	16	331	18/04/2007	0				18/04/2007	1096	0
G-BMCW	16	337	20/04/2007	0				20/04/2007	1102	0
G-BMCW	16	350	16/05/2007	0				16/05/2007	1115	0
G-BMCW	16	374	09/07/2007	2	PMC Creation	5 Pitch change links worn		09/07/2007	1139	0
G-BMCW	16	435	27/10/2007	3	50hr INSP.	50hr INSPECTION	50hr INSP	27/10/2007	1200	0
G-BMCW	16	467	16/11/2007	1	Bearings worn			03/11/2007	1211	13
G-BMCW	16	539	19/12/2007	0				19/12/2007	1271	0
G-TIGC	32	276	18/04/2007	1	Black t/r sleeve suspect wear.			18/04/2007	1888	0
G-TIGC	32	291	02/05/2007	1	Pitch change boot damaged			20/04/2007	1893	12
G-TIGC	33	136	11/08/2008	0				11/08/2008	2387	0

Registration	ComponentFitID	Sequence	Date	Number of associated maintenance records	Maintenance action description for first maintenance action	Maintenance action description for second maintenance action	Maintenance action description for third maintenance action	alert_time	alert_index	Maintenance_lag (days)
G-TIGC	33	146	18/09/2008	0				18/09/2008	2397	0
G-TIGC	33	155	25/09/2008	2	Worn	Worn		23/09/2008	2405	2
G-TIGE	36	18	27/09/2006	2	T/R FLAPPING HINGE BEARINGS WORN	T/R Pitch Links Worn Bearings		27/09/2006	2494	0
G-TIGE	36	70	13/11/2006	1	flapping hinge bearings worn			13/11/2006	2546	0
G-TIGE	36	259	04/05/2007	1	Pilot Reports Vibration Tail Rotor			03/05/2007	2733	1
G-TIGE	37	152	20/08/2007	2	Forgotten to raise PMC	During pull offs red spindle u/s		31/07/2007	2875	20
G-TIGE	37	603	09/10/2008	0				09/10/2008	3368	0
G-TIGE	37	612	20/10/2008	1	BLK & BLUE TR sleeve binding			16/10/2008	3376	4
G-TIGF	41	63	15/11/2006	1	RTB'S required on Tail rotor			14/11/2006	3516	1
G-TIGF	41	112	30/01/2007	1	IHUMS T/R RTB's			30/01/2007	3566	0

Registration	ComponentFitID	Sequence	Date	Number of associated maintenance records	Maintenance action description for first maintenance action	Maintenance action description for second maintenance action	Maintenance action description for third maintenance action	alert_time	alert_index	Maintenance_lag (days)
G-TIGF	41	124	26/03/2007	1	blue sleeve and spindle timex			08/03/2007	3576	18
G-TIGF	41	261	27/09/2007	0				27/09/2007	3715	0
G-TIGF	41	277	31/10/2007	1	T/R spider bearing replaced			15/10/2007	3723	16
G-TIGF	42	131	05/09/2008	1	tail rotor gear box leaking			04/09/2008	3914	1
G-TIGF	42	193	03/11/2008	1	Tail rotor pitch links.			19/10/2008	3955	15
G-TIGF	42	272	30/12/2008	1	Red TR flapping hinge			29/12/2008	4055	1
G-TIGJ	47	74	11/10/2006	1	tail rotor pitch link worn			03/10/2006	4114	8
G-TIGJ	47	144	10/11/2006	1	T/R pitch links worn			08/11/2006	4196	2
G-TIGJ	48	343	30/04/2008	1	Flapping hinge bearing/sleeve,spin.			21/04/2008	4563	9
G-TIGO	55	492	29/12/2007	0				29/12/2007	5320	0
G-TIGS	66	20	15/09/2006	2	TAIL ROTOR BALANCE	IHUMS tail rotor vib exceedance		14/09/2006	5357	1
G-TIGS	66	705	06/09/2007	0				06/09/2007	6006	0

Registration	ComponentFitID	Sequence	Date	Number of associated maintenance records	Maintenance action description for first maintenance action	Maintenance action description for second maintenance action	Maintenance action description for third maintenance action	alert_time	alert_index	Maintenance_lag (days)
G-TIGS	66	1021	20/05/2008	1	Sleeve/Spindles brinelling			15/05/2008	6354	5
G-TIGS	66	1041	06/06/2008	0				06/06/2008	6379	0
G-TIGS	66	1083	05/07/2008	1	TR Pitch links worn			15/06/2008	6393	20
G-TIGS	66	1152	03/09/2008	0				03/09/2008	6490	0
G-TIGS	67	1	15/09/2008	0				15/09/2008	6500	0
G-TIGS	67	8	22/09/2008	3	tail rotor vibrations excessive	T/R Vibration Adjustments Required	tail rotor vibes spiked	22/09/2008	6507	0
G-TIGV	75	298	26/01/2007	0				26/01/2007	7230	0
G-TIGG	80	39	01/09/2008	0				01/09/2008	7996	0
G-TIGG	80	72	08/10/2008	2	TR pitch change spider boot missing	PITCH LINKS FOUND WORN [50h]		06/10/2008	8027	2
G-TIGG	80	87	17/11/2008	3	T/R inner race RTS G-TIGF	Flapping hinge RTS G-TIGE	TGB 750H inspection	17/11/2008	8044	0
G-BWWI	89	74	10/10/2006	0				10/10/2006	8189	0

Registration	ComponentFitID	Sequence	Date	Number of associated maintenance records	Maintenance action description for first maintenance action	Maintenance action description for second maintenance action	Maintenance action description for third maintenance action	alert_time	alert_index	Maintenance_lag (days)
G-BWWI	89	108	28/10/2006	1	red flapping hinge brg worn			27/10/2006	8222	1
G-BWWI	89	128	06/11/2006	0				06/11/2006	8243	0
G-BWWI	89	141	13/11/2006	2	Tail rotor sleeve guide.	Flapping hinge.		13/11/2006	8256	0
G-BWWI	89	318	30/01/2007	1	IHUMS ADJUSTMENT REQUIRED			30/01/2007	8433	0
G-BWWI	89	328	02/02/2007	0				02/02/2007	8443	0
G-BWWI	89	359	19/02/2007	3	High T/R vertical balance (IHUMS)	Tail rotor pitch links	Tail Rotor balance	17/02/2007	8472	2
G-BWWI	89	390	12/03/2007	1	T/R Vib's T/R Flapping Hinge Bearings Inner races:Inspection.:Vib's. T/R Flapping Hinge Bearings I			25/02/2007	8483	15
G-BWWI	89	413	27/03/2007	0				27/03/2007	8528	0
G-BWWI	90	64	06/05/2007	0				06/05/2007	8593	0
G-BWWI	90	98	12/06/2007	1	IHUMS t/r bal adj.			15/05/2007	8602	28
G-BWWI	90	550	25/04/2008	1	IHUMS warning			23/04/2008	9078	2

Registration	ComponentFitID	Sequence	Date	Number of associated maintenance records	Maintenance action description for first maintenance action	Maintenance action description for second maintenance action	Maintenance action description for third maintenance action	alert_time	alert_index	Maintenance_lag (days)
G-BWZX	93	737	17/09/2007	0				17/09/2007	10088	0
G-BWZX	93	759	26/09/2007	1	brg,s worn			25/09/2007	10109	1
G-BWZX	94	726	23/12/2008	0				23/12/2008	10863	0
G-PUMI	104	503	20/12/2007	1	LBE raised for pics.			19/12/2007	11379	1
G-PUMI	104	555	08/02/2008	0				08/02/2008	11434	0
LN-OLC	107	98	05/06/2007	0				05/06/2007	11546	0

4.4.2.2 Anomaly model using the SG smoothed harmonic amplitudes

The alerts for the 1T, 2T and 3T harmonics across all 11,616 TR acquisitions are shown in Figure 4-29. The charts show both the PA parameter and the filtered alerts. The corresponding 4T, 5T and 10T harmonics are a shown in Figure 4-30. The 1T model generated a total of 12 alerts. The alerts and corresponding maintenance are shown in Table 4-10. As would be expected in comparison to the raw amplitude model outputs most of the high PA values trigger alerts using the smoothed harmonics. Eight of the 12 T1 alerts coincide with the outputs of the model based on 1T raw amplitude data. From visual inspection of the data a number of alerts appear to exist in multiple individual harmonic models. In particular alerts can be seen in the 1T, 4T, 5T and 10T model outputs at approximate index 1100, also in the 1T, 2T, 4T, 5T and 10T model outputs at approximate index 6500 (Component Fit 66), and in the 1T, 2T, 4T, 5T and 10T harmonics at approximate index 8600 (Component Fit 90).

These results are shown for the two Component Fits that had anomalies appearing in all harmonics (except 3T) in Figure 4-32 and Figure 4-33; Figure 4-32 shows the 1T harmonic and PA for Component Fit 66, while Figure 4-33 shows the corresponding values for Component Fit 90. The anomalies occur where the signals flat line. This is characteristic of an instrumentation fault. Since a fault in the signal will typically produce anomalies in all TR harmonics it would be expected that anomalies would be detected in all these harmonics. It is interesting to note that the flat line signal was not identified as an anomaly by the raw amplitudes methods. Nevertheless, while a genuine fault can generate anomalies in several harmonics, a fault that appears in all (or the majority of) harmonics is likely to be due to instrumentation.

The results of the individual harmonics were combined by taking at each acquisition the maximum PA value of any of the harmonic data. The alert filtering algorithm was then applied to the combined PA parameter to generate a combined alert parameter. The combined model generated a total of 61 alerts. The alerts and corresponding maintenance are shown in Table 4-11. 35 of the alerts could be associated with any maintenance action while of those only 22 occurred less than 10 days after the alert.

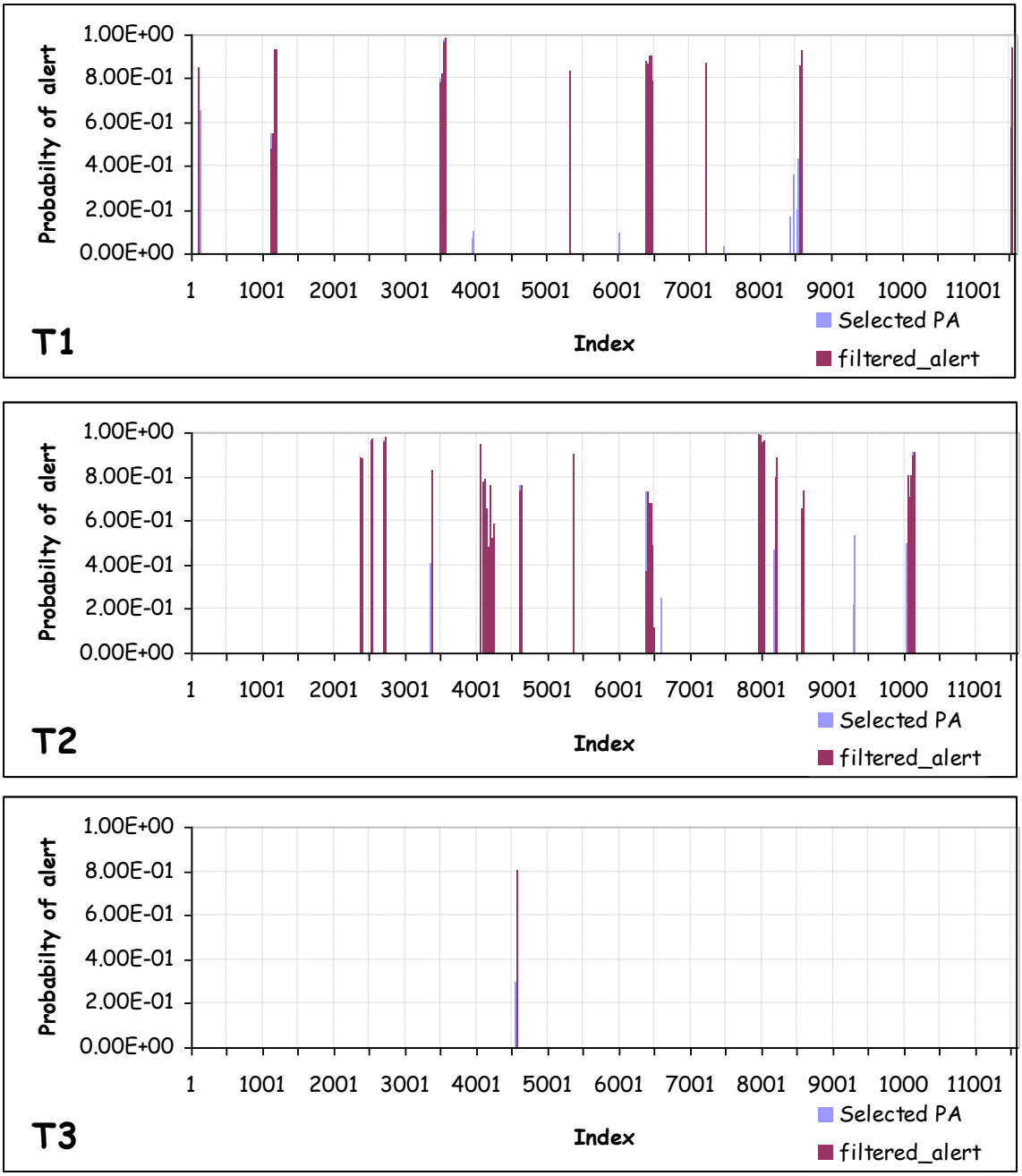

Figure 4-29: Alerts for 1/2/3T Harmonics from SG Smoothed Amplitude Anomaly Model

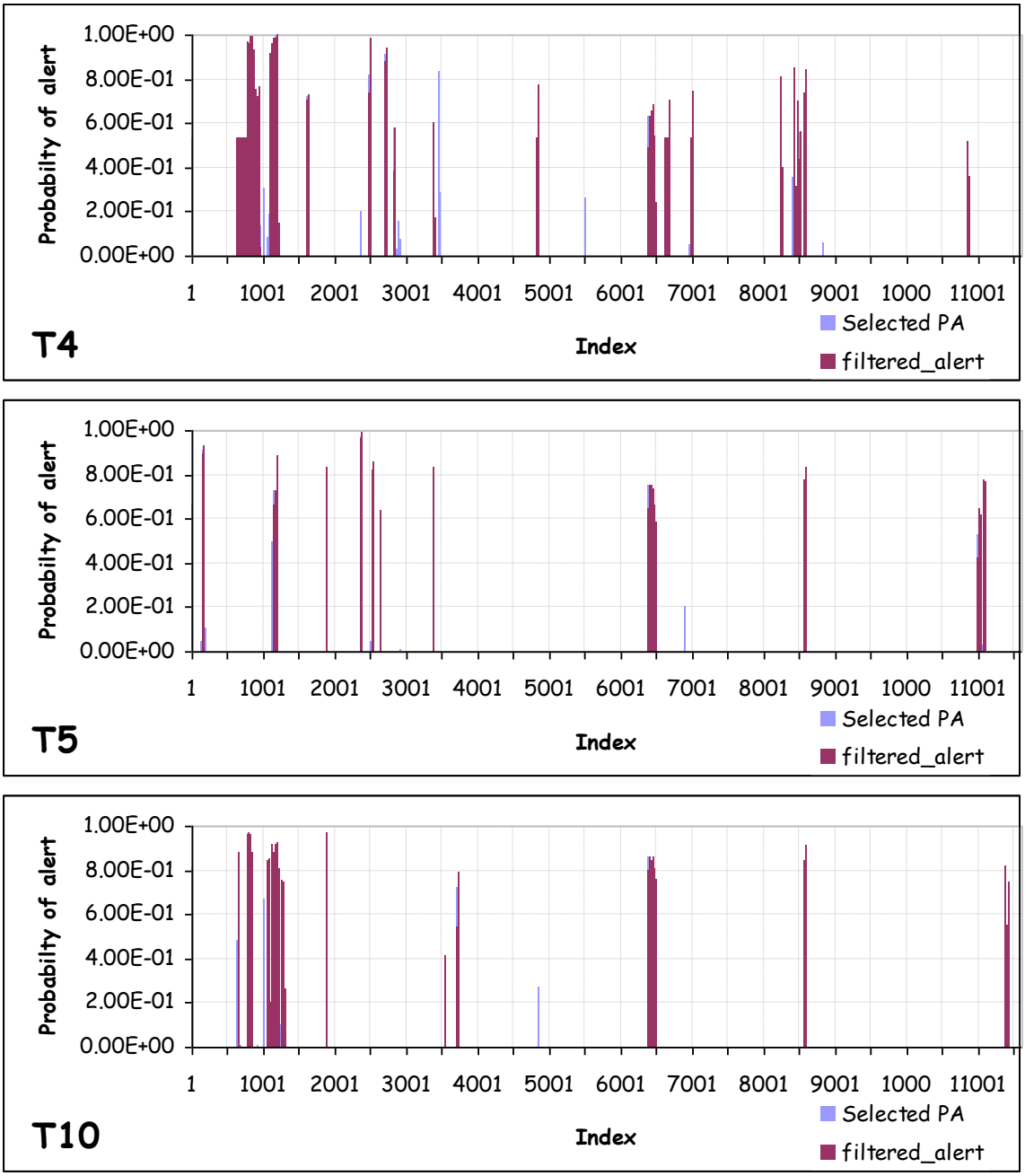

Figure 4-30: Alerts for 4/5/10T Harmonics from SG Smoothed Amplitude Anomaly Model

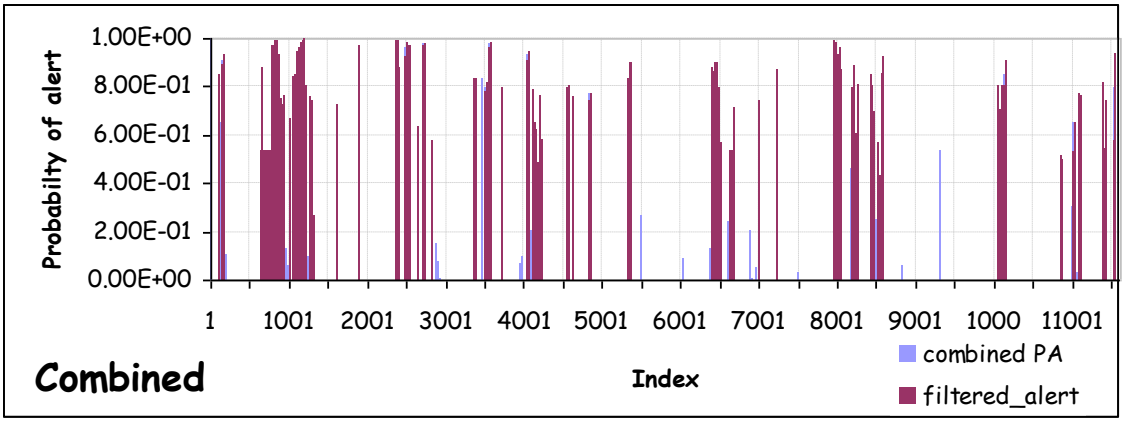

Figure 4-31: Combined Alerts for 1/2/3/4/5/6T Harmonics from SG Smoothed Amplitude Anomaly Models

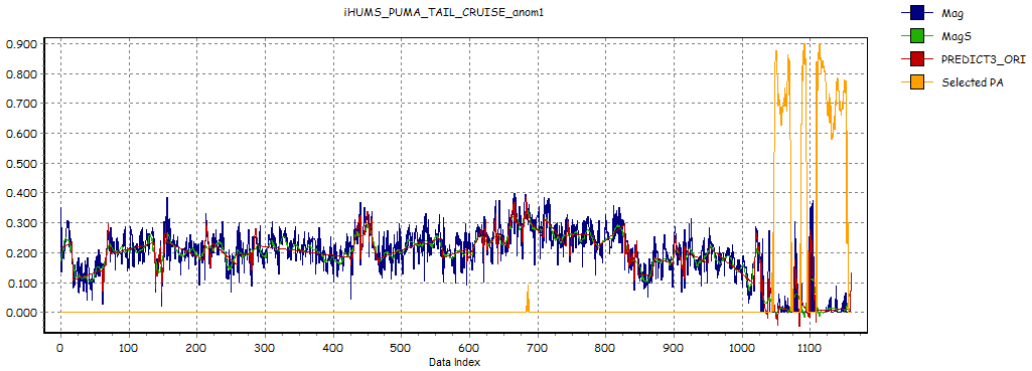

Figure 4-32: 1T Harmonic for Component Fit 66 (SG smoothed amplitude result)

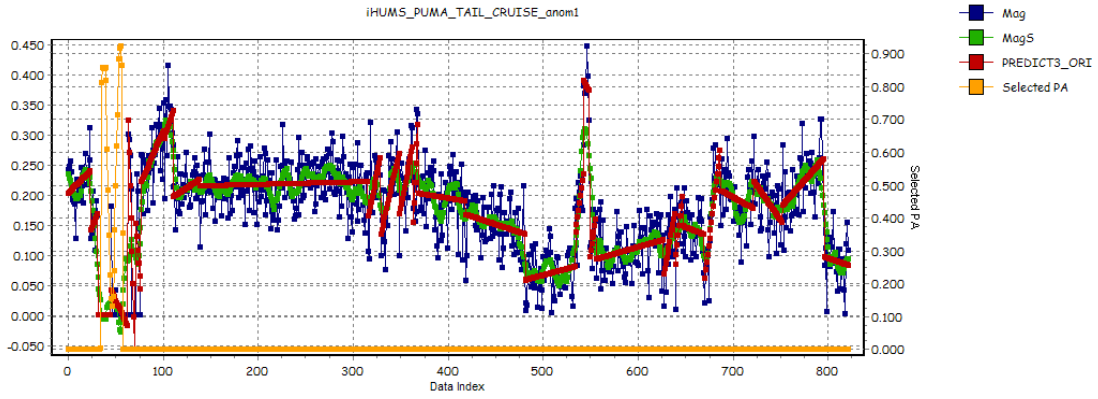

Figure 4-33: 1T Harmonic for Component Fit 90 (SG smoothed amplitude result)

Table 4-10: Alerts and Associated Maintenance Actions 1T Harmonic, Anomaly Model Derived from SG Smoothed Harmonic Amplitudes

Registration	Component Fit ID	Sequence	Date	Number of associated maintenance records	Maintenance action description for first maintenance action	Maintenance action description for second maintenance action	Maintenance action description for third maintenance action	alert_time	alert index	Maintenance_lag (days)
G-BLPM	3	105	07/03/2007	1	Yell & Blu. Flapping brngs. worn.			05/03/2007	103	2
G-BMCW	16	374	09/07/2007	2	PMC Creation	5 Pitch change links worn		20/06/2007	1132	19
G-BMCW	16	418	09/10/2007	1	RTB Adjustments			09/10/2007	1183	0
G-TIGF	41	61	14/11/2006	1	Investigate T/R. Vibration.			14/11/2006	3515	0
G-TIGF	41	112	30/01/2007	1	IHUMS T/R RTB's			29/01/2007	3565	1
G-TIGO	55	489	27/12/2007	0				27/12/2007	5317	0
G-TIGS	66	1083	05/07/2008	1	TR Pitch links worn			27/06/2008	6412	8
G-TIGS	66	1150	18/07/2008	0				18/07/2008	6435	0
G-TIGS	66	1156	08/09/2008	0				08/09/2008	6494	0
G-TIGV	75	298	29/01/2007	0				29/01/2007	7232	0
G-BWWI	90	98	03/05/2007	0				03/05/2007	8588	0
LN-OLC	107	97	05/06/2007	0				05/06/2007	11545	0

Table 4-11: Alerts and Associated Maintenance Actions Combined 1T/2T/3T/4T/5T/10T Harmonics, Anomaly Models Derived from Individual SG Smoothed Harmonic Amplitudes

Registration	ComponentFitID	Sequence	Date	Number of associated maintenance records	Maintenance action description for first maintenance action	Maintenance action description for second maintenance action	Maintenance action description for third maintenance action	alert_time	alert_index	Maintenance_lag (days)
G-BLPM	3	105	07/03/2007	1	Yell & Blu. Flapping brngs. worn.			05/03/2007	103	2
G-BLPM	4	55	05/06/2007	1	tail rotor boot torn			15/05/2007	162	21
G-BMCW	16	97	07/11/2006	0				07/11/2006	862	0
G-BMCW	16	154	12/12/2006	0				12/12/2006	919	0
G-BMCW	16	193	08/01/2007	1	Red t/r pitch link			28/12/2006	944	11
G-BMCW	16	252	12/02/2007	1	Blk,Yel' & Wte T/R Pitch Links Worn			02/02/2007	1003	10
G-BMCW	16	315	03/04/2007	1	%x T/R. pitch links worn.			16/03/2007	1062	18
G-BMCW	16	435	27/10/2007	3	50hr INSP.	50hr INSPECTION	50hr INSP	25/10/2007	1198	2
G-BMCW	16	467	16/11/2007	1	Bearings worn			05/11/2007	1213	11
G-BMCW	16	508	20/12/2007	0				20/12/2007	1273	0
G-BMCW	16	539	25/01/2008	1	PMC.			22/01/2008	1301	3
G-TIGC	32	18	20/09/2006	1	Sleeve and Spindle assy's U/S			07/09/2006	1621	13
G-TIGC	32	291	02/05/2007	1	Pitch change boot damaged			19/04/2007	1891	13
G-TIGC	33	155	25/09/2008	2	Worn	Worn		22/09/2008	2403	3
G-TIGE	36	18	27/09/2006	2	T/R FLAPPING HINGE BEARINGS WORN	T/R Pitch Links Worn Bearings		19/09/2006	2492	8

Registration	ComponentFitID	Sequence	Date	Number of associated maintenance records	Maintenance action description for first maintenance action	Maintenance action description for second maintenance action	Maintenance action description for third maintenance action	alert_time	alert_index	Maintenance_lag (days)
G-TIGE	36	70	13/11/2006	1	flapping hinge bearings worn			13/11/2006	2546	0
G-TIGE	36	170	14/02/2007	2	T/R Slider Guide Worn	Black pitch rod bearings worn		02/02/2007	2635	12
G-TIGE	36	259	04/05/2007	1	Pilot Reports Vibration Tail Rotor			03/05/2007	2734	1
G-TIGE	37	102	27/07/2007	1	Post maintenance Check			05/07/2007	2830	22
G-TIGE	37	628	05/11/2008	1	Blue T/R flapping hinge u/s			30/10/2008	3388	6
G-TIGF	41	61	14/11/2006	1	Investigate T/R. Vibration.			14/11/2006	3515	0
G-TIGF	41	92	06/01/2007	1	Spider end cap disturbed			06/01/2007	3546	0
G-TIGF	41	112	30/01/2007	1	IHUMS T/R RTB's			29/01/2007	3565	1
G-TIGF	41	277	28/09/2007	0				28/09/2007	3717	0
G-TIGF	42	272	30/12/2008	1	Red TR flapping hinge			29/12/2008	4055	1
G-TIGJ	47	74	11/10/2006	1	tail rotor pitch link worn			04/10/2006	4118	7
G-TIGJ	47	87	18/10/2006	0				18/10/2006	4145	0
G-TIGJ	47	118	01/11/2006	0				01/11/2006	4176	0
G-TIGJ	47	144	10/11/2006	1	T/R pitch links worn			09/11/2006	4200	1
G-TIGJ	47	157	21/11/2006	0				21/11/2006	4215	0
G-TIGJ	48	102	26/11/2006	0				26/11/2006	4227	0
G-TIGJ	48	343	30/04/2008	1	Flapping hinge bearing/sleeve,spin.			21/04/2008	4564	9

Registration	ComponentFitID	Sequence	Date	Number of associated maintenance records	Maintenance action description for first maintenance action	Maintenance action description for second maintenance action	Maintenance action description for third maintenance action	alert_time	alert_index	Maintenance_lag (days)
G-TIGJ	48	401	21/07/2008	2	Tail rotor balance req'd.	TR White flapping bearing U/S.		18/07/2008	4624	3
G-TIGO	55	75	04/01/2006	0				04/01/2006	4842	0
G-TIGO	55	489	27/12/2007	0				27/12/2007	5317	0
G-TIGS	66	20	15/09/2006	2	TAIL ROTOR BALANCE	IHUMS tail rotor vib exceedance		13/09/2006	5356	2
G-TIGS	66	1083	05/07/2008	1	TR Pitch links worn			01/07/2008	6418	4
G-TIGS	66	1150	21/07/2008	0				21/07/2008	6436	0
G-TIGS	67	8	22/09/2008	3	tail rotor vibrations excessive	T/R Vibration Adjustments Required	tail rotor vibes spiked	15/09/2008	6501	7
G-TIGT	71	68	27/09/2006	1	Links worn to limit			07/09/2006	6678	20
G-TIGV	75	17	14/02/2006	0				14/02/2006	7006	0
G-TIGV	75	298	29/01/2007	0				29/01/2007	7232	0
G-TIGG	80	87	16/10/2008	0				16/10/2008	8041	0
G-BWWI	89	108	28/10/2006	1	red flapping hinge brg worn			25/10/2006	8219	3
G-BWWI	89	141	13/11/2006	2	Tail rotor sleeve guide.	Flapping hinge.		09/11/2006	8253	4
G-BWWI	89	390	12/03/2007	1	T/R Vib's T/R Flapping Hinge Bearings Inner races:Inspection.:Vib's. T/R Flapping Hinge Bearings I			23/02/2007	8479	17
G-BWWI	90	1	28/03/2007	0				28/03/2007	8530	0
G-BWWI	90	98	03/05/2007	0				03/05/2007	8589	0

Registration	ComponentFitID	Sequence	Date	Number of associated maintenance records	Maintenance action description for first maintenance action	Maintenance action description for second maintenance action	Maintenance action description for third maintenance action	alert_time	alert_index	Maintenance_lag (days)
G-BWZX	93	700	03/09/2007	0				03/09/2007	10051	0
G-BWZX	93	759	26/09/2007	1	brg,s worn			16/09/2007	10087	10
G-BWZX	93	760	26/09/2007	0				26/09/2007	10111	0
G-BWZX	94	241	08/10/2007	0				08/10/2007	10138	0
G-BWZX	94	737	30/12/2008	0				30/12/2008	10874	0
G-PUMI	104	125	08/11/2006	0				08/11/2006	11004	0
G-PUMI	104	196	15/12/2006	1	T/R Brng Worn.			20/11/2006	11029	25
G-PUMI	104	210	27/12/2006	0				27/12/2006	11089	0
G-PUMI	104	233	04/01/2007	0				04/01/2007	11106	0
G-PUMI	104	503	20/12/2007	1	LBE raised for pics.			19/12/2007	11379	1
G-PUMI	104	519	05/01/2008	0				05/01/2008	11398	0
G-PUMI	104	553	02/02/2008	0				02/02/2008	11432	0
LN-OLC	107	97	05/06/2007	0				05/06/2007	11545	0

4.4.2.3 Anomaly model using trended harmonic amplitudes

The alerts for the 1T, 2T and 3T harmonics across all 11,616 TR acquisitions are shown in Figure 4-34. The charts show both the PA parameter and the filtered alerts. The corresponding 4T, 5T and 10T harmonics are a shown in Figure 4-35. The 1T model generated a total of 15 alerts. The alerts and corresponding maintenance are shown in Table 4-12. Eight of the 15 T1 alerts coincide with the outputs of the model based on 1T raw amplitude data. Six alerts coincide with alerts from using the smoothed amplitude data. Three alerts were identified that were not previously highlighted. Similarly to the smoothed amplitude models, from visual inspection of the data a number of alerts appear to exist in multiple individual harmonic models. In particular are alerts that appear at indexes of approximately 4500, 6500 and 8500.

The results of the individual harmonics were combined by taking at each acquisition the maximum PA value of any of the harmonic data. The alert filtering algorithm was then applied to the combined PA parameter to generate a combined alert parameter. The combined model generated a total of 51 alerts. The alerts and corresponding maintenance are shown in Table 4-12. Thirty-one of the alerts could be associated with maintenance action: 21 alerts occurred less than 10 days after the alert.

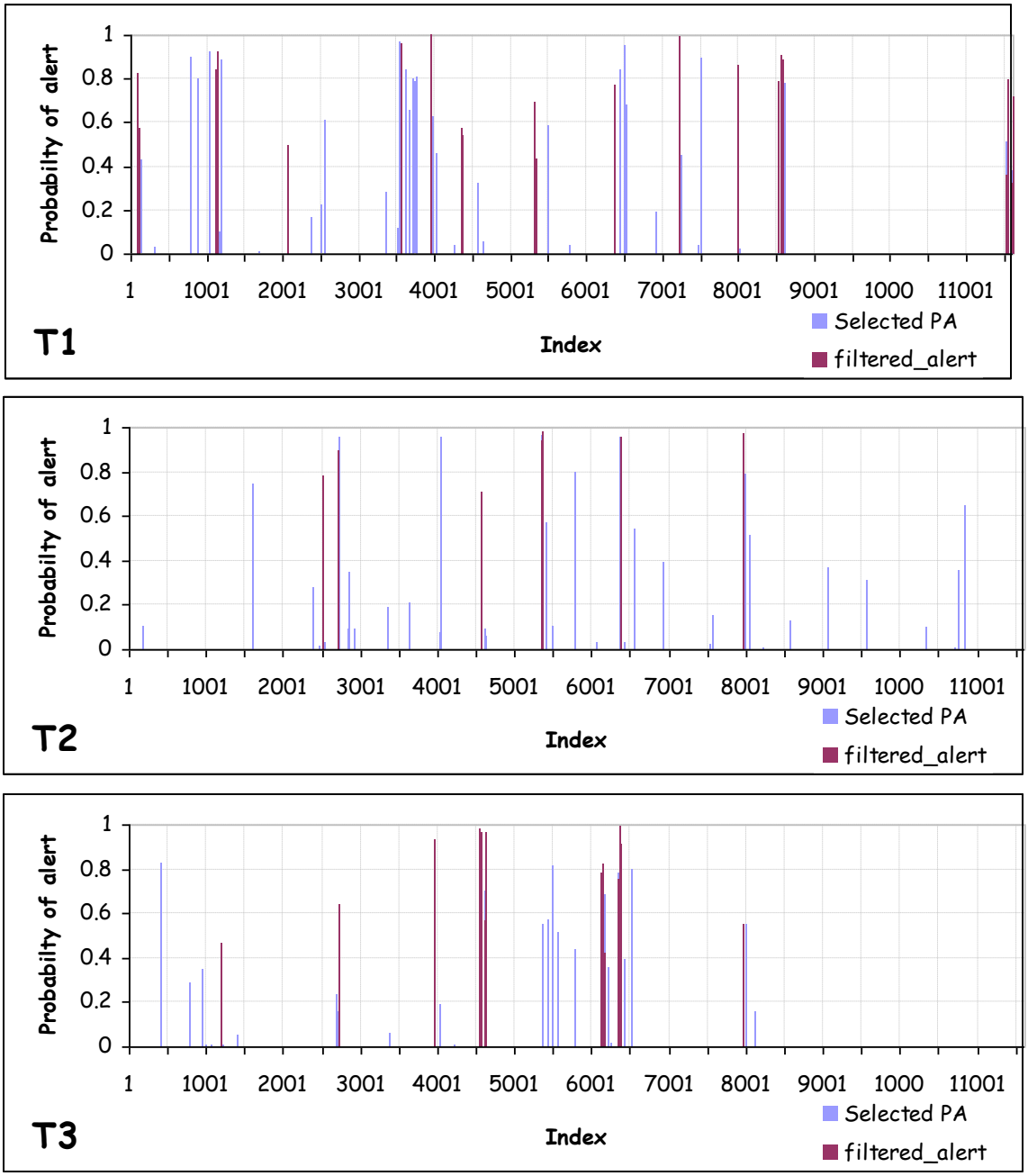

Figure 4-34: Alerts for 1/2/3T Harmonics from Trended Amplitude Anomaly Model

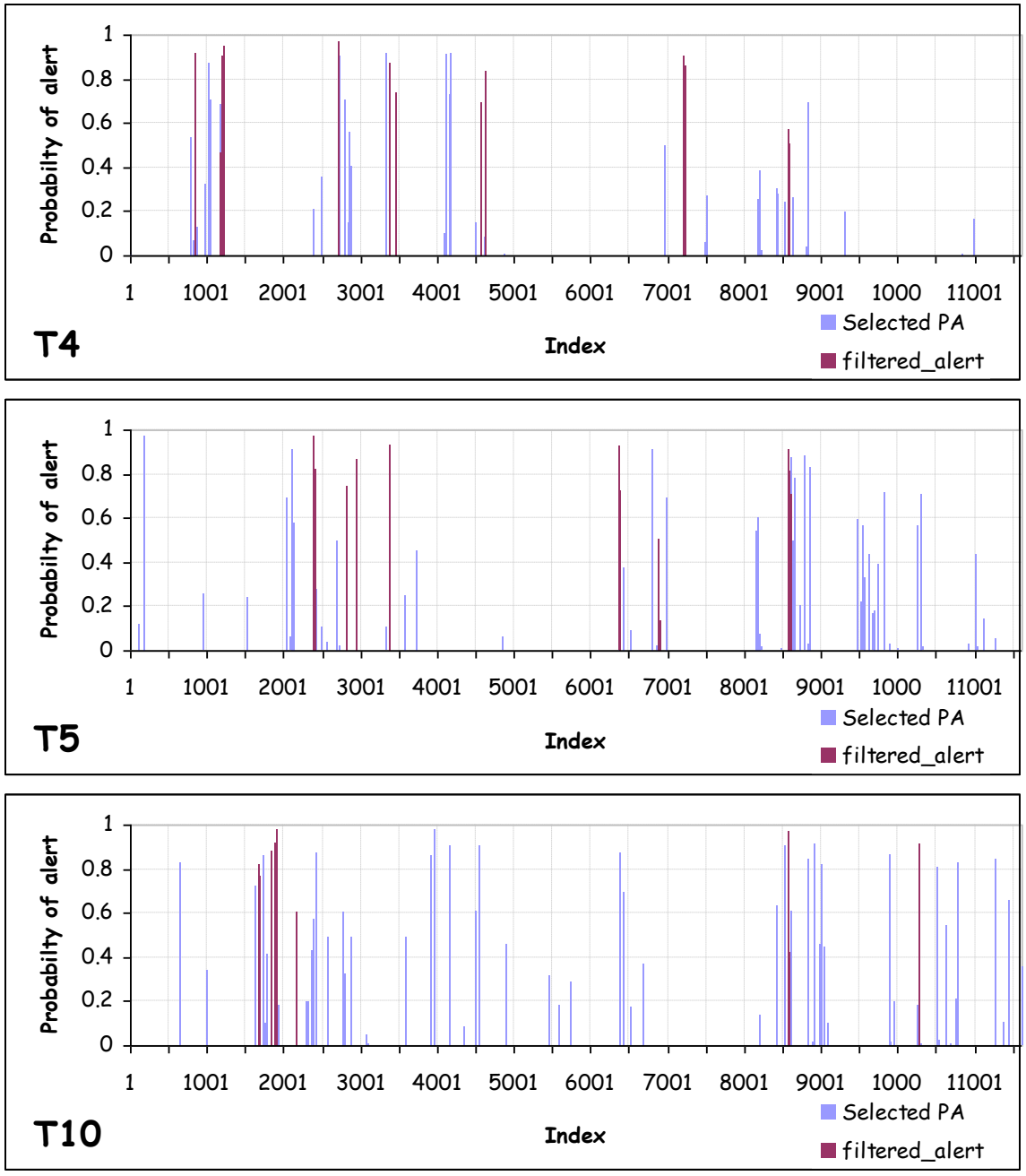

Figure 4-35: Alerts for 4/5/10T Harmonics from Trended Amplitude Anomaly Model

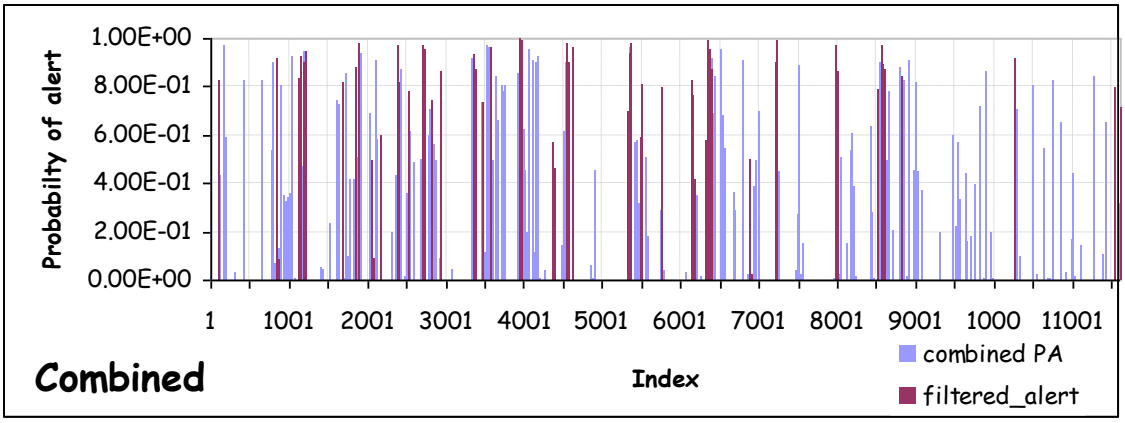

Figure 4-36: Combined Alerts for 1/2/3/4/5/6T Harmonics from Trended Amplitude Anomaly Models

Table 4-12: Alerts and Associated Maintenance Actions 1T Harmonic, Anomaly Model Derived from Trended Harmonic Amplitudes

Registration	ComponentFitID	Sequence	Date	Number of associated maintenance records	Maintenance action description for first maintenance action	Maintenance action description for second maintenance action	Maintenance action description for third maintenance action	alert_time	alert index	Maintenance_lag (days)
G-BLPM	3	105	07/03/2007	1	Yell & Blu. Flapping brngs. worn.			02/03/2007	101	5
G-BMCW	16	364	15/06/2007	0				15/06/2007	1129	0
G-BMCW	16	374	09/07/2007	2	PMC Creation	5 Pitch change links worn		27/06/2007	1135	12
G-TIGC	32	493	26/10/2007	1	TAIL ROTOR BOOT TORN			02/10/2007	2066	24
G-TIGF	41	112	30/01/2007	1	IHUMS T/R RTB's			25/01/2007	3562	5
G-TIGF	42	193	03/11/2008	1	Tail rotor pitch links.			20/10/2008	3956	14
G-TIGJ	48	173	24/04/2007	0				24/04/2007	4378	0
G-TIGO	55	502	08/01/2008	0				08/01/2008	5330	0
G-TIGS	66	1083	05/07/2008	1	TR Pitch links worn			04/06/2008	6377	31
G-TIGV	75	298	29/01/2007	0				29/01/2007	7232	0
G-TIGG	80	72	02/09/2008	0				02/09/2008	7998	0
G-BWWI	89	410	25/03/2007	0				25/03/2007	8525	0
G-BWWI	90	98	07/05/2007	0				07/05/2007	8594	0
LN-OLC	107	96	03/06/2007	0				03/06/2007	11544	0
LN-OLC	107	167	31/10/2007	0				31/10/2007	11615	0

Table 4-13: Alerts and Associated Maintenance Actions Combined 1T/2T/3T/4T/5T/10T Harmonics, Anomaly Models Derived from Individual Trended Harmonic Amplitudes

Registration	ComponentFitID	Sequence	Date	Number of associated maintenance records	Maintenance action description for first maintenance action	Maintenance action description for second maintenance action	Maintenance action description for third maintenance action	alert_time	alert_index	Maintenance_lag (days)
G-BLPM	3	105	07/03/2007	1	Yell & Blu. Flapping brngs. worn.			02/03/2007	101	5
G-BMCW	16	79	29/10/2006	0				29/10/2006	844	0
G-BMCW	16	193	01/11/2006	0				01/11/2006	851	0
G-BMCW	16	364	15/06/2007	0				15/06/2007	1129	0
G-BMCW	16	374	09/07/2007	2	PMC Creation	5 Pitch change links worn		27/06/2007	1135	12
G-BMCW	16	418	09/10/2007	1	RTB Adjustments			01/10/2007	1180	8
G-BMCW	16	435	27/10/2007	3	50hr INSP.	50hr INSPECTION	50hr INSP	22/10/2007	1190	5
G-BMCW	16	467	16/11/2007	1	Bearings worn			29/10/2007	1202	18
G-TIGC	32	86	25/10/2006	1	2 bearings worn			15/10/2006	1679	10
G-TIGC	32	265	10/04/2007	2	Pitch links worn	BEARINGS WORN		13/03/2007	1835	28
G-TIGC	32	276	18/04/2007	1	Black t/r sleeve suspect wear.			18/04/2007	1888	0
G-TIGC	32	291	02/05/2007	1	Pitch change boot damaged			29/04/2007	1900	3
G-TIGC	32	493	26/10/2007	1	TAIL ROTOR BOOT TORN			02/10/2007	2066	24
G-TIGC	32	569	14/12/2007	1	White tail rotor pitch link worn			05/12/2007	2171	9

Registration	ComponentFitID	Sequence	Date	Number of associated maintenance records	Maintenance action description for first maintenance action	Maintenance action description for second maintenance action	Maintenance action description for third maintenance action	alert_time	alert_index	Maintenance_lag (days)
G-TIGC	33	155	14/08/2008	0				14/08/2008	2392	0
G-TIGE	36	45	26/10/2006	1	t/rotor pitch links worn			25/10/2006	2519	1
G-TIGE	36	234	18/04/2007	1	Tail rotor			18/04/2007	2710	0
G-TIGE	36	259	04/05/2007	1	Pilot Reports Vibration Tail Rotor			04/05/2007	2735	0
G-TIGE	37	102	27/07/2007	1	Post maintenance Check			28/06/2007	2819	29
G-TIGE	37	240	01/10/2007	1	T/R pitch links worn			04/09/2007	2948	27
G-TIGE	37	612	20/10/2008	1	BLK & BLUE TR sleeve binding			20/10/2008	3377	0
G-TIGF	41	18	01/10/2006	2	Link bearings worn	Pitch links worn		28/09/2006	3471	3
G-TIGF	41	112	30/01/2007	1	IHUMS T/R RTB's			29/01/2007	3565	1
G-TIGF	42	193	03/11/2008	1	Tail rotor pitch links.			20/10/2008	3956	14
G-TIGJ	48	173	24/04/2007	0				24/04/2007	4378	0
G-TIGJ	48	317	07/04/2008	0				07/04/2008	4543	0
G-TIGJ	48	343	30/04/2008	1	Flapping hinge bearing/sleeve,spin.			21/04/2008	4563	9
G-TIGJ	48	412	28/07/2008	1	Worn bearings.			21/07/2008	4628	7
G-TIGO	55	502	08/01/2008	0				08/01/2008	5330	0
G-TIGS	66	20	15/09/2006	2	TAIL ROTOR BALANCE	IHUMS tail rotor vib exceedance		14/09/2006	5357	1
G-TIGS	66	160	30/11/2006	2	IHUMS adjustment required	Tail rotor		30/11/2006	5498	0

Registration	ComponentFitID	Sequence	Date	Number of associated maintenance records	Maintenance action description for first maintenance action	Maintenance action description for second maintenance action	Maintenance action description for third maintenance action	alert_time	alert_index	Maintenance_lag (days)
G-TIGS	66	438	17/04/2007	4	Black T/R Pitch Change Link Brng	Red,Blu & Whi' In/Out Brngs Worn.	Red T/R pitch link.	12/04/2007	5775	5
G-TIGS	66	808	08/12/2007	0				08/12/2007	6146	0
G-TIGS	66	814	11/12/2007	0				11/12/2007	6152	0
G-TIGS	66	832	20/12/2007	2	all 5 trpcl's worn	tail rotor needs weight		20/12/2007	6170	0
G-TIGS	66	1000	15/04/2008	0				15/04/2008	6338	0
G-TIGS	66	1021	20/05/2008	1	Sleeve/Spindles brinelling			20/05/2008	6359	0
G-TIGS	66	1083	05/07/2008	1	TR Pitch links worn			09/06/2008	6380	26
G-TIGT	72	91	27/09/2007	0				27/09/2007	6898	0
G-TIGV	75	224	16/01/2007	0				16/01/2007	7217	0
G-TIGV	75	298	29/01/2007	0				29/01/2007	7232	0
G-TIGG	80	19	08/08/2008	1	Aircraft rough in cruise			01/08/2008	7971	7
G-TIGG	80	72	02/09/2008	0				02/09/2008	7998	0
G-BWWI	89	410	25/03/2007	0				25/03/2007	8525	0
G-BWWI	90	65	07/05/2007	0				07/05/2007	8594	0
G-BWWI	90	75	16/05/2007	0				16/05/2007	8604	0
G-BWWI	90	98	12/06/2007	1	IHUMS t/r bal adj.			25/05/2007	8618	18
G-BWWI	90	292	16/10/2007	4	T/R adjustments	pics	Tail rotor spindles	11/10/2007	8819	5
G-BWZX	94	241	18/12/2007	0				18/12/2007	10268	0
LN-OLC	107	96	03/06/2007	0				03/06/2007	11544	0
LN-OLC	107	167	31/10/2007	0				31/10/2007	11615	0

4.4.3 Trend model summary

The three methods presented are not mutually exclusive and all three models may be used to confirm a potential fault. The raw magnitudes model does not process the data so will not mask a fault by contaminating the data through an applied process; if a fault is present and manifests itself in the recorded data it should be detected by the anomaly model. Nevertheless, a significant amount of alerts will be false due to the high levels of noise. In addition, this model is based on absolute values only, and may not be particularly effective at reacting to developing trends due to localised variations in the vibration amplitudes.

The SG smoothing model is less affected by noise and can identify developing underlying trends. The use of SG filters means that rapidly developing short term trends are preserved. Nevertheless, sudden changes, due to step changes in the data, for example, will be smoothed.

The (linear) trended harmonic model, unlike the SG smoothing model, is able to react to sudden step changes in the data that could indicate the onset of a fault condition. Also, by tracking linear trends in the data it is able to indicate when there has been a change in behaviour in the harmonic amplitudes, e.g. a change from a constant trend in amplitude to an increasing trend. However, in this work this aspect of the model has not been investigated due to limited available time. Nevertheless it could be useful to detect changes in trends before they become large enough to trigger alerts in the anomaly models.

The trended harmonic model provides a high degree of smoothing and in this regard is similar to the SG smoothing model. It will remove a substantial part of the background noise that can obscure trends in the raw harmonics model, although further work should be considered to improve the robustness of the model to outliers. However because it is also able to react to step changes that would be smoothed by the SG smoothing model it can be seen to compliment both the raw magnitudes model and the smoothed models to provide additional information. Therefore the different models would be expected to identify different anomalies.

Nevertheless, significant anomalies that develop over a period sufficiently long not to be considered noise and removed with the smoothing models would be expected to alert in all three models. Therefore one approach for improving the robustness of the models is to identify faults that are detected by multiple models. Measured over all the anomaly models that used individual harmonic inputs, the total number of unique anomalies identified was 123. 44 of the anomalies were identified by two model techniques. Of these 23 were identified by the raw amplitude and the SG smoothed amplitude models. 13 anomalies were identified by all three methods.

The 13 anomalies detected by all three models are shown in Table 4-14. The table also shows any corresponding maintenance action carried out within one month of the alert. It can be noted that all bar one of the alerts could be associated with a maintenance action within this period whilst 7 of the actions occurred within 10 days of the alerts and a further 3 actions occurred within 13 days. This shows a high correlation between maintenance action and events where all three model types alerted.

A summary of the numbers of alerts generated by the absolute models and the trend models is shown in Table 4-15. The table shows the alerts for the individual harmonic absolute and trend models, the absolute models that used multiple

harmonic inputs and the combined alerts of the individual trend models. The table also shows the number of alerts that could be associated with maintenance actions. For the trend models these are the actions that occurred within 10 days of the alert. Highlighted in the table are the alerts for the individual harmonic models that demonstrated the highest correlation with maintenance actions. For many of the individual harmonic models the SG smoothed model generated the most alerts that could be associated with a maintenance action. Overall, the results indicate that there is an advantage to developing models based on smoothed and trended the data, as well as raw amplitude data. As indicated above, models based on individual harmonics can potentially be used to distinguish instrumentation faults. However, the number of anomalies that could be associated with maintenance actions are lower than previously obtained using a single anomaly model with multiple (e.g. 2T—10T) harmonic inputs. There is no reason therefore that simple anomaly models based on 1T and 2T—10T inputs should not be used.

Table 4-14: Alerts Identified by all Approaches

Registration	Component Fit ID	Sequence	Date	Number of associated maintenance records	Maintenance action description for first maintenance action	Maintenance action description for second maintenance action	Maintenance action description for third maintenance action	alert time	alert index	Maintenance lag (days)
G-BLPM	3	105	07/03/2007	1	Yell & Blu. Flapping brngs. worn.			03/03/2007	102	4
G-BMCW	16	193	08/01/2007	1	Red t/r pitch link			27/12/2006	937	12
G-BMCW	16	435	27/10/2007	3	50hr INSP.	50hr INSPECTION	50hr INSP	27/10/2007	1200	0
G-BMCW	16	467	16/11/2007	1	Bearings worn			03/11/2007	1211	13
G-BWWI	90	98	12/06/2007	1	ihums t/r bal adj.			15/05/2007	8602	28
G-TIGC	32	291	02/05/2007	1	Pitch change boot damaged			20/04/2007	1893	12
G-TIGC	33	155	25/09/2008	2	Worn	Worn		23/09/2008	2405	2
G-TIGE	36	259	04/05/2007	1	Pilot Reports Vibration Tail Rotor			03/05/2007	2733	1
G-TIGF	41	112	30/01/2007	1	IHUMS T/R RTB's			30/01/2007	3566	0
G-TIGJ	48	343	30/04/2008	1	Flapping hinge bearing/sleeve,spin.			21/04/2008	4563	9
G-TIGS	66	20	15/09/2006	2	TAIL ROTOR BALANCE	IHUMS tail rotor vib exceedance		14/09/2006	5357	1
G-TIGS	66	1083	05/07/2008	1	TR Pitch links worn			15/06/2008	6393	20
G-TIGV	75	298	19/03/2007	0				26/01/2007	7230	

Table 4-15: Alert and Associated Maintenance Summary Across Models

Harmonics in model	absolute		Trend					
			Raw harmonics		SG Smoothed harmonics		Linear trended harmonics	
	Number of alerts	Correlated Maintenance	Number of alerts	Correlated Maintenance*	Number of alerts	Correlated Maintenance*	Number of alerts	Correlated Maintenance*
T1	12	7	20	10	12	8	15	2
T2	7	6	16	10	23	18	19	11
T3	17	13	1	1	1	1	13	7
T4	10	9	20	8	22	12	12	5
T5	7	1	12	4	16	6	9	1
T10	-	-	16	6	20	11	8	4
T1-T10 (combined)	-	-	74	32	61	24	51	22
T234	25	19						
T1234	14	11						
T12345	17	13						

*Correlated maintenance actions are those occurring within 10 days of an alert

4.5 Combining TR and gearbox databases

The large amount of noise in the data and the significant variance of the recorded values can make it difficult to distinguish a genuine anomaly from one caused by an artefact of the data. Previous research focusing on the TR gearbox determined that some anomalies identified in the gearbox were caused by the TR itself (Reference [1]). Therefore, it is anticipated that combining the measurements in the TR database with the gearbox database could enhance the ability to detect faults by including a measure of cross validation. The main advantage of this approach is that the TR sensors are separate from the gearbox sensors. A genuine fault may be sensed by both the TR sensors and the gearbox sensors. An instrumentation error in one sensor would not affect the other sensor, while the likelihood of instrumentation errors in both sensors at the same time is much lower than the likelihood of this occurring in any one sensor. Therefore, anomalies that are identified in one TR sensor but do not appear in the other may be caused by an instrumentation problem. A limitation of this approach is that the gearbox sensor only outputs SO1 and SO2 (1/rev and 2/rev vibration), therefore only the TR 1T and 2T harmonics could be cross validated in this way.

A second difficulty in cross validating anomalies in the two sensor measurements is the different acquisition times and regimes for the gearbox and TR. Previous attempts to merge the data resulted in the loss of a large amount of data and made developing models from the reduced data sets unviable. An alternative approach is to build separate anomaly models for the TR and gearbox data sets, then combine the outputs from the models using reasoning logic to determine the presence of a fault.

A limited exercise was performed building a gearbox SO1 model and a TR 1T model, then comparing alerts triggered by the two models. Only a relatively small proportion of the alerts could be directly correlated, therefore the analysis was not pursued any further. However, it is still considered that there is merit in cross validating information from separate sensors to provide robustness when instrumentation faults affect the data.

Nevertheless, the correlated results for the three model types (raw, SG smoothed and linear trended) and the corresponding maintenance actions are shown in Table 4-16, Table 4-17 and Table 4-18. The individual raw parameter model for the TR 1T harmonic indicated 21 alerts of which 11 alerts could be correlated with a maintenance action within 30 days of the alert. Of those alerts 10 could be correlated with a maintenance action within 10 days. The corresponding individual raw parameter model for the gearbox SO1 parameter indicated 40 alerts of which 18 alerts could be associated with maintenance within 30 days. Of those alerts 15 could be correlated with a maintenance action within 10 days. The combined gearbox\TR 1T model results are shown in Table 4-16. The table shows that only 3 alerts were common between the two models with 2 alerts having maintenance action within 10 days whilst the third alert could not be associated with any action. Therefore there were 58 individual alerts across the two models with only 3 common to both (5.1%).

The individual smoothed parameter model for the TR 1T harmonic indicated 39 alerts where 20 alerts could be correlated with maintenance within 30 days. Of those alerts, 17 could be correlated within 10 days. For the corresponding gearbox model 29 alerts were recorded. However, only 13 alerts were correlated with maintenance within 30 days and only 9 alerts with maintenance within 10 days. The

combined gearbox\TR 1T model results are shown in Table 4-17. This model showed a slight increase in the number of alerts common to both TR and gearbox models. A total of 9 combined alerts were identified, i.e. a total of 59 unique alerts were identified of which 9 were common to both models (15.2%). Of the 9 common alerts, 6 could be associated with a maintenance action and 3 could not. The correlated maintenance actions all occurred within 10 days of the alert.

The individual linear trended parameter model for the TR 1T harmonic generated 30 alerts whilst the corresponding gearbox model generated 44 alerts. Of the 30 alerts for the TR1T harmonic 13 could be associated with maintenance within 30 days of the alert and 6 could be associated with maintenance within 10 days. Of the 44 gearbox alerts 24 could be correlated with maintenance within 30 days of the event. Of those events 17 could be correlated with maintenance within 10 days. However, as shown in Table 4-18 only 2 events were common to both the TR 1T harmonic model and the gearbox model. This represents only 3% of the unique alerts. Neither alert was correlated with any maintenance action.

As indicated above, the limited number of combined gearbox\TR 1T harmonic alerts and the limited resources available meant that the analysis was not pursued further at this stage. However, it should be noted that in this work the models focused on cross-correlating gearbox model outputs with TR 1T harmonic model outputs using data recorded in the MPOG phase. Better correlations might have been obtained if the data recorded during the Cruise phase were used.

Table 4-16: Alerts and Associated Maintenance Actions Combined Gearbox and 1T Harmonic, Anomaly Model Derived from Raw Harmonic Amplitudes

Registration	ComponentFitID	Sequence	Date	associated maintenance	Maintenance action description for first maintenance action	Maintenance action description for second maintenance action	Maintenance action description for third maintenance action	alert_time	alert index	Maintenance_ lag (days)
G-BLPM	3	287	07/03/2007	1	Yell & Blu. Flapping brngs. worn.			07/03/2007	288	0
G-TIGE	36	532	04/05/2007	1	Pilot Reports Vibration Tail Rotor			02/05/2007	4483	2
G-TIGV	75	382		0				25/01/2007	10499	

Table 4-17: Alerts and Associated Maintenance Actions Combined Gearbox and 1T Harmonic, Anomaly Model Derived from SG Smoothed Harmonic Amplitudes

Registration	ComponentFitID	Sequence	Date	associated maintenance	Maintenance action description for first maintenance action	Maintenance action description for second maintenance action	Maintenance action description for third maintenance action	alert_time	alert index	Maintenance_ lag (days)
G-BLPM	3	290	08/03/2007	0				08/03/2007	291	0
G-BLPM	4	13	09/04/2007	1	Tail Rotor Balance			02/04/2007	310	7
G-TIGE	36	532	04/05/2007	1	Pilot Reports Vibration Tail Rotor			02/05/2007	4484	2
G-TIGF	41	90	15/11/2006	1	RTB'S required on Tail rotor			13/11/2006	5560	2
G-TIGJ	48	585	20/07/2008	1	TR White flapping bearing U/S.			18/07/2008	7180	2
G-TIGS	66	1457	05/08/2008	0				05/08/2008	9554	0
G-TIGS	66	1480	14/08/2008	0				14/08/2008	9577	0
G-TIGS	66	1523	03/09/2008	2	T/R balance reqd	BLK & YEL TR SL/SP to be replaced		26/08/2008	9606	8
G-TIGS	67	15	19/09/2008	1	tail rotor vibes spiked			16/09/2008	9644	3

Table 4-18: Alerts and Associated Maintenance Actions Combined Gearbox 1T Harmonic, Anomaly Model Derived from Trended Harmonic Amplitudes

Registration	ComponentFitID	Sequence	Date	associated maintenance	Maintenance action description for first maintenance action	Maintenance action description for second maintenance action	Maintenance action description for third maintenance action	alert_time	alert index	Maintenance_ lag (days)
G-BWWI	90	129	12/06/2007	0	.			11/04/2007	12126	
G-PUMI	105	18	20/11/2008	0				20/11/2008	15668	0

4.6 Further analysis of CF AHUMS™ TR data

It is anticipated that while rotor balance may be successively determined using the radial data, some TR faults will be more easily detected in the axial data; and while the axial sensor is fitted to the IHUMS aircraft the data is not currently recorded. The HUMS database for the CF412 aircraft has available both axial and radial TR data, although in this case there is no related maintenance information. Nevertheless, to determine whether it would beneficial to routinely record axial data a quick experiment was performed to configure anomaly models using the axial and radial TR measurements in the CF412 database.

Pre-processing of the data was carried out by quickly configuring and applying a data correction algorithm. The algorithm is designed to identify complex short period corruptions in signal data and was used to eliminate, where possible, noise in the harmonic measurements. Once a period of corruption has been identified it is removed and replaced with synthesised data linearly interpolated from valid data either side of the corruption. The corrected data was subsequently interrogated to ensure any genuine anomalies were identified.

Although, due to the action of the fin, the TR is usually not highly loaded in the cruise, it is probably more loaded in that flight condition than at minimum pitch on the ground (MPOG). Therefore it was anticipated that any anomalies due to faults would be more easily detected during cruise conditions and the investigation concentrated on data in the Normal Cruise database.

Separate anomaly models were built for the radial and axial data. Each set of anomaly models were built using both SG smoothed amplitudes and trended measurements, applying the processing described in Section 4.4.1. For each technique two anomaly models were constructed: one model was built using the 1T harmonic while the second model combined the harmonics 2T, 3T, 4T, 5T and 6T, i.e. 4 models were built for each set of radial and axial TR data. Higher harmonics were not included; however, research indicated that no significant information was excluded. Any Component Fit that was identified as having corrupt data by the correction algorithm was excluded from the anomaly model training set, however all the data was used for anomaly prediction. Predictions were based on corrected data and not the raw data. In the following charts both raw and corrected data are shown.

For each of the four models the minimum Fitness Score was extracted and ranked. In addition, the minimum Fitness Score from all of the four models was calculated and ranked. An example of the ranked data is given in Table 4-19. It should be noted that Component Fit 2 is the accident aircraft. It was assumed that the models that would be able to identify Component Fit 2 as significant would be better able to detect rotor faults; at least those that exhibited the same type of fault characteristics in the data. From Table 4-19 it is seen that it is seen that the models using the axial data ranked the significance of Component Fit 2 higher than those using the radial data. Looking at the ranking of the separate model outputs it was determined that all the models ranked Component Fit 2 higher using the axial data rather than the radial.

Table 4-19: Fitness Score Rankings for Axial and Radial CF412 Anomaly Models

Axial		Radial	
ComponentFitID	Fitness Score	ComponentFitID	Fitness Score
152	-375.08	272	-432.002
332	-105.96	442	-348.714
172	-86.664	542	-296.39
112	-82.512	492	-234.723
2	-62.698	552	-172.485
202	-54.802	432	-100.13
432	-43.719	482	-99.7755
442	-39.14	2	-94.9918
542	-36.221	342	-90.4163
222	-36.21	152	-68.8218
92	-31.929	82	-67.3459
362	-16.389	202	-41.1262
562	-12.788	362	-39.3949
472	-10.743	192	-27.979

Further insight into the results for the axial and radial models can be gained by considering the rank correlation. It can be argued that it is not beneficial to record TR axial data if the radial data contains similar information to the axial data. If information in the radial measurements is similar to the information in the axial measurements this would lead the models to react in a similar manner and rank anomalies in the Component Fits in a similar order: at least for the most significant anomalies.

It was shown in Section 3.2.3 for the IHUMS data that similar behaviour between two models gave similar rankings for the minimum Fitness Score value, and high ranked correlations, when measured over aircraft ordered by rank. It was also argued that rank statistics are more robust; if the rank correlation indicates a linear relationship then it is genuine, whereas the normal linear correlation calculation can indicate a relationship when no relationship exists.

For each model the minimum Fitness Score values for each aircraft were extracted. The values for the axial models were averaged and a rank value assigned to each aircraft. The values for the radial models were processed in the same way. The axial and radial model rank values for the 51 Component Fits are shown in Figure 4-37, where the ranks for the radial models have been plotted against the ranks for the axial models. The rank correlation between the two sets of calculations is quite low at 0.32. In particular if the axial and radial models contain similar information it would be anticipated that the most significant anomalies, and therefore the highest ranked Component Fit (based on minimum Fitness Score values) at least would be very similar as indicated by the IHUMS example shown in Figure 3-48. A running rank correlation was calculated after ordering the ranks by the order of the axial models, Figure 4-38. Table 4-20 shows the rank correlation for the top 20 aircraft when ordered by the axial model ranking values. The figure and the table indicate that there is very poor rank correlation at any level of ranking (comparison can be

made with the IHUMS example Figure 3-49). This indicates that the axial and radial models are behaving in different ways, and not necessarily reacting to the same anomalies.

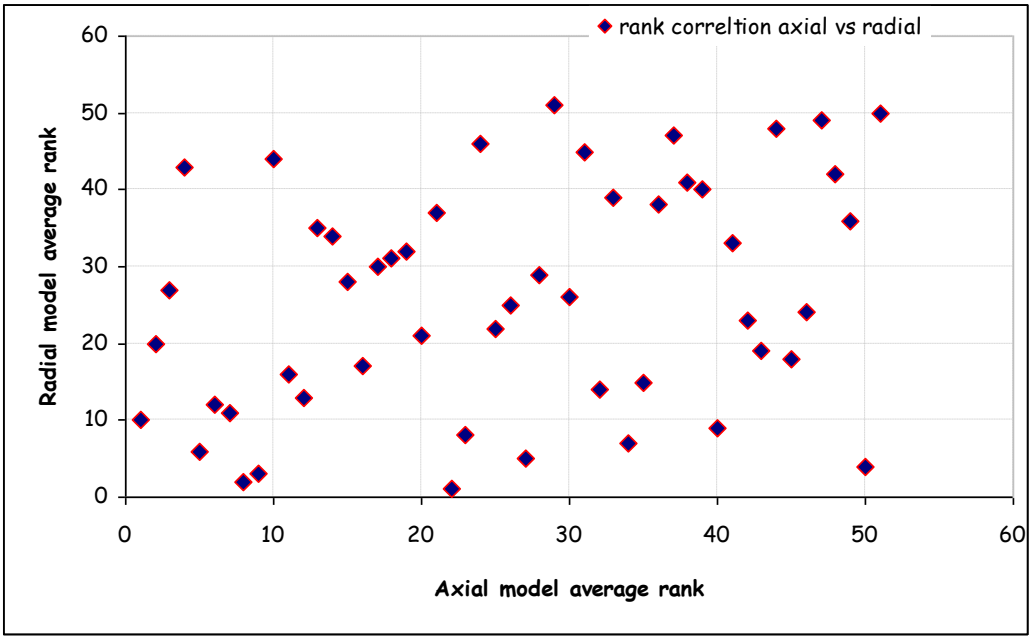

Figure 4-37: Average Axial Model Ranking vs. Average Radial Model Ranking for CF412 Anomaly Models

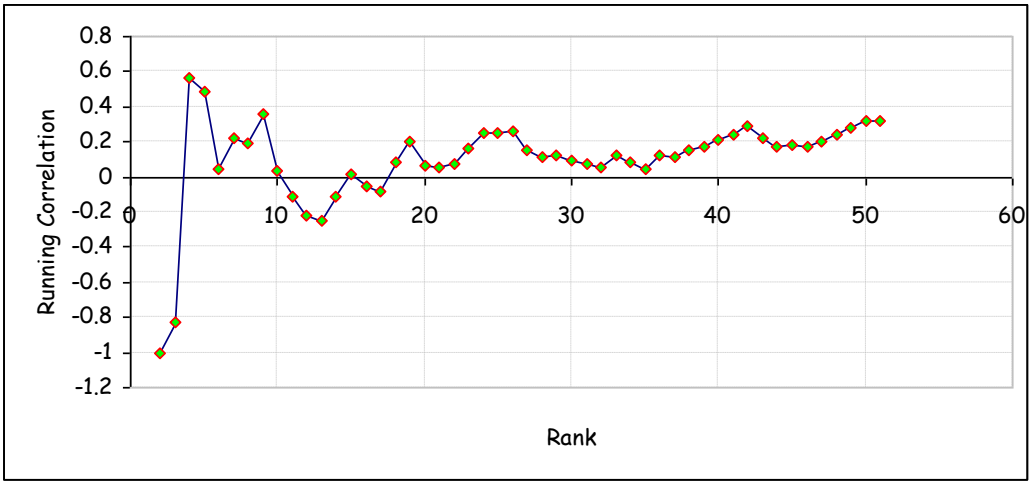

Figure 4-38: Running Rank Correlation between Axial and Radial CF412 Anomaly Models Ordered by Axial Rank

Table 4-20: Top 20 Running Rank Correlation between Axial and Radial CF412 Anomaly Models Ordered by Axial Rank: Top 20

Axial Models		Radial Models		Running Correlation
ComponentFitID	Rank	ComponentFitID	Rank	
272	1	272	22	
442	2	442	8	-1.000
542	3	542	9	-0.832
492	4	492	50	0.561
552	5	552	27	0.481
2	6	2	5	0.041
342	7	342	34	0.226
482	8	482	23	0.196
82	9	82	40	0.363
152	10	152	1	0.040
432	11	432	7	-0.107
202	12	202	6	-0.218
362	13	362	12	-0.253
192	14	192	32	-0.115
392	15	392	35	0.013
92	16	92	11	-0.058
312	17	312	16	-0.081
62	18	62	45	0.087
382	19	382	43	0.200
332	20	332	2	0.068

It can be noted that this simple experiment does not mean that anomalies identified by the different models are mutually exclusive; anomalies may be identified in both the radial and axial models and may be used to validate a genuine anomaly from an instrumentation fault (because the axial and radial measurements use different sensors). Nevertheless, these results indicate that the radial and axial models are driven by different effects and contain different information. This indicates that both sets of measurements should be recorded.

The distribution of minimum Fitness Score values is shown in Figure 4-39 and indicates that several Component Fits have anomalies. A number of interesting Component Fits are now discussed:

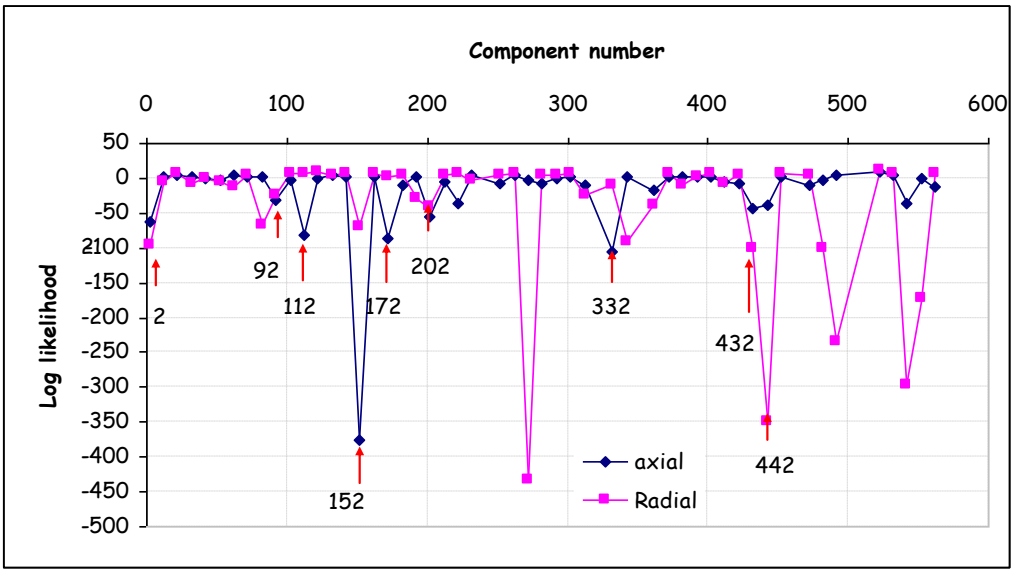

Figure 4-39: Minimum Fitness Score Values for CF412 Anomaly Models

Component Fit 112: this shows a strong trend in the axial data that starts at index 71 (10/09/07), Figure 4-40. In fact in this case, the interesting trend was identified as corrupt by the correction algorithm and removed. Nevertheless a related trend possibly exists in the radial data but at much lower amplitude, such that this feature looks genuine rather than an instrumentation fault. Since the trend was removed from the axial data this feature did not trigger the low Fitness Score value observed in the output. This was due to a step change in the 3T, and 5T data at index 50 (24/07/07). It is also seen in the 1T although this did not lead to a significant 1T Fitness Score result.

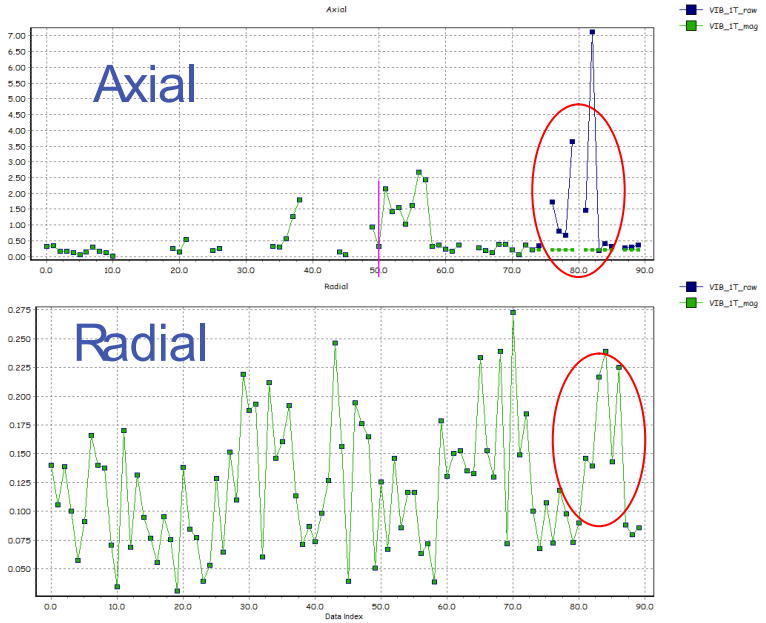

Figure 4-40: Component Fit 112 1T Harmonic

Component Fit 152: this shows low values in the axial data up to index 145 (23/06/07) where there is a step change and an increase in signal activity, Figure 4-41. There is a behaviour change in the radial data at this point too and some of the data has been corrected. This could be indicative of a maintenance action to repair or replace a faulty axial sensor.

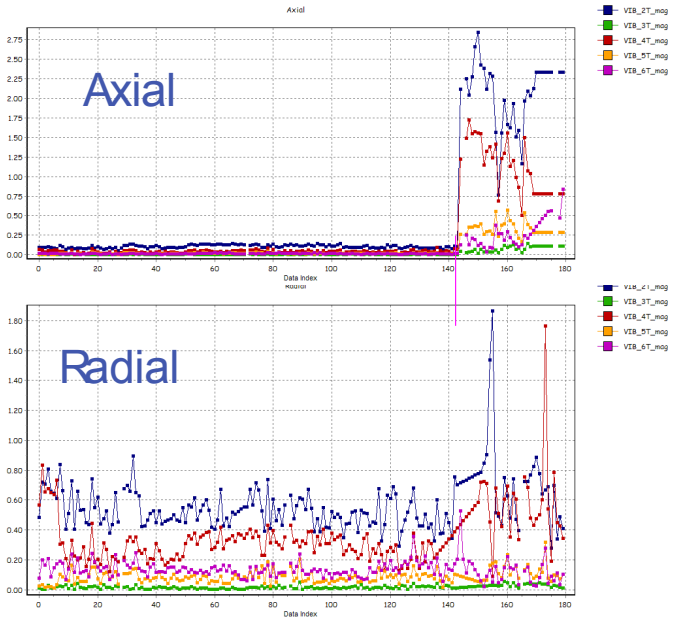

Figure 4-41: Component Fit 152 2/3/4/5/6T Harmonics

Component Fit 172: this exhibits similar behaviour to Component Fit 152 where there is a step change in activity of the axial data at data index 8 (02/10/06) and could be due to maintenance action on the axial sensor, Figure 4-42. This is particularly obvious in the 2T and 4T harmonics. No such step change is observed in the radial data.

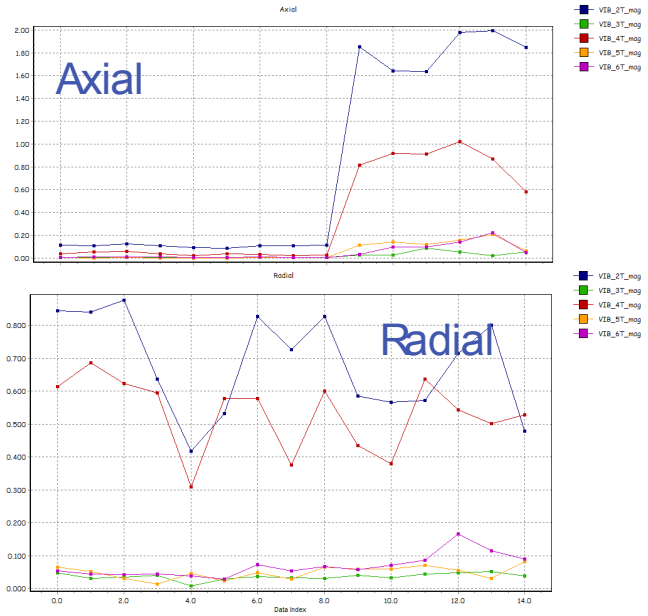

Figure 4-42: Component Fit 172 2/3/4/5/6T Harmonics

Component Fit 332: this exhibits an increasing trend in the axial 1T values from index 12 (17/06/06), Figure 4-43. In the radial data 1T is also trending up at this point although in comparison with the preceding data no significant increase in the amplitude is observed. In addition, the trend in the radial data starts earlier from about index 8, (16/06/06). Further examination of the data indicates that similar upward trends are observed in the other axial harmonics. Downward trends are observed in the radial data for the remaining harmonics although the amplitudes of the trends are not significant. However, the nature of the increasing trend in the axial data is more characteristic of a developing fault rather than the large amplitude, random data characteristic of instrumentation errors.

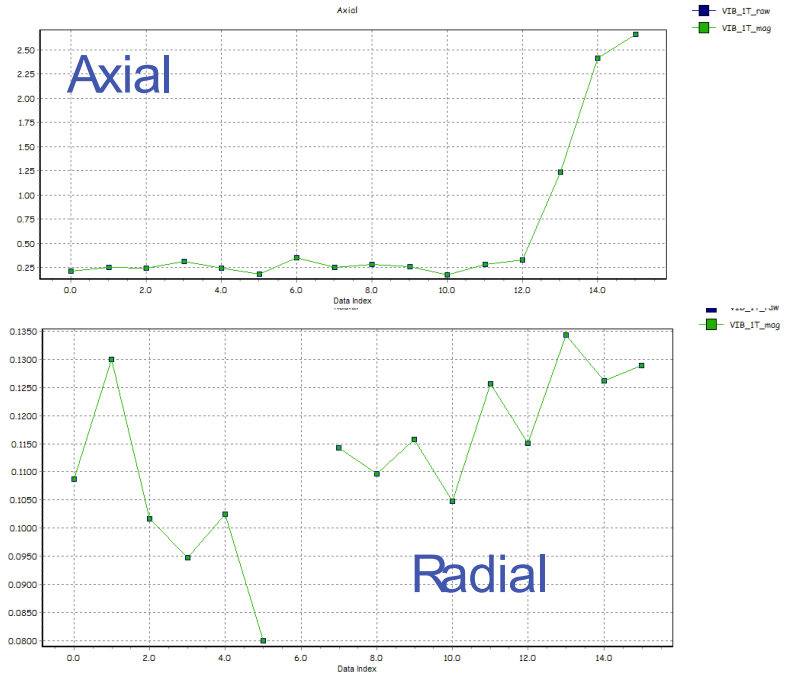

Figure 4-43: Component Fit 332 1T Harmonic

Component Fit 442: this shows significant activity in all the axial harmonics from index 79 (30/05/07). The 1T harmonic is shown in Figure 4-44 while the 2/3/4/5/6T harmonics are shown in Figure 4-45. The amplitudes were sufficient to trigger data correction in the 2T, 3T, 4T and 5T harmonics. After a significant upward trend over 4 or 5 points there is more random, large amplitude variations which would be more indicative of instrumentation faults. However, similar behaviour is also observed in the radial data indicating that this may not be the case. Recording both axial and radial data is useful to cross-correlate datasets to help identify both instrumentation and TR faults.

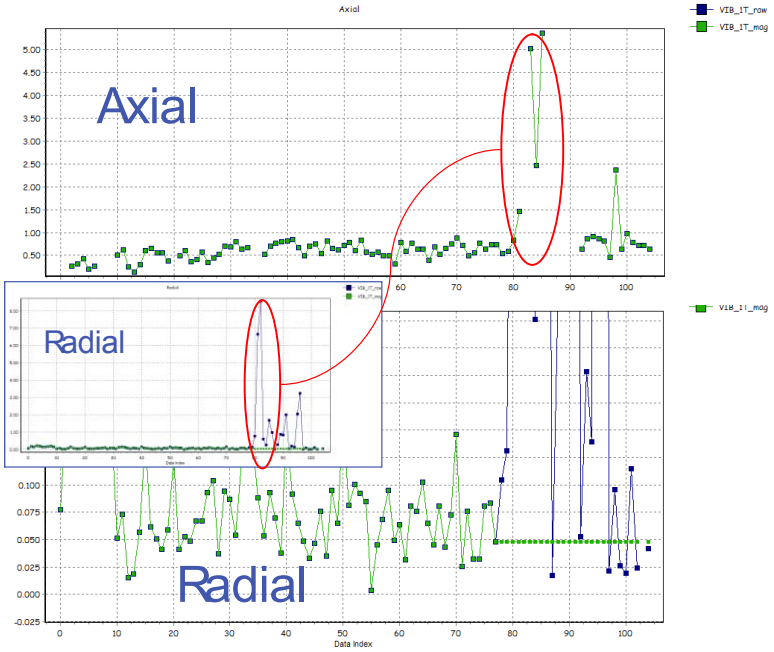

Figure 4-44: Component Fit 442 1T Harmonic

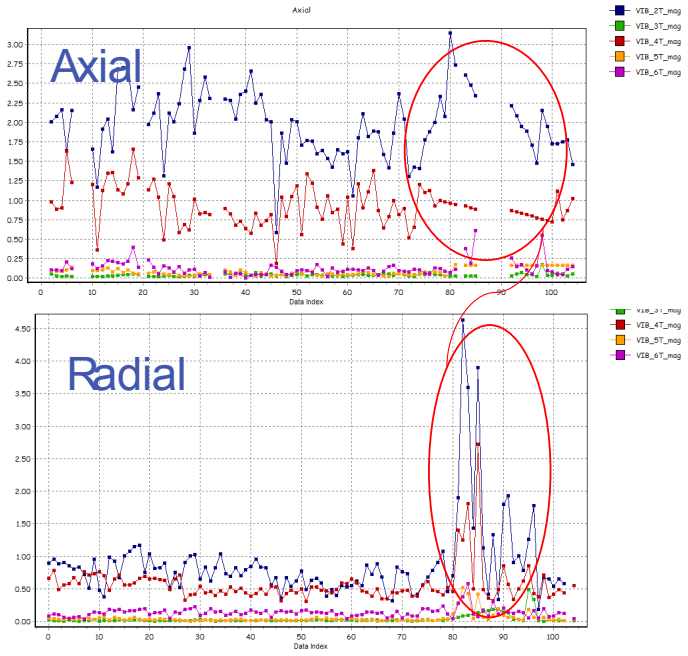

Figure 4-45: Component 442 Fit 2/3/4/5/6T Harmonics

5 Conclusions and Recommendations

5.1 Conclusions

Under an extension to Contract No. 841, GE Aviation conducted a helicopter rotor HUMS study to review the status of rotor health monitoring research, and also accidents caused by rotor system failures. This study identified two Main Rotor (MR) failure cases and three Tail Rotor (TR) cases for which HUMS data was available. In neither of the MR cases (a MR blade failure and a cracked blade yoke) was there any evidence in the currently acquired HUMS data of fault-induced changes that could have provided warning of the failure. However, in all three TR cases (failure of a flapping hinge retainer; failure of a pitch change spider; and a blade failure) an investigation performed after the incident or accident revealed some fault-related information in the HUMS vibration data. In one case an increase in 1/rev vibration had triggered a HUMS alert, but an inspection failed to detect the fault. In the other two cases there were increases in vibration harmonics for which thresholds are not currently set. It was therefore concluded that there is potential to improve airworthiness through the application of Advanced Anomaly Detection (AAD) to HUMS TR vibration data.

Under a further extension to Contract No. 841, GE Aviation has applied its AAD technology to HUMS vibration data from two TR-related accidents and one TR-related incident, and also a database of historical Bristow 332L IHUMS data (with TR faults identified in a separate maintenance database) to evaluate the potential airworthiness and maintenance benefits that could be obtained. The analysis consisted of three primary elements; anomaly modelling of single and multiple TR harmonics, merging data from different acquisitions stored in different database tables (e.g. to allow TR axial and radial data to be modelled together), and automated trend analysis.

A blade failure occurred on the two bladed TR of a Bell 412 helicopter. The clearest failure related trends were in 1T and 5T axial and radial vibration. The 1T vibration would be expected as a result of the defection of the cracked blade. However the 5T trend could not have been predicted, and is believed to be due to excitation of a blade bending mode, as the frequencies of the blade modes would decrease as the crack developed. Several anomaly models built with different combinations of vibration harmonics responded to the fault. An axial 5T univariate model had the highest anomaly ranking, identifying the significance of the 5T axial data; however fusing multiple TR harmonics in an anomaly model also gave a clear fault indication. A trend detection algorithm showed that the last 3 data points from the accident aircraft could be identified as part of a trend. The results indicated that a TR AAD alert could have been triggered on the flight prior to a refuelling stop that occurred before the final flight.

A failure occurred on one of the arms of the pitch change spider on the 5 bladed TR of a Super Puma. The clearest failure related trends were in 1T, 4T and 6T axial and radial vibration. In this case, the frequencies could be predicted from a knowledge of the failure mode (causing 1/rev modulation of the blade pass frequency). Multiple anomaly models were built using axial and radial TR data and all models clearly responded to the failure. The trend detection algorithm identified a clear trend on the accident aircraft; however this was only detected on the last two data points. The results show that a TR alert could have been triggered after the first flight of the day of the accident, with the failure occurring on the second flight.

The third incident involved a Super Puma with a cracked flapping hinge retainer on one of the 5 TR blades. The available accident data was limited to published plots of HUMS Tail rotor Gearbox (TGB) output SO1 data and 'composite' TR vibration measurements. An anomaly model was built using recreated TGB output SO1 data and the accident aircraft was identified as anomalous. A trend detection algorithm also identified a clear trend in the data. In this case the existing IHUMS had triggered an alert, but a subsequent maintenance inspection failed to identify the developing flapping hinge retainer crack.

For the two accident cases an anomaly alert could have been triggered before the final flight, however to prevent the accident it would have been necessary for the HUM system to report a warning, and for this to have been acted upon, between two flights on the same day. In the case of the incident, an anomaly warning could have been generated several flights before the failure. In both accident cases the effects of the faults were clearest in the TR axial data as opposed to the radial data. Radial measurements can be affected by both TR unbalance and component faults, whereas axial measurements are in the axis of thrust generated loadings, which could exercise faults. As for the application of AAD to the helicopter rotor drive system, in all cases the most extreme anomalies identified were believed to be due to HUMS instrumentation issues.

For TR failures, there can be a very limited time interval between the point at which damage propagates to an extent that it affects the vibration measurements and the final failure. As HUMS data is not downloaded and analysed after every landing (the aircraft may be away from its operating base), if all three accidents/incidents were to have been prevented it would probably be necessary to implement AAD in the on-board system and provide a cockpit indication on the ground before take-off. There may then be a problem of nuisance alerts due to HUMS instrumentation issues. However, even without this capability, applying AAD to HUMS TR data would still improve fault detection as multiple TR harmonics can be modelled, including ones that do not currently have HUMS thresholds.

The Bristow Super Puma TR 'maintenance study' (analysing maintenance-related TR faults) used IHUMS data that was limited to radial measurements only, but included both amplitude and phase. The TR maintenance actions identified typically related to TR balance, pitch link bearings, flapping hinge bearings, and sleeve and spindle bearings. According to the maintenance data, there were repeat occurrences of similar faults, however the TR vibration data showed trends in different TR harmonics, and it was not possible to identify any consistent pattern between the harmonics in the TR vibration data and particular documented fault types. However instrumentation faults could affect all harmonics. The analysis indicated that multiple TR harmonics can be combined in a single model to provide a general fault detection capability, while a separate 1T model remains useful to identify balance issues.

An analysis of the TR phase data identified phase shifts caused by maintenance actions, but did not highlight any clear trends in phase information that could be correlated with developing faults. Results showed that the outputs from anomaly models combining amplitude and phase information were primarily dependent on magnitude rather than phase. Therefore it was concluded that using the phase data did not provide any improvement in the ability to detect TR faults.

The Bristow IHUMS data was affected by frequent TR maintenance and servicing actions, with noise also being present due to suspected instrumentation issues. Smoothing the data and applying trend analysis to identify underlying trends was

useful, suppressing the effects of data noise. However, smoothing techniques must be treated with caution as the accident analysis showed that TR faults causing accidents can develop quickly.

To complete the project, some limited further analysis was performed on the Bell 412 HUMS TR data. This data was pre-processed using a smoothing filter, and anomaly models were built on the smoothed magnitude data. A trend algorithm was also applied to automatically identify and extract linear trends in the data, and trend models were built on differences in linear trend data. Anomaly models were built on the smoothed magnitudes and trends in the 1T and 2-6T harmonics of the data from the radial and axial accelerometers. Like the previously analysed Bristow 332L IHUMS data, the Bell 412 data also appeared to be affected by HUMS instrumentation issues. It was concluded from this short final anomaly modelling exercise that TR faults appear to be generally more visible in the axial dataset rather than the radial. Cross correlating axial and radial data sets can help to distinguish between instrumentation errors and potential faults.

5.2 Recommendations

It is recommended that, when implementing an AAD capability for the helicopter rotor drive system, AAD models are also included for the TR. While there may be aircraft specific modeling requirements, for an optimum balance between good fault detection and diagnostic capabilities and reduced false alarms, it is generally recommended that four model configurations are implemented. These are two univariate models; 1T radial and 1T axial, and two multivariate models; 2 to n+1T radial, 2 to n+1T axial (where n = 4 or the number of TR blades, whichever is larger). 1T radial and axial measurements could be included in a single model, however it would involve combining results from different data acquisitions (this has not been implemented in current AAD systems).

Consideration should be given to the application of appropriate data pre- and post processing techniques to enhance the AAD results. Pre-processing may include the use of techniques to identify data trends (building models on trend data) and the careful use of smoothing techniques if data is noisy. Post-processing can include anomaly model output trend identification and severity assessment.

TR vibration monitoring may provide a late indication of a potential TR hub or blade failure. Therefore, where possible, HUMS data should be downloaded and reviewed between flights. For system upgrades and future systems, consideration should be given to the feasibility of providing on-ground indications of MR and TR vibration monitoring alerts on a Multi-Functional Display in the cockpit. Providing on-ground cockpit alerts based on AAD would also require the implementation of an AAD capability in the on-board system. Alternatively, where the facilities exist, MR and TR vibration measurements and alerts could be included in data transmitted from aircraft via a Satcom link in flight or a Wifi link at a landing site.

As TRs can have different numbers of blades, there will be some differences in the TR vibration measurements between different aircraft types, for example in the number of harmonics measured. However it is recommended that, for TR VHM, the measurement set is standardised where possible. Data should be acquired from both radial and axial accelerometers and should, as a minimum, include measurements at MPOG and in normal cruise of all harmonics up to nT+1 where n = 4 or the number of TR blades, whichever is larger.

Vibration monitoring can provide TR health information, however instrumentation problems can cause a significant number of false alarms. Providing high reliability instrumentation and the elimination of signal noise should be key requirements for the design and installation of accelerometers and wiring harnesses for TR vibration monitoring.

The analysis described in this report was performed on TR data from early generation HUM systems and, in the case of the Bristow IHUMS, on data from a radial sensor only. TR data could be analysed from more modern aircraft (e.g. the EC225 or AW139), with different TR hub designs and possibly more reliable instrumentation. However, no further accident data is available and, whilst further analysis may yield new information, it would be unlikely to change the overall conclusions of the work.

As there are similar limitations with MR and TR VHM, consideration should be given to further research into health monitoring techniques that would be applicable to both the MR and TR. This could include areas such as the investigation of the potential use of vibration data acquired during unsteady flight conditions, and the investigation of the emergent rotating-frame sensing technologies including data transfer from the rotor system to the non-rotating fuselage equipment.

6 References and Acknowledgement

1 CAA Paper 2011/01: “Intelligent Management of Helicopter Vibration Health Monitoring Data”, May 2012.

2 CAA Paper 2008/05: “HUMS Extension to Rotor Health Monitoring”, March 2009.

3 “Report on the Incident to Aerospatiale AS332L Super Puma, G-PUMH over North Sea on 27 September 1995”, AAIB Aircraft Incident Report 2/98.

4 Canadian Forces Flight Safety Investigation Report (FSIR) – Final Report, File Number 1010-CH146420 (DFS 2-2), 24 June 2005.

5 GE Aviation report REP1649(3), “MHS Aircraft 9M-STT Ditching – Analysis of HUMS Data”, September 2005.

Acknowledgement

GE Aviation wishes to acknowledge the assistance given by the following organisations in providing data and information for this work: Meggitt Avionics, Bristow Helicopters, CHC Helicopters, DND Canada, Malaysian Helicopter Services and Eurocopter.